SAPIENZA
UNIVERSITÀ DI ROMA

FACOLTÀ DI SCIENZE MATEMATICHE FISICHE E NATURALI

DOTTORATO DI RICERCA IN BIOLOGIA AMBIENTALE ED EVOLUZIONISTICA – BOTANICA

PhD thesis

Giulia De Angelis

Internalization mechanisms of biopolymeric nanoparticles in plants and fungi and application in integrated pest management

Tutor:

Prof.ssa Gabriella Pasqua

A.Y. 2021/2022

Index

Chapter 1: Introduction

1.1. Nanotechnology in agricolture

The economy of most developing countries is based on agriculture, which has been fundamental to the rise of human civilization, with more than 60 percent of the population depending on it for their sustenance (Brock et al., 2011; Jan et al., 2020). To date, many factors such as climate changes, industrialization, use of resources, environmental issues such as the pesticide and fertilizer use, and increasing food demand caused by the growing population, place the agricultural sector in front of continuous challenges. In this context, nanotechnology has grown rapidly in recent years, and advances in the era of nanostructured materials and nanodevices have opened up new possibilities in many applications. By developing more efficient and less contaminant agrochemicals (nanoformulations), nanosensor for detecting biotic and abiotic stresses before they affect production (nanosensors), or new genetic manipulation techniques that allow more efficient plant breeding (Pérez-de-Luque and Hermosín, 2013; Fraceto et al., 2016) and allow active ingredients like pesticides, micronutrients, and elicitors to be delivered to plant roots, agriculture can benefit. Currently, the pesticides on the market help prevent the spread of pests and diseases in global trade and in stored agricultural products and also

the use of pesticides protect crops and prevent post-harvest losses, thus contributing to food security. However, despite their relevance in plant protection, more recently evidence of the severe impacts on the environment have emerged (FAO/WHO, 2016). In fact, most of the agrochemicals (including pesticides) applied to the crops are lost because of several factors including leaching, hydrolysis, photolysis, and microbial degradation. Consequently, a large part of agrochemicals does not reach the plant target site, and at the same time, they could cause groundwater and soil pollution with consequent damage to soil microorganisms, plants and animals (McKnight et al., 2015). The generation of drug delivery systems based on nanomaterials or nanoparticles (NPs) represents a potentially alternative to develop novel formulations to successfully fight fungal infections and overcome the fungal multi-resistance to existent drugs. The main advantage of these nanoformulations could be that they can protect the load from volatilization, infiltration, outflow, leaching and photo, chemio- or biodegradation. Moreover, nanoformulations offer a promising alternative in plant disease management and have many benefits over conventional products and approaches, which are associated with enhanced efficacy, reduced input, and lower eco-toxicity (Elmer and White, 2018; Sathiyabama and Manikandan, 2018).

However, concerning the nanoformulation of agrochemicals, most of them have only been *in vitro* tested and many questions are still open. At first, several aspects need to be solved including the mechanisms of

internalization of NPs, sorting and targeting into plant and fungal cells according to morphology and physico-chemical properties of NPs.
It has not been assessed whether the nanocarrier penetrates in fungal and plant cells and reaches root or leaf tissues releasing its load inside, or if the active compounds are released outside in proximity of the plant and fungus. Answering to these questions could hold the key for a definitive use of nanotechnology in agriculture. Currently, we find a reduced number of antifungal nanoformulations on the market, compared to traditional pesticides. Few chemical companies have recently advertised microencapsulated nanoscale pesticides for sale. Some Syngenta products in Switzerland (Karate ZEON, Subdue MAXX, Ospray's Chyella, Penncap-M) and Australia (Primo MAXX, Banner MAXX, Subdue MAXX) and microencapsulated pesticides from BASF, fall into this category (Prasad et al., 2017). In summary, nanotechnology in agriculture could offer enormous promise; however, most of the research studies are still ongoing and awaiting field assays and extensive testing.

1.1.1. Biopolymeric nanoparticles

The term nanoparticle is often used about any nanometre-sized particle. However, the International Union of Pure and Applied Chemistry (IUPAC) suggests a specific terminology for different types of

nanoparticles. As regards controlled delivery systems, IUPAC recognizes several types of nanoparticles (Fig. 1) including: nanocapsules, nanospheres, liposomes, dendrimers and micelles (Su and Kang, 2020).

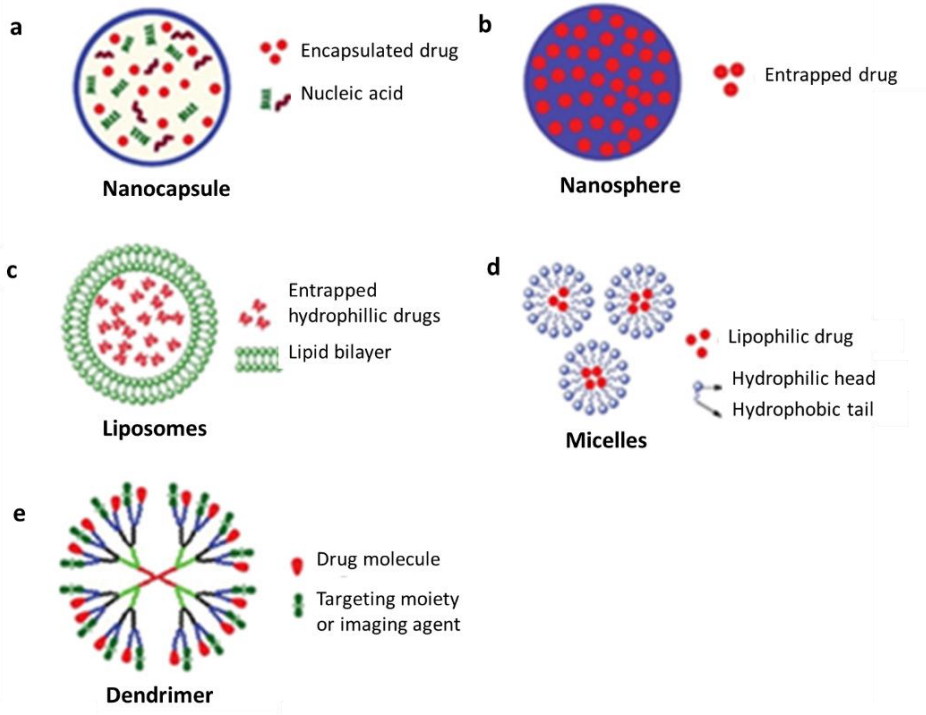

Figure 1: Schematic representation of the main types of nanoparticles used for drug delivery (Modified from Xu et al., 2013).

Nanocapsules (10-1000 nm) can encapsulate large amounts of drugs and nucleic acids. Nanosphere (20-200 nm) are typically made from biodegradable polymers. Liposomes (100-400 nm) are small spherical artificial vesicles typically made from lipid bilayers. Micelles (10-100 nm) are self-assembled amphiphilic particles that can encapsulate lipophobic or lipophilic compounds stabilized by surfactants. Dendrimers (3-20 nm) are monodisperse macro-molecules that can be utilized to covalently encapsulate or conjugate drugs (Xu et al., 2013).
In particular, nanocapsules (Fig. 1a) are of interest for applications in the agronomic field. The active substance is confined within a cavity surrounded by a polymeric shell (Pascoli et al., 2018), but it can also be adsorbed on the outer surface of the shell. The release of the entrapped substances takes place by diffusion through the polymeric shell and is influenced by both the chemical composition of the shell and the encapsulation method, which in turn affects the shell's size, shape and thickness.
Biodegradable nanovectors are particularly important both in the biomedical and agronomic fields, which are mainly applied in drug delivery for human's therapy drugs and pesticides. The term "biodegradable" refers to materials of natural or synthetic origin that can be degraded *in vivo*, enzymatically or otherwise. The products of their degradation are not toxic, or at least the risk of toxicity can be defined as negligible and are able to enter the normal metabolic pathways. Therefore, they are defined as biocompatible materials,

remembering that biocompatibility is a property that must be related to the organism tolerability and the biological environment (Makadia and Siegel, 2011).

Among these materials, PLGA (poly lactic-co-glycol acid) (Fig. 2) shows the greatest potential. It is characterized by high biocompatibility, physical resistance and ability to successfully transport drugs, proteins, nucleic acids and other macromolecules (Makadia and Siegel, 2011) and it is approved by the FDA (US Food and Drug Administration). PLGA is synthesized primarily by polymerization through opening of the cyclic diesters ring. This is the most used method thanks to the shorter times requested and the higher conversion rate of monomers (Stevanovic and Uskokovic, 2009). Since PLGA is a copolymer of PLA (poly lactic acid) and PGA (poly glycolic acid), both these components determine its chemico-physical properties. One of the advantages of using PLGA compared to other materials is the possibility of adjusting dosage and release of the cargo through alteration of some parameters such as molecular weight, the size of the vector, and the glycol/lactide ratio (Makadia and Siegel 2011). Diffusion and bio-erosion are the two main mechanisms by which PLGA nanoparticles release the load. For what concerns the bio-erosion, it has been shown that the water hydrolyses the copolymer, causing an increase in the matrix pore size, until the complete degradation of the nanoparticle. Furthermore, the water solubilizes the carrier's load, allowing it to spread through the pores of the matrix.

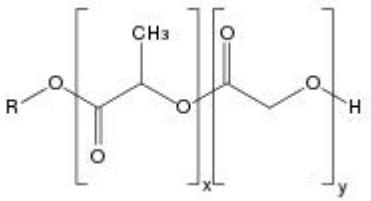

Figure 2: Structure of poly lactic-co-glycolic acid (x is the number of lactic acid units and y is number of glycolic acid units).

1.2. Internalization mechanisms of biopolymeric nanoparticles in plants

1.2.1. Endocytosis in plant cells

A major pathway for membrane proteins, lipids, and extracellular molecules to enter a cell is endocytosis. New findings indicate that multiple cellular processes require endocytosis, including signaling transduction, nutrient uptake, and plant–microbe interactions (Qi et al., 2018). Different endocytic pathways seem to be responsible for the endocytosis in animal cells, including phagocytosis, macropinocytosis, clathrin-mediated, and cavaeole-mediated endocytosis (Doherty and McMahon, 2009). Compared to the well-defined endocytic networks in animals, the understanding of endocytic mechanisms and their

physiological role in plants has lagged far behind. A variety of endocytic pathways also appear to be involved in endocytosis in the plant cells, and these may be clathrin-dependent or -independent (Fan et al. 2015). The last mentioned includes fluid-phase endocytosis, endocytosis associated with membrane microdomains, and phagocytosis-like uptake of rhizobia in plants (Malinsky et al., 2013). As in animal cells, clathrin-mediated endocytosis (CME) occurs through the invagination of clathrin-coated membranes, also called clathrin-coated pits (Fig. 3) (Fan et al., 2015). CME can be divided into five steps, as described extensively by Fan and collaborators in 2015: "CME can be divided into five steps. (1) Clathrin-coated endocytic vesicle formation begins with the association of adaptor protein complex 2 (AP2) with the plasma membrane (PM) via binding to phosphatidylinositol-4,5-bisphosphate [PI(4,5)P2]. (2) clathrin and unidentified accessory proteins are recruited by the membrane-associated AP2. After initiation, AP2 binds to various cargo proteins through its s2 and m2 subunits. With the aid of accessory proteins, AP2 continues to recruit clathrin, which polymerizes and forms a clathrin coat around the newly formed membrane invagination. (3) When the clathrin-coated vesicles (CCVs) mature, the GTPase dynamin-related protein (DRP) is recruited at the neck of the vesicle and (4) is responsible for the detachment of the vesicle from the PM. (5)". After the vesicles have been peeled off, the coated components are

disassembled and the endocytic vesicles containing the cargo are released into the cytoplasm (Fan et al., 2015).

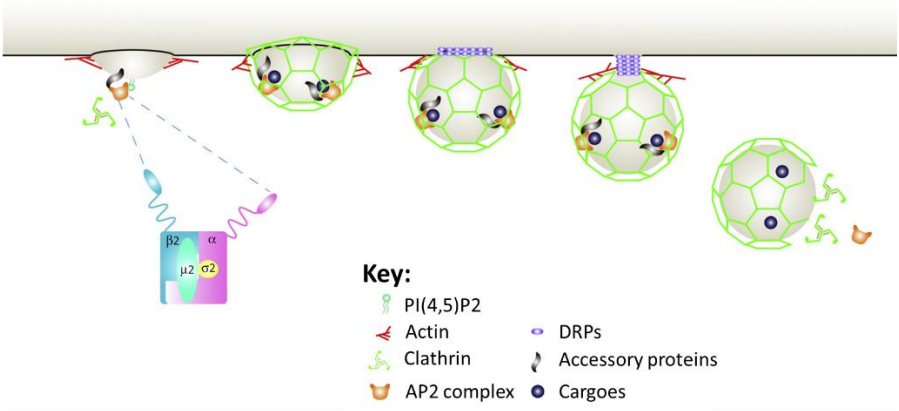

Figure 3: A proposed model of clathrin-mediated endocytosis (CME) in plants (Modified from Fan et al., 2015).

In clathrin-mediated endocytosis, an essential protein for vesicle detachment is dynamin, a GTPase protein (Fan et al., 2015). Nonetheless, in addition to clathrin-dependent endocytosis pathway, different researches have revealed several clathrin-independent pathways in plant cells, not all dependent on dynamin (Mayor and Pagano, 2007; Hemalatha and Mayor, 2019) (Fig. 4).

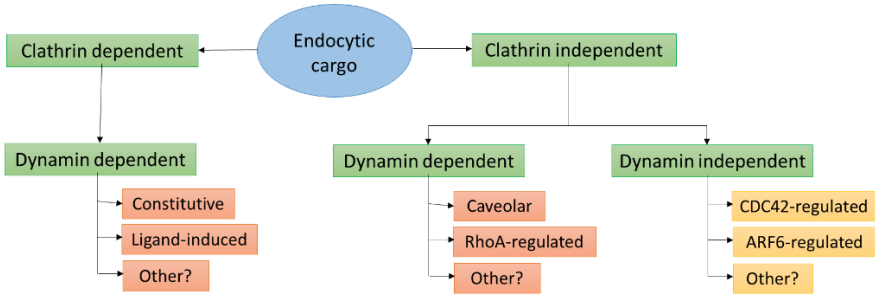

Figure 4: Classification system for endocytic mechanisms. A cargo protein can be endocytosed by either clathrin-dependent or clathrin-independent (CI) mechanisms. CI pathways can be further classified according to their dependence on the large GTPase dynamin (Modified from Mayor and Pagano, 2007).

In this context, recent studies have revealed microdomain-associated endocytosis (nanodomains associated to the plasma membrane rich in sterols and sphingolipids). Two membrane microdomain marker proteins are flotillin and remorin, and flotillin has been shown to participate in a clathrin-independent endocytic pathway in plant cells (Fan et al., 2015). The proteins flotillin may have a role in selecting lipid cargo for dynamin-independent endocytosis (Mayor and Pagano, 2007).

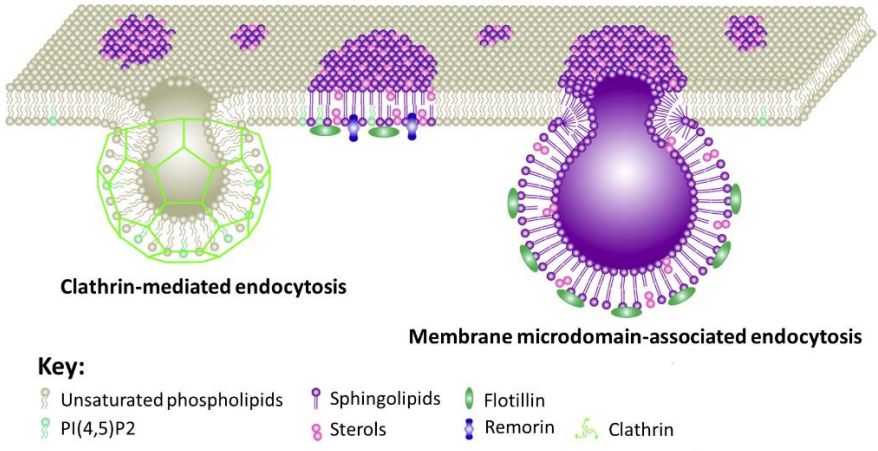

Figure 5: Two endocytic pathways identified in plant, clathrin-mediated endocytosis (CME) and membrane microdomain-associated endocytosis (Modified from Fan et al., 2015).

1.2.1.1. Dynasore, a dynamin inhibitor

Dynamin is fundamental for clathrin-coated vesicle formation in endocytosis, in transport from the trans Golgi network, and for ligand uptake through caveolae (Haucke and Kozlov, 2018; Makaraci and Kim, 2018). In clathrin-mediated endocytosis, accumulating evidence suggests that dynamine is critical for the pinching and release of a completed clathrin-coated pit from the plasma membrane, which

becomes a fully enclosed coated vesicle. Infact, dynamin assembles like a collar on the neck of a budding pit, and the cooperative conformational change that accompanies GTP hydrolysis results in neck constriction and scission (Macia et al., 2006).

Chemical inhibitors continue to be the most commonly used method to investigate endocytotic internalization mechanisms. Over the years several types of inhibitors have been investigated (Li et al., 2012), among them Dynasore has been shown to be extremely effective. Dynasore inhibits the GTPase activity of mitochondrial dynamin (Drp1), dynamin1, and dynamin2, but not those of other small GTPases *in vitro*. Consequently, Dynasore acts as a potent inhibitor of endocytic pathways known to depend on dynamin preventing the detachment of the coated vesicle from the membrane (Macia et al., 2006).

1.2.2 NPs uptake in plant cells

In the last decades, many studies have been conducted on the ability of nanomaterials to interact with eukaryotic cells (Farnoud and Nazemidashtarjandi, 2019). Currently, this ability is mainly utilized for nanomedicine applications, to deliver bioactive compounds to animal cells (Wang et al., 2021), and only recently researchers have been starting to explore the potential of nanocarriers in the field of plant biology (Sanzari et al., 2019). Different endocytic pathways appear to

be responsible for the internalization of NPs in animal cells, including macropinocytosis phagocytosis, clathrin-mediated, and cavaeole-mediated endocytosis (Manzanares and Ceña, 2020). However, plant cells have the cell wall, an additional barrier outside the plasma membrane, so these results cannot be used to model internalization in plant cells. Several mechanisms have been suggested for NP uptake in plant cells (e.g., by binding to carrier proteins, through ion channels, aquaporins, by binding to organic chemicals in the environmental media or creating new pores) (Lv et al., 2019). It has been proven that the capability of NPs to penetrate the plant cells depends on both the plant species and NP composition (Etxeberria et al., 2016). The cellular uptake also depends on NP dimensions, in relation to the diameter of cell wall pores and endocytic vesicles (Varma and Dey, 2021) as a result that cell wall and plasma membrane are selective barriers that allow the entry into the plant cell only to NPs within a specific size range (Tripathi et al., 2017). TEM analyses carried out on grapevine cells suggest that PLGA NPs are internalized by endocytic vesicles (Valletta et al., 2014). TEM observations suggest that internalized PLGA NPs are able to creep into the matrix spaces of the cell wall. The use of labeled NPs, labeled endocytic vesicles and specific clathrin-dependent endocytosis inhibitors indicate that NPs enter in suspended cells of *V. vinifera* through clathrin-dependent and clathrin-independent endocytosis, with a prevalence of the first route on the second (Palocci et al., 2017). The absence of PLGA NPs into the vacuole was supported

by fluorescence and electron microscopy and this is particularly interesting for the application of PLGA NPs as carriers for the delivery of bioactive compounds into the plants. However, further studies are necessary to understand the mechanisms by which PLGA NPs penetrate the plant cell.

1.2.3 NPs uptake in plant tissues and organs

The uptake of nanomaterials by plants is affected by several factors, including the particle's nature, but also the plant's physiology and its interaction with its environment (Pérez-de-Luque, 2017). It has been suggested that size is an important limiting factor for NPs penetration into plant tissues, with plants usually allowing NPs to move and accumulate within cells no larger than 40-50 nm in size; as shown by the administration of Au-NPs spheres to *Solanum lycopersicum* roots, or Quantum Dots coated to poly(acrylic acid-ethylene glycol) in *A. thaliana* leaves (Wang et al., 2016; Fincheira et al., 2020). In addition, the type of NPs, its chemical composition and its morphology are other factors that influence NPs uptake in plant (Raliya et al., 2016). It is possible to alter the properties of the nanomaterials by functionalizing and coating their surface, affecting how they are absorbed and accumulated in plants (Judy et al., 2012). Moreover, plant species may differ in their physiology, resulting in variations in NPs uptake; NPs also interact with the environment, which can affect their properties and

their possibility to be absorbed (Verma et al., 2021). In order to determine the effectiveness of nanomaterials to be internalized in plants, methods of application turn out to be crucial. NPs are absorbed into plants by the roots, which are specialized in absorbing nutrients and water, or by the leaves which are specialized in gas exchange through the stomata (Fig. 6 A and B). Two ways for nanoparticles to move through tissues are available once they penetrate the plant: the apoplast and the symplast (Fig. 6 C). Apoplastic transport occurs through the cell wall, and in the extracellular spaces (Sattelmacher., 2001), while symplastic transport occurs within adjacent cells' cytoplasm through plasmodesmata (Roberts and Oparka, 2003) and sieve plates (Roberts and Oparka, 2003). The movement of NPs toward the root central cylinder occurs by means of apoplastic transport, which promotes the movement of NPs toward the aerial part of the plant following the transpiration flow through the xylem (Sanzari et al., 2019; Sun et al., 2014).

Before reaching the xylem, the NPs must cross the endodermis through the symplastic pathway. In the endodermis, the Casparian strip, can stop the passage of NPs that accumulate, such as the case of mesoporous silica nanoparticles and ZnO nanoparticles. (Sanzari et al., 2019). For foliar applications, nanomaterials could enter through stomata or cross the cuticle barrier through either lipophilic or hydrophilic pathways. A lipophilic route involves diffusion through the cuticular wax, whereas

a hydrophilic route involves the polar aqueous pores in the cuticle and/or stomata (Lv et al., 2019).

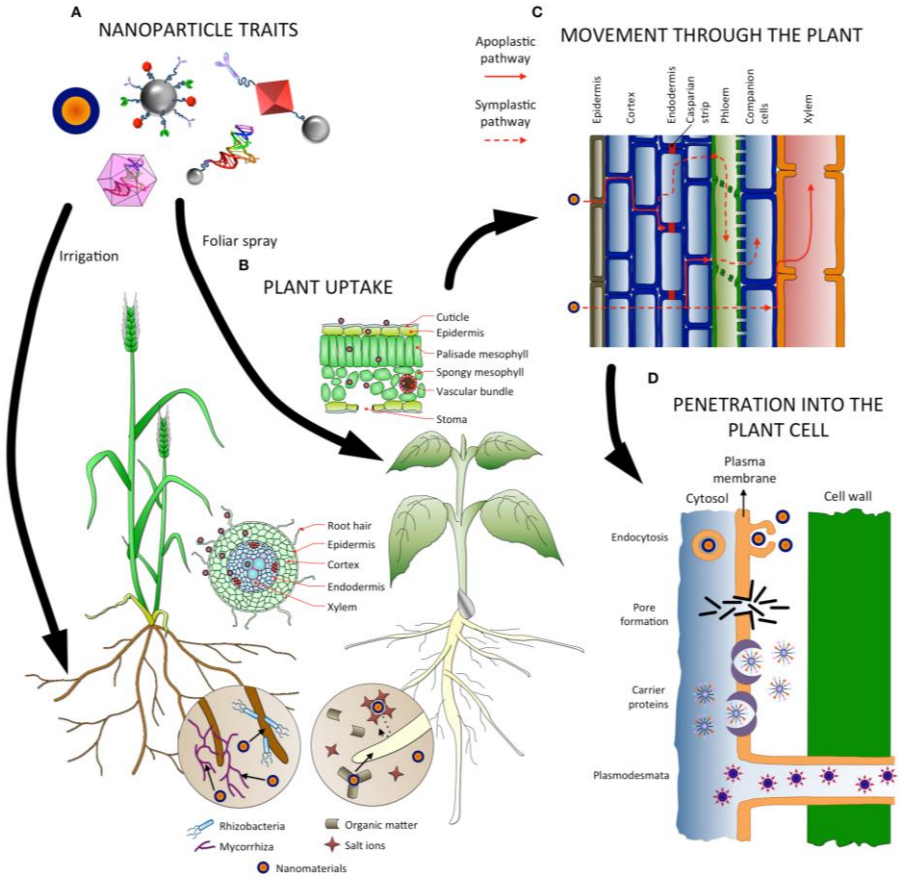

Figure 6: Nanoparticles absorption, uptake, transport, and penetration in plants. (A) Nanoparticle characteristics influence their absorption and

translocation, as well as the method of application. (B) Tissues and barriers in roots or leaves that must be passed through before nanoparticles can be taken up by vascular tissues. In soil, microorganisms and compounds can facilitate or hinder nanoparticle taking up. (C) For moving up and down, nanomaterials can follow apoplastic and/or symplastic pathways, and can switch from one pathway to another by radial movement. (D) Nanoparticles can be internalized through different mechanisms, such as pores, endocytosis, carrier proteins, and plasmodesmata (Modified from Pérez-de-Luque, 2017).

Internalization of NPs by the plant cell and crossing of the plasma membrane are required for them to enter the symplastic pathway (Fig. 6 D). There are various ways for nanoparticles to do this (Pérez-de-Luque, 2017):

- Endocytosis: the plasma membrane invaginates, incorporating NPs, giving rise to a vesicle that can reach different cellular compartments.
- Pore formation: NPs can induce the formation of pores in the plasma membrane throught carrier proteins: NPs bind to cell membrane proteins that act as carriers for internalization. Aquaporins, for instance, were suggested as nanomaterial transporters in the cell, but their tiny pore sizes (ranging between 2.8 and 3.4 Å) make them unlikely to penetrate NPs.
- Ion channels: there is only the possibility for small NPs to successfully cross the membrane by exploiting ion channels,

but these channels have a size of about 1 nm so this is the upper limit.

- Plasmodesmata: this involves specialized structures for transporting nanomaterials, which are already within the symplast, between cells.

However, any mechanism will use the NPs to get to the vascular tissues then they will accumulate in the leaves, flowers and fruits.

1.2.4 *Arabidopsis thaliana*: model plant selected for the NPs uptake studies

Arabidopsis thaliana (Fig. 7) is a small, annual, rosette plant. It is a member of the Brassicaceae family, in the eudicotyledon group of angiosperm vascular plants, and it is distributed in Asia, Europe, and North America (Kramer, 2015). Several different ecotypes have been harvested and are available for experimental analysis. The accepted ecotypes for genetic and molecular studies are Columbia and Landsberg (Meinke et al., 1998). The full life cycle (seed germination, formation of a rosette plant, bolting of the main stem, flowering, and maturation of the first seeds) takes place in a short period of time about 6 weeks (Fig. 7). In terms of size, the flowers are 2 mm long, self-pollinate at bud opening and may be easily crossed by applying pollen to the stigma. The fruits, called siliques, produce 0.5 mm long at maturity seeds. Seedlings grow in rosette plants from 2 to 10 cm in diameter, based on

growth conditions. Small unicellular hairs, called trichomes, cover the leaves and are convenient models for studying cell morphogenesis and differentiation (Meinke et al., 1998). In a greenhouse or in climate chamber, plants can be cultured in petri plates or grown in pots. Flowering is rapid and, prior to senescence, the inflorescence forms a progression of flowers and siliques for several weeks (Meinke et al., 1998). Four green sepals form the outer whorl, and four white petals compose the inner whorl of the flowers. The flowers have six pollen-bearing stamens and a gynoecium forming the silique. Hundreds of siliques with more than 5000 seeds are produced by the mature plants, which reach about 20 cm in height. The roots are easy to investigate in culture, have a simple structure, and do not establish symbiotic relationships with nitrogen-fixing bacteria (Meinke et al., 1998). Currently, several studies have been carried out using *A. thaliana* as a model plant (Chapter 3). For these reasons, *A. thaliana* has been chosen as model plant for NPs uptake studies.

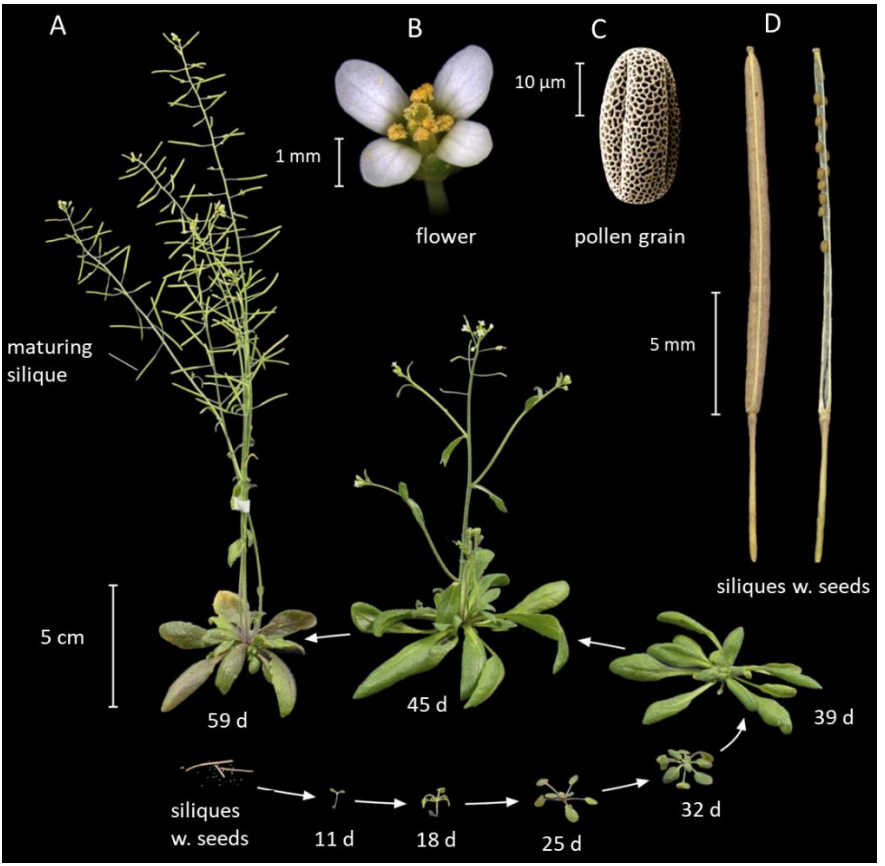

Figure 7: *Arabidopsis thaliana*. (A) *A. thaliana* at different stages of its life cycle. (B) *A. thaliana* flower (C) pollen grain (scanning electron micrograph) and (D) mature siliques (seed pods; left: closed; right: open with a few remaining unshattered seeds) (modified from Krämer, 2015).

1.3 Uptake of PLGA NPs in plant pathogenic fungi: is it a sustainable strategy for pest management?

Fungi have developed a multitude of strategies to colonize plants, and these interactions result in a wide spectrum of consequences ranging from beneficial interactions to death of the host. Regarding plant pathogens, fungi represent probably the most diversified group of ecologically and economically relevant threats. The plant pathogen fungi belong mainly to the phyla Ascomycota and Basidiomycota. Fungal infections cause a wide spectrum of disease symptoms. Conventionally, fungal plant pathogens are classified into two main groups: biotrophic pathogens, which form intimate interactions with plants and can persist in and use living tissues (biotrophs), and necrotrophic pathogens, which kill the tissue to draw out nutrients (necrotrophs). In addition to these two groups, there are hemibiotrophic pathogens, which start as biotrophs and then switch to become necrotrophs (Doehlemann et al., 2017). Plant pathogenic fungi have been a destructive threat over the history of agriculture. Some of these include *Botrytis cinerea*, which is responsible for “gray mould" (Bolívar-Anillo et al., 2020); and *Aspergillus* species that are not considered primary causes of plant diseases but are found as opportunistic storage moulds (Varga et al., 2007). Even if in modern

agriculture most fungal pathogens can principally be controlled by modern crop management, massive outbreaks still occur with devastating yield losses. New sustainable strategies to control plant pathogenic fungi in agriculture is necessary. Some studies in which nanoformulates have been used to control harmful fungi is reported in chapters 4 and 5. *B. cinerea* and *Penicillium expansum* can be significantly inhibited by zinc oxide nanoparticles (He et al., 2011); NPs self-assembled from fungicide fenhexamid and polyhexamethylene biguanide have shown high antimicrobial activity against *B. cinerea*, and *Sclerotinia sclerotiorum* (Tang et al., 2021); *Aspergillus niger* is more susceptible to carvacrol and thymol essential oils loaded into mesoporous silica nanoparticles (Bernardos et al., 2015); and cyazofamid encapsulated in PLGA NPs inhibited *Phytophthora infestans* zoospore release and reduced tomato leaf infection (Fukamachi et al., 2019).

1.3.1 *Botrytis cinerea*

Botrytis cinerea (Fig. 8) is a necrotrophic fungus and is considered the second most important plant pathogen in the world, making it one of the most studied fungal phytopathogens (Dean et al., 2012). It causes diseases known as ‘‘grey mould’’ which are responsible for considerable economic damage (Bolívar-Anillo et al., 2020). This

parasite attacks the green and particularly rich in water tissues, but not the lignified ones (Coertze et al., 2001). The infection appears as chlorotic spots that progressively become brown and develops necrosis. Leaf infection is characterized by the typical grey mould; on shoots, brownish areas appear with necrotic lesions and longitudinal striations. *B. cinerea* germination occurs in a temperature ranging between 5 and 30 °C, with an optimum of about 15 °C, after 15 hours of wetting. In fact, prolonged rain and high relative humidity are the ideal conditions for the development of this pathogen (Zitter, 2005).

B. cinerea has a broad host range that causes severe pre- and post-harvest losses, so it has an evident global impact on plants and plant products. For instance, *B. cinerea* infect grape inflorescences at flowering stages (beginning, full, and end of flowering) (Ciliberti et al., 2015). Similarly, in blueberries, flowers are more susceptible from preflowering to full bloom (Abbey et al., 2019). Although flower infection on the field is significant, *B. cinerea* is the most important postharvest pathogen of table grapes because of the massive economic losses due to berry wilt, rot and biochemical alteration that reduce the quality of wine (Abbey et al., 2019).

Figure 8: *Botrytis cinerea*, etiological agent of gray mold. A) Conidia of *B. cinerea*, B) scanning electron micrograph of *B. cinerea* infection on a leaf C) gray mold on *V. vinifera* bunch.
(Figure source: https://www.microbiologiaitalia.it/micologia/botrytis-cinerea-la-muffa-nobile-e-i-vini-botritizzati/;
https://www.sciencephoto.com/media/14714/view/grey-mould-sem;
https://it.wikipedia.org/wiki/Botrytis_cinerea)

1.3.2 *Aspergillus* section *Nigri*

Black aspergilli (*Aspergillus* section *Nigri*) include 28 accepted species, among them, *Aspergillus niger*, *A. tubingensis*, *A. heteromorphus*, *A. ellipticus*, *A. carbonarius*, *A. brasiliensis*, *A. japonicus* and *A. aculeatus*. *Aspergillus* species are mostly found as opportunistic storage molds, although they are not considered primary causes of plant diseases. Several agricultural products, including grape-derived products, coffee, and cocoa (Varga et al., 2007), are defiled by mycotoxins from their presence, the most important of which are

ochratoxin A and aflatoxins (Perrone and Gallo, 2017). Different species are frequent in vineyards and are often associated with bunch rot. For example, *A. niger* is the main cause of *Aspergillus* rot in grapes before harvest and also *A. brasiliensis* had been isolated from grapes. The ochratoxin A producted by *A. carbonarius* and *A. niger* has been detected in grapes and grape products causing substantial economic loss (Leong et al., 2004) and having a negative impact on human health. Some *Aspergillus* species, mainly *A. flavus*, *A. brasiliensis* and *A. niger*, have long been noted as important pathogens in ocular infections, especially keratitis (Makijandan et al., 2010) and *A. niger* and *A. brasiliensis* were considered the main *Aspergillus* species that causes otomycosis (Sarvestani et al., 2022). For these reasons, it is indispensable to find a strategy to successfully combat Black Aspergilli infections.

1.3.3 Antifungal compounds loaded in NPs to be used against pathogenic fungi

1.3.3.1 Fluopyram and pterostilbene

In 2010, Bayer Crop Science introduced Fluopyram, a new pyridinylethylbenzamide fungicide. Fluopyram is highly efficacious in controlling a wide variety of pathogens (*B. cinerea*, *Sclerotinia spp*, *Monilia spp*) for more than 70 crops, including vines and table grapes,

vegetables and field crops, pome, and stone fruits (Zhang et al., 2014). Fluopyram has been registered in many countries including China, USA, and Canada, and it is widely used due to its high successful. This fungicide has broad-spectrum activity because it inhibits the ubiquitous enzyme succinate dehydrogenase (SDH), which is a key element of mitochondrial electron transport in fungal pathogens' tricarboxylic acid cycle (Avenot et al., 2014). Globally, over-application of fungicides causes food safety concerns and ecological risks despite offsetting yield loss (Wei et al., 2016). The LD50 value of fluopyram for mammals ranked it as a low toxic compound, but it is also highly endocrine disrupting (EDC) causing side effects on human and wildlife endocrine systems at trace levels (Skolness et al., 2011). Recent research has also found that this fungicide alters soil microbial diversity, resulting in poor soil health (Zhang et al., 2014). Due to the imbalance of the associated agricultural ecosystem, excessive and constant application of fluopyram may pose a threat to human health (Wei et al., 2016). An innovative solution to reduce the risks caused by excessive application of fluopyram in agriculture could be the delivery of this pesticide through nanoformulates. *In vitro* fungal tests revealed that fluopyram-loaded nanofibers inhibited fungal growth of *Alternaria linearіae* (Pirzada et al., 2020). However, to date, few studies on the administration of this pesticide in nanoformulation are available.

Currently, numerous studies are directed in the search for natural bioactive compounds that counteract the spread of fungal plant

pathogens with reduced harm to humans and the environment, these include pterostilbene. Plant extracts have traditionally been used for the treatment of several diseases due to their various medicinal activities, such as anti-proliferative, antifungal, antimicrobial, anti-inflammatory, anti-androgenic, antioxidant, and others (Simonetti et al., 2018).

Roots, leaves, stems, flowers, and fruits of medicinal plants are used in Ayurvedic medicine as well as European, Asiatic and Russian, and folk medicine to treat different infections caused by fungi, bacteria, virus, parasite, as well as metabolic disorders (Chuang et al., 2007). Plant extracts contain a multitude of biologically active molecules of pharmaceutical interest, but only a small percentage of plants have been explored for their antifungal activity. Pterostilbene (PTE; trans-3,5-dimethoxy-4′ -hydroxystilbene), a trans-stilbene compound, is a methylated derivative of resveratrol which has a higher, more stable bioavailability than resveratrol (Zhao et al., 2021). PTE has a number of biological activities, such as antioxidation, lowering blood lipids and blood glucose, fungi inhibition and anti-tumorigenesis (Tsai et al., 2017). In addition, it has a variety of preventive and therapeutic effects on cardiovascular diseases, neurological diseases, metabolic diseases and blood diseases (Liu et al., 2019). Li et al., (2014) reported that PTB has a strong *in vitro* and *in vivo* activity against *C. albicans* biofilm. They also demonstrated the antifungal activity of PTB against plant fungal pathogens, such as *Phomopsis viticola, P. obscurans*, and *B. cinerea*. Simonetti et al., (2019) demonstrated that Anti-*Candida*

biofilm activity of PTB loaded PLGA NPs was higher than free formulations. Other information about the effect of PTB in plants can be found in chapters 4 and 5. PTB showed high bioavailability and no toxicity and for these reasons it is a promising compound for use in agriculture against pathogenic fungi. Nanotechnology combined with synthetic or natural compounds (e.g., fluopyram or pterostilbene, respectively) could offer an intelligent solution for crop disease control. It has been shown that compared with free oils, chitosan nanoparticles loaded with clove oil exhibited improved performance against *A. niger* isolated from spoiled pomegranates (Hasheminejad et al., 2019). Compared to pure fungicide, chitosan-pectin nanoparticles containing carbendazim were more effective against *Fusarium oxysporum* and *Aspergillus parasiticus* (Kumar et al., 2017); Polyethylene glycol (PEG) nanoparticles encapsulated with azomethine enhanced *in vitro* inhibitory activities against *Sclerotium rolfsii*, *Rhizoctonia bataticola*, and *Rhizoctonia solani*. (Mondal et al. 2017). Nanotechnology could increase agrochemical efficiency and reduce the indiscriminate use of conventional pesticides through their controlled delivery, protecting the encapsulated active ingredients from premature degradation or increasing their efficacy for a longer period.

References

Abbey, J. A., Percival, D., Abbey, L., Asiedu, S. K., Prithiviraj, B., & Schilder, A. (2019). Biofungicides as alternative to synthetic fungicide control of grey mould (*Botrytis cinerea*)–prospects and challenges. *Biocontrol Science and Technology*, *29*(3), 207-228.

Avenot, H. F., Van Den Biggelaar, H., Morgan, D. P., Moral, J., Joosten, M. H. A. J., & Michailides, T. J. (2014). Sensitivities of baseline isolates and boscalid-resistant mutants of *Alternaria alternata* from pistachio to fluopyram, penthiopyrad, and fluxapyroxad. *Plant Disease*, 98(2), 197-205.

Bernardos, A., Marina, T., Žáček, P., Pérez-Esteve, É., Martínez-Mañez, R., Lhotka, M., ... & Klouček, P. (2015). Antifungal effect of essential oil components against *Aspergillus niger* when loaded into silica mesoporous supports. *Journal of the Science of Food and Agriculture*, 95(14), 2824-2831.

Bolívar-Anillo, H. J., Garrido, C., & Collado, I. G. (2020). Endophytic microorganisms for biocontrol of the phytopathogenic fungus *Botrytis cinerea*. *Phytochemistry Reviews*, *19*(3), 721-740.

Brock, D. A., Douglas T. E., Queller, D. C., Strassmann, J. E. (2011). Primitive agriculture in a social amoeba. *Nature* 469, 393-398.

Chuang, P. H., Lee, C. W., Chou, J. Y., Murugan, M., Shieh, B. J., & Chen, H. M. (2007). Anti-fungal activity of crude extracts and essential oil of *Moringa oleifera* Lam. *Bioresource Technology*, 98(1), 232-236.

Ciliberti, N., Fermaud, M., Languasco, L., & Rossi, V. (2015). Influence of fungal strain, temperature, and wetness duration on infection of grapevine inflorescences and young berry clusters by *Botrytis cinerea*. *Phytopathology*, 105(3), 325-333.

Coertze, S., Holz, G., & Sadie, A. (2001). Germination and establishment of infection on grape berries by single airborne conidia of *Botrytis cinerea*. *Plant Disease*, 85(6), 668-677.

Dean, R., Van Kan, J. A., Pretorius, Z. A., Hammond-Kosack, K. E., Di Pietro, A., Spanu, P. D., ... & Foster, G. D. (2012). The Top 10 fungal pathogens in molecular plant patholcoerzeogy. *Molecular Plant Pathology*, 13(4), 414-430.

Doehlemann, G., Ökmen, B., Zhu, W., & Sharon, A. (2017). Plant pathogenic fungi. *Microbiology Spectrum*, *5*(1), 5-1.

Doherty, G. J., & McMahon, H. T. (2009). Mechanisms of endocytosis. *Annual Review of Biochemistry*, 78, 857-902.

Elmer, W. H., White J. C. (2018). The future of nanotechnology in plant pathology. *Annual Review of Phytopathology*, 56, 111-133.

Etxeberria, E., Gonzalez, P., Bhattacharya, P., Sharma, P., & Ke, P. C. (2016). Determining the size exclusion for nanoparticles in citrus leaves. *Hort Science*, 51(6), 732-737.

Fan, L., Li, R., Pan, J., Ding, Z., & Lin, J. (2015). Endocytosis and its regulation in plants. *Trends in Plant Science*, 20(6), 388-397.

Farnoud, A. M., & Nazemidashtarjandi, S. (2019). Emerging investigator series: interactions of engineered nanomaterials with the cell plasma membrane; what have we learned from membrane models?. *Environmental Science: Nano*, 6(1), 13-40.

Fincheira, P., Tortella, G., Duran, N., Seabra, A. B., & Rubilar, O. (2020). Current applications of nanotechnology to develop plant growth inducer agents as an innovation strategy. *Critical reviews in biotechnology*, *40*(1), 15-30.

Fraceto, L. F., Grillo, R., de Medeiros, G. A., Scognamiglio, V., Rea, G., and Bartolucci, C. (2016). Nanotechnology in agriculture: which innovation potential does it have? *Frontiers in Environmental Science*, 4:20.

Fukamachi, K., Konishi, Y., & Nomura, T. (2019). Disease control of Phytophthora infestans using cyazofamid encapsulated in poly lactic-co-glycolic acid (PLGA) nanoparticles. *Colloids and Surfaces A: Physicochemical and Engineering Aspects*, 577, 315-322.

Hasheminejad, N., Khodaiyan, F., & Safari, M. (2019). Improving the antifungal activity of clove essential oil encapsulated by chitosan nanoparticles. *Food chemistry*, 275, 113-122.

Haucke, V., & Kozlov, M. M. (2018). Membrane remodeling in clathrin-mediated endocytosis. *Journal of Cell Science*, 131(17), jcs216812.

He, L., Liu, Y., Mustapha, A., & Lin, M. (2011). Antifungal activity of zinc oxide nanoparticles against *Botrytis cinerea* and *Penicillium expansum*. *Microbiological research*, 166(3), 207-215.

Hemalatha, A., & Mayor, S. (2019). Recent advances in clathrin-independent endocytosis. F1000Research, 8.

Jan, A., Pirzadah, T. B., & Malik, B. (2020). Nanotechnology: an innovative tool to enhance crop production. *In Nanobiotechnology in Agriculture* (pp. 163-170). Springer, Cham.

Judy, J. D., Unrine, J. M., Rao, W., Wirick, S., and Bertsch, P. M. (2012). Bioavailability of gold nanomaterials to plants: importance of particle size and surface coating. *Environmental Science & Technology*, 46, 8467–8474. doi: 10.1021/es3019397.

Krämer, U. (2015). Planting molecular functions in an ecological context with *Arabidopsis thaliana*. Elife 4.

Kumar, S., Kumar, D., & Dilbaghi, N. (2017). Preparation, characterization, and bio-efficacy evaluation of controlled release carbendazim-loaded polymeric nanoparticles. *Environmental Science and Pollution Research*, *24*(1), 926-937.

Leong, S. L., Hocking, A. D., & Pitt, J. I. (2004). Occurrence of fruit rot fungi (*Aspergillus* section *Nigri*) on some drying varieties of irrigated grapes. *Australian Journal of Grape and Wine Research*, 10(1), 83-88.

Li, D. D., Zhao, L. X., Mylonakis, E., Hu, G. H., Zou, Y., Huang, T. K., ... & Jiang, Y. Y. (2014). *In vitro* and *in vivo* activities of pterostilbene against *Candida albicans* biofilms. *Antimicrobial Agents and Chemotherapy*, 58(4), 2344-2355.

Li, R., Raikhel, N. V., & Hicks, G. R. (2012). Chemical effectors of plant endocytosis and endomembrane trafficking. *Endocytosis in plants* (pp. 37-61). Springer, Berlin, Heidelberg.

Liu, H., Wu, X., Luo, J., Wang, X., Guo, H., Feng, D., ... & Qu, Y. (2019). Pterostilbene attenuates astrocytic inflammation and neuronal oxidative injury after ischemia-reperfusion by inhibiting NF-κB phosphorylation. *Frontiers in Immunology*, 10, 2408.

Lv, J., Christie, P., & Zhang, S. (2019). Uptake, translocation, and transformation of metal-based nanoparticles in plants: recent advances and methodological challenges. *Environmental Science: Nano*, 6(1), 41-59.

Macia, E., Ehrlich, M., Massol, R., Boucrot, E., Brunner, C., & Kirchhausen, T. (2006). Dynasore, a cell-permeable inhibitor of dynamin. *Developmental Cell*, 10(6), 839-850.

Makadia, H. K., Seigel, S. J. (2011) Poly Lactic-co-Glycolic Acid (PLGA) as Biodegradable Controlled Drug Delivery Carrier. *Polymers*, 3, 1377-1397.

Makaraci, P., & Kim, K. (2018). trans-Golgi network-bound cargo traffic. *European Journal of Cell Biology*, 97(3), 137-149.

Malinsky, J., Opekarová, M., Grossmann, G., & Tanner, W. (2013). Membrane microdomains, rafts, and detergent-resistant membranes in plants and fungi. *Annual Review of Plant Biology*, 64, 501-529.

Manikandan, P., Varga, J., Kocsubé, S., Revathi, R., Anita, R., Dóczi, I., ... & Kredics, L. (2010). Keratitis caused by the recently described new species *Aspergillus brasiliensis*: two case reports. *Journal of Medical Case Reports*, 4(1), 1-4.

Manzanares, D., & Ceña, V. (2020). Endocytosis: the nanoparticle and submicron nanocompounds gateway into the cell. *Pharmaceutics*, 12(4), 371.

Mayor, S., & Pagano, R. E. (2007). Pathways of clathrin-independent endocytosis. *Nature Reviews Molecular Cell Biology*, 8(8), 603-612.

McKnight, U. S., Rasmussen, J. J., Kronvang, B., Binning, P. J., Bjerg, P. L. (2015) Sources, occurrence and predicted aquatic impact of legacy and contemporary pesticides in streams. *Environmental Pollution*, 200, 64-76.

Meinke, D. W., Cherry, J. M., Dean, C., Rounsley, S. D., & Koornneef, M. (1998). *Arabidopsis thaliana*: a model plant for genome analysis. *Science*, *282*(5389), 662-682.

Mondal, P., Kumar, R., & Gogoi, R. (2017). Azomethine based nano-chemicals: development, *in vitro* and *in vivo* fungicidal evaluation against *Sclerotium rolfsii*, *Rhizoctonia bataticola* and *Rhizoctonia solani*. *Bioorganic Chemistry*, 70, 153-162.

Palocci, C., Valletta, A., Chronopoulou, L., Donati, L., Bramosanti, M., Brasili, E., ... & Pasqua, G. (2017). Endocytic pathways involved in PLGA nanoparticle uptake by grapevine cells and role of cell wall and membrane in size selection. *Plant Cell Reports*, 36(12), 1917-1928.

Pascoli, M., Lopes-Oliveira, P. J., Fraceto, L. F., Seabra, A. B., & Oliveira, H. C. (2018). State of the art of polymeric nanoparticles as carrier systems with agricultural applications: a minireview. *Energy, Ecology and Environment*, 3(3), 137-148.

Pérez-de-Luque, A. (2017). Interaction of nanomaterials with plants: what do we need for real applications in agriculture?. *Frontiers in Environmental Science*, *5*, 12.

Pérez-de-Luque, A., & Hermosín, C. (2013). Nanotechnology and its use in agriculture. *Bio-Nanotechnology: A Revolution in Food, Biomedical and Health Sciences*, 383–398.

Perrone, G., & Gallo, A. (2017). *Aspergillus* species and their associated mycotoxins. *Mycotoxigenic Fungi*, 33-49.

Pirzada, T., de Farias, B. V., Mathew, R., Guenther, R. H., Byrd, M. V., Sit, T. L., ... & Khan, S. A. (2020). Recent advances in biodegradable matrices for active ingredient release in crop protection: Towards attaining sustainability in agriculture. *Current opinion in colloid & interface science*, *48*, 121-136.

Prasad, R., Bhattacharyya, A., & Nguyen, Q. D. (2017). Nanotechnology in sustainable agriculture: recent developments, challenges, and perspectives. *Frontiers in microbiology*, *8*, 1014.

Qi, X., Pleskot, R., Irani, N. G., & Van Damme, D. (2018). Meeting report–Cellular gateways: expanding the role of endocytosis in plant development. *Journal of Cell Science*, 131(17), jcs222604.

Raliya, R., Franke, C., Chavalmane, S., Nair, R., Reed, N., and Biswas, P. (2016). Quantitative understanding of nanoparticle uptake in watermelon plants. *Frontier in Plant Science*, 7:1288. doi: 10.3389/fpls.2016.01288.

Roberts, A. G., and Oparka, K. J. (2003). Plasmodesmata and the control of symplastic transport. *Plant Cell Environment*, 26, 103–124.

Sanzari, I., Leone, A., & Ambrosone, A. (2019). Nanotechnology in plant science: to make a long story short. *Frontiers in Bioengineering and Biotechnology*, 7, 120.

Sarvestani, H. K., Seifi, A., Falahatinejad, M., & Mahmoudi, S. (2022). Black aspergilli as causes of otomycosis in the era of molecular diagnostics, a mini-review. *Journal of Medical Mycology*, 32(2), 101240.

Sathiyabama, M., & Manikandan, A. (2018). Application of copper-chitosan nanoparticles stimulate growth and induce resistance in Finger Millet (*Eleusine coracana Gaertn*.) plants against blast disease. *Journal of Agricultural and Food Chemistry*, 66, 1784-1790.

Sattelmacher, B. (2001). The apoplast and its significance for plant mineral nutrition. *New Phytologist*. 149, 167–192.

Simonetti, G., Palocci, C., Valletta, A., Kolesova, O., Chronopoulou, L., Donati, L., ... & Pasqua, G. (2019). Anti-*Candida* biofilm activity of pterostilbene or crude extract from non-fermented grape pomace entrapped in biopolymeric nanoparticles. *Molecules*, 24(11), 2070.

Simonetti, G., Valletta, A., Kolesova, O., & Pasqua, G. (2018). Plant products with antifungal activity: From field to biotechnology strategies. *Natural Products as Source of Molecules with Therapeutic Potential* (pp. 35-71). Springer, Cham.

Skolness, S. Y., Durhan, E. J., Garcia-Reyero, N., Jensen, K. M., Kahl, M. D., Makynen, E. A., ... & Ankley, G. T. (2011). Effects of a short-term exposure to the fungicide prochloraz on endocrine function and gene expression in female fathead minnows (*Pimephales promelas*). *Aquatic Toxicology*, 103(3-4), 170-178.

Stevanovic, M., & Uskokovic, D. (2009) Poly(lactide-co-glycolide)-based micro and nanoparticles for the controlled drug delivery of vitamins. *Current Nanoscience* 5, 1-14.

Su, S., & Kang, P. M. (2020). Systemic review of biodegradable nanomaterials in nanomedicine. *Nanomaterials*, 10(4), 656.

Sun, D., Hussain, H. I., Yi, Z., Siegele, R., Cresswell, T., Kong, L., et al. (2014). Uptake and cellular distribution, in four plant species, of fluorescently labeled mesoporous silica nanoparticles. *Plant Cell Reports*. 33, 1389–1402.

Tang, G., Tian, Y., Niu, J., Tang, J., Yang, J., Gao, Y., ... & Cao, Y. (2021). Development of carrier-free self-assembled nanoparticles based on fenhexamid and polyhexamethylene biguanide for sustainable plant disease management. *Green Chemistry*, 23(6), 2531-2540.

Tripathi, D. K., Singh, S., Singh, S., Pandey, R., Singh, V. P., Sharma, N. C., ... & Chauhan, D. K. (2017). An overview on manufactured nanoparticles in plants: uptake, translocation, accumulation and phytotoxicity. *Plant Physiology and Biochemistry*, 110, 2-12.

Tsai, H. Y., Ho, C. T., & Chen, Y. K. (2017). Biological actions and molecular effects of resveratrol, pterostilbene, and 3′-hydroxypterostilbene. *Journal of Food and Drug Analysis*, 25(1), 134-147.

Valletta, A., Chronopoulou, L., Palocci, C., Baldan, B., Donati, L., & Pasqua, G. (2014). Poly (lactic-co-glycolic) acid nanoparticles uptake by *Vitis vinifera* and grapevine-pathogenic fungi. *Journal of Nanoparticle Research*, 16(12), 1-14.

Varga, J., Kocsube, S., Toth, B., Frisvad, J. C., Perrone, G., Susca, A., ... & Samson, R. A. (2007). *Aspergillus brasiliensis* sp. nov., a biseriate black Aspergillus species with world-wide distribution. *International Journal of Systematic and Evolutionary Microbiology*, 57(8), 1925-1932.

Varma, S., & Dey, S. (2021). Cellular uptake pathways of nanoparticles: process of endocytosis and factors affecting their fate. *Current Pharmaceutical Biotechnology*, 3(5), 679-706.

Verma, Y., Singh, S. K., Jatav, H. S., Rajput, V. D., & Minkina, T. (2021). Interaction of zinc oxide nanoparticles with soil: Insights into the chemical and biological properties. *Environmental Geochemistry and Health*, 1-14.

Wang, M., Qu, Y., Hu, D., Niu, T., & Qian, Z. (2021). Nanomedicine applications in treatment of primary central nervous system lymphoma: current state of the art. *Journal of Biomedical Nanotechnology*, 17(8), 1459-1485.

Wang, P., Lombi, E., Zhao, F. J., & Kopittke, P. M. (2016). Nanotechnology: a new opportunity in plant sciences. *Trends in Plant Science, 21*(8), 699-712.

Wei, P., Liu, Y., Li, W., Qian, Y., Nie, Y., Kim, D., & Wang, M. (2016). Metabolic and dynamic profiling for risk assessment of fluopyram, a

typical phenylamide fungicide widely applied in vegetable ecosystem. *Scientific Reports*, 6(1), 1-12.

Xu, Q., Kambhampati, S. P., & Kannan, R. M. (2013). Nanotechnology approaches for ocular drug delivery. *Middle East African Journal of Ophthalmology*, 20(1), 26.

Zhang, Y., Xu, J., Dong, F., Liu, X., Wu, X., & Zheng, Y. (2014). Response of microbial community to a new fungicide fluopyram in the silty-loam agricultural soil. *Ecotoxicology and Environmental Safety*, 108, 273-280.

Zhao, X., Shi, A., Ma, Q., Yan, X., Bian, L., Zhang, P., & Wu, J. (2021). Nanoparticles prepared from pterostilbene reduce blood glucose and improve diabetes complications. *Journal of Nanobiotechnology*, 19(1), 1-18.

Zitter, S. M. (2005). The biology and control of *Botrytis* bunch rot (*Botrytis cinerea*) in grapevines: ontogenic, physical, and cultural factors affecting initiation and spread of the disease. *Cornell University*.

Chapter 2: Project aims

In this PhD project, PLGA NPs were used for a dual purpose. The first one was to clarify the mechanisms of internalization of PLGA NPs, sorting and targeting into plants and fungi according to morphology and physico-chemical properties of NPs. The second one was to use NPs as vectors for the delivery of antifungals directed against plant pathogenic fungi that cause immeasurable economic damage to agriculture every year.

The main objectives of this research are summarized as follows:

1) to study the mechanism of endocytosis of PLGA nanoparticles (PLGA NPs) in plants, *A. thaliana* cultured cells and seedlings have been used as model systems. In plant cells the major route for the internalization of PLGA NPs seems to be clathrin-mediated endocytosis, which starts with the formation of clathrin-coated membrane invaginations, also termed clathrin-coated pit. An essential protein for vesicle detachment is dynamin, a GTPase protein. However, in addition to clathrin-dependent endocytosis pathway, emerging researches have revealed several clathrin-independent pathways in plant cells, not all dependent on dynamin. To investigate the uptake of NPs, a fluorescent molecule, coumarin-6, was selected to be loaded into the NPs and followed in the pathway by microscopy. Briefly, 30 nm NPs were synthesized by the microfluidic method, loaded with the coumarin-6 fluorescent probe (Cu6-PLGA NPs), administered to plant

cultured cells and seedlings, and observed by confocal microscopy at different times after administration. In addition, to investigate the mechanism/s of PLGA NPs uptake, the dynamine inhibitor Dynasore was tested on *Arabidopsis* cultured cells and seedling roots before the administration of NPs (manuscript in preparation).

2) The second objective is the study PLGA NPs uptake in *B. cinerea* and *Aspergillus* section *Nigri* and the use of natural or synthetic compounds antifungal activity entrapped in PLGA NPs against *B. cinerea* conidia and mycelium and *A. brasiliensis* biofilm.
In order to examine the nanoparticle uptake, *B. cinerea* conidia and mycelium and *A. brasiliensis* conidia mycelium and biofilm were treated with PLGA NPs uploaded with high fluorescent probe coumarin-6 (Cu6-PLGA NPs) and microscopically analyzed using the ApoTome fluorescence microscope. In order to examine whether PLGA NPs could be used as an attractive strategy for integrating plant disease management, pterostilbene and fluopyram were encapsulated in PLGA NPs and administered at different stages of the development of *B. cinerea* to investigate their antimicrobial activity. In addition, pterostilbene encapsulated in PLGA NPs was tested for antifungal ability against *A. brasiliensis* biofilm. The results of this research led to the publication of two papers (chapters 4 and 5).

Chapter 3:

Biopolymeric PLGA nanoparticles uptake in *Arabidopsis* cultured cells and plantlets

De Angelis Giulia, Badiali Camilla, Possenti Marco, Chronopoulou Laura, Palocci Cleofe, D'Angeli Simone, Brasili Elisa*, Pasqua Gabriella.

Introduction

Biopolymeric nanoparticles for the delivery of bioactive substances are an increasingly promising strategy in the agronomic field (Fortunati et al., 2019). The use of biodegradable Poly lactic-co-glycolic acid-Nanoparticles (PLGA NPs) has shown great potential as drug delivery carrier due to their proven biocompatibility and biodegradability (Makadia and Siegel, 2011). Nevertheless, few information is available on the absorption, uptake, moving and interaction processes of nanoparticles in plant systems (Pérez-de-Luque, 2017). In addition, tracking of these systems inside plants requires complex probe tagging strategies (Proença et al., 2022). Most of the studies on PLGA NPs have been carried out on mammalian and human systems and few information is available about the PLGA NPs uptake plant cells (Valletta et al., 2014; Palocci et al., 2017; Chronopoulou et al., 2019). Transmission Electron Microscopy (TEM) analyses carried out on

grapevine cells suggest that PLGA NPs are internalized by endocytic vesicles (Valletta et al. 2014).

The most investigated and validated mechanism for the cargo molecules internalization in cells seemed to be clathrin-mediated endocytosis (CME), however the endocytic pathway in plants is poorly characterized and its hypothesized mechanism is largely inferred from studies in mammalian and yeast systems, where CME components are highly conserved (Narasimhan et al., 2020). The process of CME begins with the formation of clathrin-coated membrane invaginations, also known as clathrin-coated pits. An essential protein for vesicle detachment is dynamin, a GTPase protein (Fan et al., 2015). Nonetheless, in addition to the clathrin-dependent endocytosis pathway, different researches have revealed several clathrin-independent pathways in plant cells, not all dependent on dynamin (Mayor and Pagano 2007). Clathrin-independent pathways have been implicated in studies of tobacco (*Nicotiana tabacum*) cells grown in suspension cultures (Onelli et al., 2008) and in epidermal cells of *Arabidopsis* root (Li et al., 2012), but neither of these pathways has been well characterized with respect to the identity of cargo handled or the endocytic mechanisms below the epidermis. Through fluorescence microscopy, it has been established that PLGA NPs can enter grapevine leaf tissues through stomata openings and that they can be absorbed by the roots and transported to the shoot through vascular tissues. In addition, in grapevine, cells PLGA NP-containing vesicles were

observed exclusively in the cytoplasm, the absence of PLGA NPs in the vacuoles suggested that the mechanism clathrin-independent endocytosis might have been the main internalization pathway (Valletta et al., 2014). The results obtained by administering PLGA NPs to grapevine cells, after treatment with clathrin-dependent endocytosis inhibitors ikarugamycin and wortmannin, led to the hypothesis that PLGA NPs uptake largely follows the clathrin-independent endocytic route (Palocci et al., 2017). But the question remained open, because these inhibitors are not chemical modulators of protein trafficking components involved in early steps of CME (Mishev et al., 2013). Ikarugamycin is an antibiotic with antiprotozoal activity that exhibited strong cytotoxicity (Minamidate et al., 2021). Ikarugamycin caused redistribution of the clathrin heavy chain and the adaptor protein 2 (Elkin et al., 2016), however, its precise mechanism of action remains unclear. Wortmannin is an inhibitor of phosphatidylinositol-3 kinase a component essential for the formation of internal vesicles (Robinson et al., 2008). Treatment with wortmannin, leads to a perturbation of receptor recycling in yeasts and mammals (Arighi et al., 2004). Further studies about endocytic mechanisms in plant cells and tissues are indispensable to shed light on the uptake of molecules in plants.

It's important to highlight that not all the clathrin-independent pathways require dynamin activity. Differently, the clathrin-dependent pathway is closely linked to the activity of dynamin (Fan et al., 2015). In 2006, Macia et al., screened about 16,000 small molecules identifying

Dynasore, that interferes *in vitro* with the GTPase activity of dynamin1, dynamin2, and Drp1, the mitochondrial dynamin, but not of other small GTPases. Dynasore acts as a potent inhibitor of endocytic pathways known to depend on dynamin by blocking the GTPase activity of dynamin by preventing vesicles from detaching from the membrane and rapidly blocking coated vesicle formation in HeLa cells transferrin uptake (Macia et al., 2006).

In the present study PLGA NPs uptake has been carried out in *A. thaliana* cultured cells and in 10-day-old plantlets. PLGA NPs were loaded with the fluorescent probe coumarin6 (Cu6-PLGA NPs) and administered in aqueous suspension to cells and to *A. thaliana* seedling roots. To clarify whether Cu6-PLGA NPs penetrated plant cells through the dynamin-like-dependent or dynamin-like-independent endocytic pathway, the inhibitor Dynasore was used both in experiments in cultured cells and in plant roots. In addition, we investigated the possible mechanisms of PLGA NPs translocation at a distance.

Materials and methods

PLGA NPs preparation

As reported previously (Chronopoulou et al., 2014), microfluidic preparation of PLGA NPs with a diameter of 30 nm, empty or entrapping coumarin 6 was performed. At a flow rate of 50 μL min^{-1},

PLGA (2 mg mL^{-1}) was dissolved in acetone and injected into the middle channel of a microfluidic reactor. For the preparation of fluorescent NPs, Coumarin 6 was added in a ratio of 1:50 with respect to PLGA. Water was injected in the two side channels of the reactor at a flow rate of 2000 µL min^{-1}. The dispersed and continuous phase meet in a cross junction and nanoprecipitation occurs in the successive outlet mixing channel, at whose end PLGA-based NPs can be recovered. Under reduced pressure, organic phase was eliminated, and PLGA-based NPs were stored at 4 °C until used.

Plant growth conditions

Arabidopsis thaliana (L.) Heynh var. Columbia (Col-0) seeds were used the experiments. Plantlets were vertically grown in petri dishes and in aseptic conditions for 10 days on solid Murashige and Skoog medium in a controlled environment chamber under a photoperiod of 16/8 h (light/dark) and at 26 ± 1 °C (photon flux density, 70 µmol m^{-2} s^{-1}).

Cell suspension cultures

According to May et al., 1993, callus formation was induced by placing stem explants on agarised medium (Gamborg B5, Glc 2% [w/v], agar 0.8% [w/v], Mes 0.5 g/L, 2,4-D 0.5 mg/L, kinetin 0.05 mg/L), maintained in a growth chamber at 26 ± 1 °C under continuous darkness

and subcultured every 25 days. Suspension cultures were obtained by inoculation of 300 mg of rapidly dividing, friable, white callus into 50 mL of Murashige and Skoog medium containing 0.5 mg/L naphthaleneacetic acid, 0.05 mg/L kinetin, 3% (w/v) sucrose, and incubated on a rotary shaker at 100 rpm (May et al., 1993). Cell suspensions were subcultured every 25 days for 3 months by decanting 60% of the medium and replacing it with fresh medium. The pH of all media was adjusted to 5.6 by adding 1N NaOH before autoclaving at a temperature of 121 °C and 1 atm for 20 min.

Uptake experiments in cultured cells and plantlet roots

PLGA NPs in aqueous suspension were sonicated for 30 minutes before adding them to the *A. thaliana* Col-0 cell suspensions and plantlets.

For the culture cell experiments, Cu6-PLGA NPs were added to the liquid culture media at a final concentration of 15 mg L^{-1} (at day 10 of subculture) incubating them under continuous darkness on a rotary shaker at 100 rpm. The observations were carried out at different times after Cu6-PLGA NPs supplementation: 0 min, 10 min, 30min, 1h, 2h, 24h.

Dynasore (purchased from Sigma-Aldrich, Milan, Italy) was added to cultured cells to a final concentration of 80 or 160 μM to investigate whether the Cu6-PLGA NPs endocytic process is prevented from this inhibitor. Cells were incubated with Dynasore for 10 or 30 min and then Cu6-PLGA NPs were added to cell suspensions (15 mg L^{-1} final

concentration) and cells were observed at confocal microscope 10 minutes later.

For the root uptake experiments, *A. thaliana* plantlets were transferred from agarized medium to multiwell plate (6 plates) filled with 5 ml of liquid culture media, being careful not to damage the roots, and Cu6-PLGA NPs were added to the medium at a final concentration of 15 mg L^{-1} under continuous darkness on a rotary shaker at 100 rpm. To evaluate Cu6-PLGA NPs absorption, confocal microscopy observations were carried out at 0 min, 10 min, 30 min, 80 min, 5 h. To investigate the root endocytic uptake of NPs, Dynasore was added to plantlets to a final concentration of 80, 160 or 320 μM. Specifically, plantlets were incubated with Dynasore for 30 min, 60 min and 120 min and then the roots were treated with 15 mg L^{-1} of NPs and were observed at confocal microscope 10 minutes later.

Cytotoxicity test

Propidium iodide water solution (12,5 μg/ml) was used. Plantlet roots treated with different Dynasore concentration and timing, were mounted on microscope slides and root cells viability was assessed by confocal microscopy. Cells were considered nonviable if propidium iodide filled the cytoplasm; cells were considered viable if propidium iodide was excluded. The excitation wavelength of the reader was 530 nm with an emission filter of 620 nm.

NPs translocation analysis

To investigate the translocation of PLGA NPs within the plantlets, 13 days old plantlets showing 1.5/2 cm root length, were transferred from the petri dish into eppendorf. The roots were placed in contact with liquid HF medium. Following one hour of treatment with Cu6-PLGA NPs in liquid culture media (15 mg L^{-1}), the aerial part of the plantlets was excised, placed on a microscope slide, and observed with ApoTome fluorescence microscopy.

Confocal microscopy

In order to investigate the uptake of Cu6-PLGA NPs by cells, differential interference contrast (DIC) and confocal microscopy were used. The analyses were performed on an inverted Z.1 microscope (Zeiss, Germany) equipped with a Zeiss LSM 700 spectral confocal laser scanning unit (Zeiss, Germany). For 6 coumarin detection, a 488 nm, 10 mW solid laser with an emission wavelength of 520 nm was employed, while for propidium iodide detection, a 555 nm, 10 mW solid laser with an emission split at 550 nm/LP 640 was employed.

ApoTome fluorescence microscopy

Image analysis was conducted with an Axio Imager M2 fluorescence microscope equipped with an Apotome 2 module (Zeiss, Germany), a fringe projection module, motorized on the 3 axes, using a FITC filter

(λ excitation BP 455-495 nm; λ emission BP 505-555 nm) for Cu6-PLGA NPs treated cell and roots

Results and Discussion

PLGA NPs uptake in cells and roots

Cu6-PLGA NPs (30 nm) at a concentration of 15 mg L^{-1}, were able to be rapidly internalized by *A. thaliana* cultured cells (**Fig. 1**), as revealed by the small highly fluorescent round bodies (endosomes) and a low diffuse background observed after 10 min by confocal microscopy. At increasing of observation times (30 min), these bodies were coalescing by appearing to be less numerous and greatest. NPs were accumulated in the cytoplasm and seemed to be stable over time: at 24 h from Cu6-PLGA NPs treatment, the fluorescence distribution pattern was similar to the one observed at 60 min. In some cells, at different times, cells with larger spherical bodies were observed as shown in **Fig. 1g**. The treatment with Dynasore, at 80 μM (Macia et al., 2006) or 160 μM for 10 minutes before the addition of 15 mg L^{-1} NPs did not prevent the NPs uptake, as revealed by fluorescence visible in the cytoplasm and in spherical vesicles (**Fig. 1h and i**).

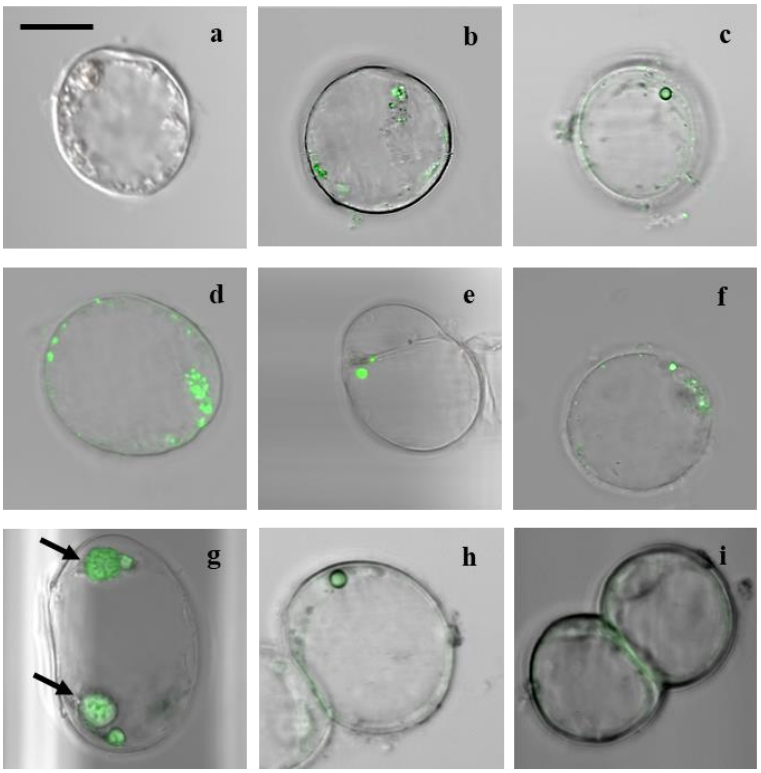

Fig 1. Cell suspension cultures of *A. thaliana* treated with 30 nm NPs and observed at confocal microscope at different times (a: 0 min; b: 10 min; c: 30 min; d: 1 hour; e: 2 hours; f: 24 hours). Fluorescence is localized within spherical bodies. g: arrows indicate big spherical bodies observed in some cells at different times. h; i: *A. thaliana* suspended cells observed by confocal microscopy after treatment with Dynasore at 80 µM (h) or 160 µM (i) for 10 minutes before the addition of 15 mg L^{-1} NPs. Fluorescence in the cytoplasm and vesicles are still visible. Merge (brieght field / fluorescence) images. The scale bar represents 10 µm.

The confocal microscopy analysis of *in vitro A. thaliana* plantlet roots, showed that 15 mg L^{-1} Cu6-PLGA NPs penetrated in the roots in a few minutes after the treatment (**Fig. 2**). In particular, Cu6-PLGA NPs penetrated through the root hairs already 10 min after treatment (**Fig. 2a**), and at longer times (30 and 80 min), fluorescence was visible not only in the root hairs but in almost all cells of the epidermis (**Fig. 2b, 2c and 2d**). Cu6-PLGA NPs remained at the level of the epidermis also after 5 hours (**Fig. 2e**). The treatment with Dynasore at 80 or 160 µM for 30 and 60 minutes before the addition of 15 mg L^{-1} Cu6-PLGA NPs for 10 minutes did not prevent the uptake of NPs observed in the epidermis (**Fig 3a, b, c, d**). Even treating the roots with a higher concentration of Dynasore (320 µM) for 30 and 60 minutes before Cu6-PLGA NPs treatment, intense fluorescence continued to be visible in the root epidermis (**Fig. 4a, b**). Differently, the treatment with 320 µM of Dynasore for a longer time (120 minutes) before the addition of NPs, caused the absence of the fluorescent signal in the root cells (**Fig. 5a**). The cytotoxicity test with propidium iodide showed that the root cells were not viable after 120-minute treatment with Dynasore at the highest concentration (320 µM) (**Fig. 5b)**. Consequently, the absence of fluorescence in the epidermis root cells was not caused by inhibition of Cu6-PLGA NPs uptake but was due to the inability of Cu6-PLGA NPs to enter into the cells since they were dead. It is known that propidium iodide is a membrane-impermeable dye that is generally excluded from viable cells and, conversely, fills the cytoplasm of non-viable cells

(Jones and Senft, 1985). Cytotoxicity test on roots treated with Dynasore at 80 µM for 120 minutes showed that the roots were viable and, after Cu6-PLGA NPs treatment fluorescence was clearly visible in the epidermis (**Fig. 6a and b**). These results showed that Dynasore did not inhibit the uptake of PLGA NPs 30 nm loaded with 6-coumarin suggesting that the internalization of NPs follows the dynamin-independent pathway since the GTPase activity of dynamin, which causes the detachment of the neo-formed endocytic vesicle, was not required.

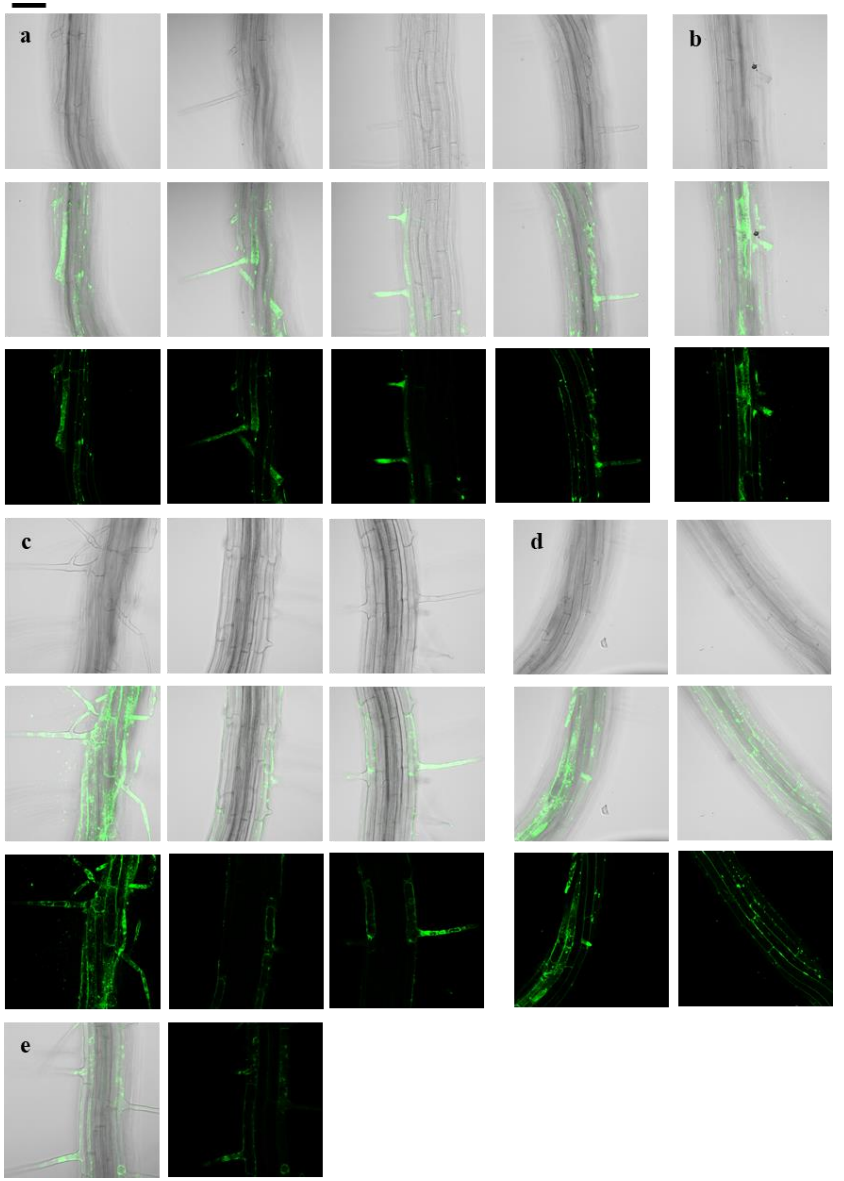
a
b
c
d
e

Fig. 2 *A. thaliana* plantlet roots treated with 30 nm NPs (15 mg L^{-1}) and observed by confocal microscopy at different time of Cu6-PLGA NPs supplementation (10, 30, 80 minutes and 5 hours). Bright Field, Merge (bright field / fluorescence) and fluorescence images. a) *A. thaliana* roots treated for 10 minutes with Cu6-PLGA NPs. Cu6-PLGA NPs penetrated through the root hairs; b) *A. thaliana* roots treated for 30 minutes with Cu6-PLGA NPs; c and d) Two *A. thaliana* roots treated for 80 minutes with Cu6-PLGA NPs and observed at different focal planes. Cu6-PLGA NPs were not only visible in root hairs but in almost all cells of the epidermis. e) *A. thaliana* roots treated for 5 hours with Cu6-PLGA NPs. Cu6-PLGA NPs penetrated the root epidermis through the root hairs and remained at the level of the epidermis. The scale bar represents 20 µm.

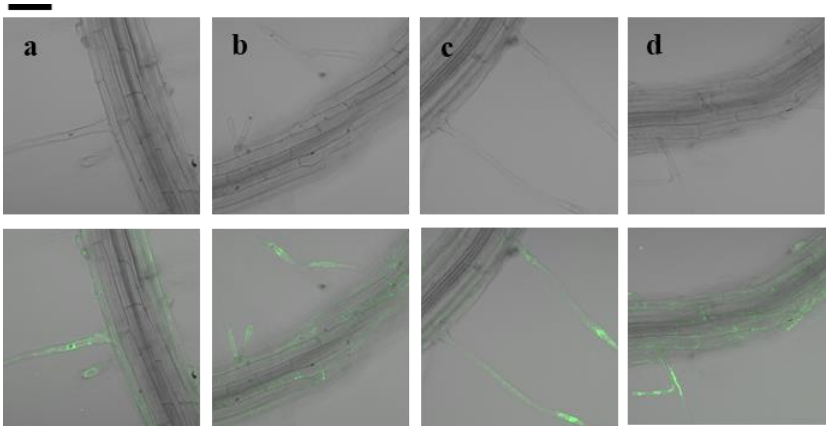

Fig. 3 *A. thaliana* seedling roots treated with Dynasore at 80 or 160 µM for 30 and 60 minutes before the addition of 15 mg L^{-1} Cu6-PLGA NPs for 10 minutes. Bright Field, Merge (bright field / fluorescence) images. a) Treatment with Dynasore at 80 µM for 30 minutes before the Cu6-PLGA NPs supplementation; b) treatment with Dynasore at 80 µM for 60 minutes before the Cu6-PLGA NPs supplementation; c) treatment with Dynasore at 160 µM for 30 minutes before the Cu6-PLGA NPs supplementation; d) treatment with Dynasore at 160 µM for 60 minutes before the Cu6-PLGA NPs supplementation. Cu6-PLGA NPs penetrated the root epidermis through the root hairs and remained at the level of the epidermis. The scale bar represents 20 µm.

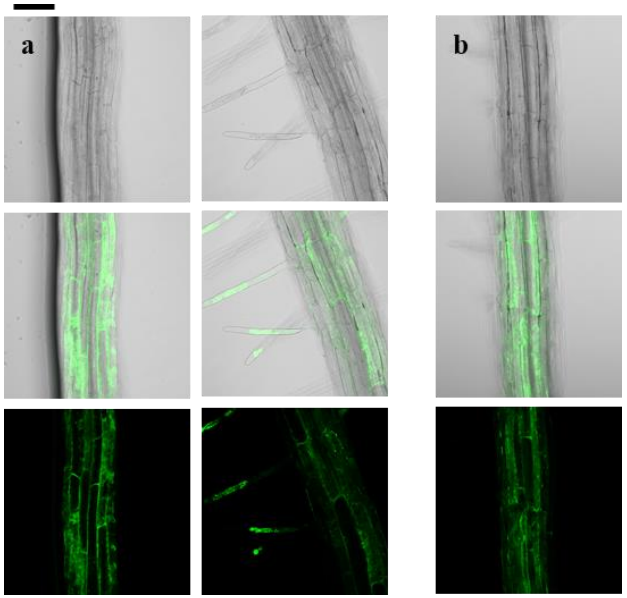

Fig. 4 *A. thaliana* plantlet roots treated with Dynasore at 320 µM for 30 and 60 minutes before the addition of 15 mg L^{-1} Cu6-PLGA NPs for 10 minutes. Bright Field, Merge (bright field / fluorescence) and fluorescence images. a) Two *A. thaliana* plantlet roots treated with Dynasore at 320 µM for 30 minutes before the Cu6-PLGA NPs treatment; b) *A. thaliana* plantlet roots treated with Dynasore at 320 µM for 60 minutes before the Cu6-PLGA NPs treatment. Cu6-PLGA NPs penetrated the root epidermis through the root hairs and remained at the level of the epidermis. The scale bar represents 20 µm.

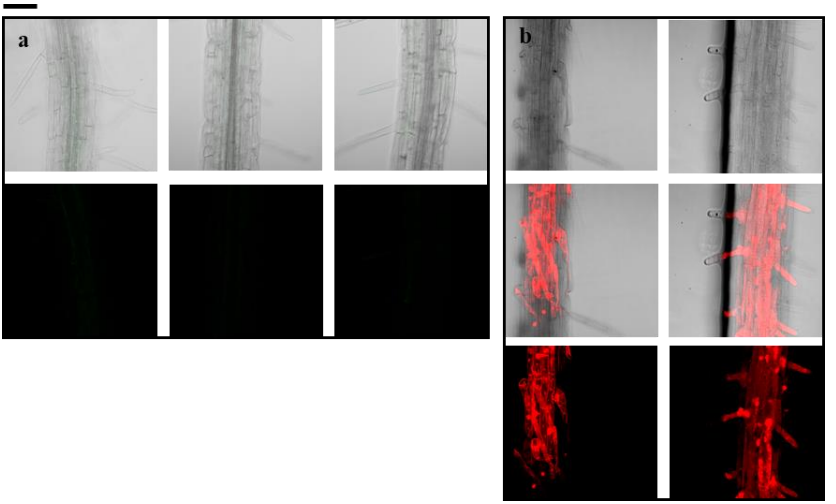

Fig. 5 *A. thaliana* seedling roots treated with Dynasore at 320 µM for 120 minutes before the addition of 15 mg L^{-1} Cu6-PLGA NPs for 10 minutes or before propidium iodide treatment for cytotoxicity test. a) *A. thaliana* different roots treated with Dynasore at 320 µM for 120 minutes before the Cu6-PLGA NPs supplementation. Absence of fluorescence in the roots. Merge (bright field / fluorescence) and fluorescence images; b) *A. thaliana* roots treated with Dynasore at 320 µM for 120 minutes before the propidium treatment. In red are the nonviable cells, almost all cells are found to be nonviable. Bright Field, Merge (bright field / fluorescence) and fluorescence images. The scale bar represents 20 µm.

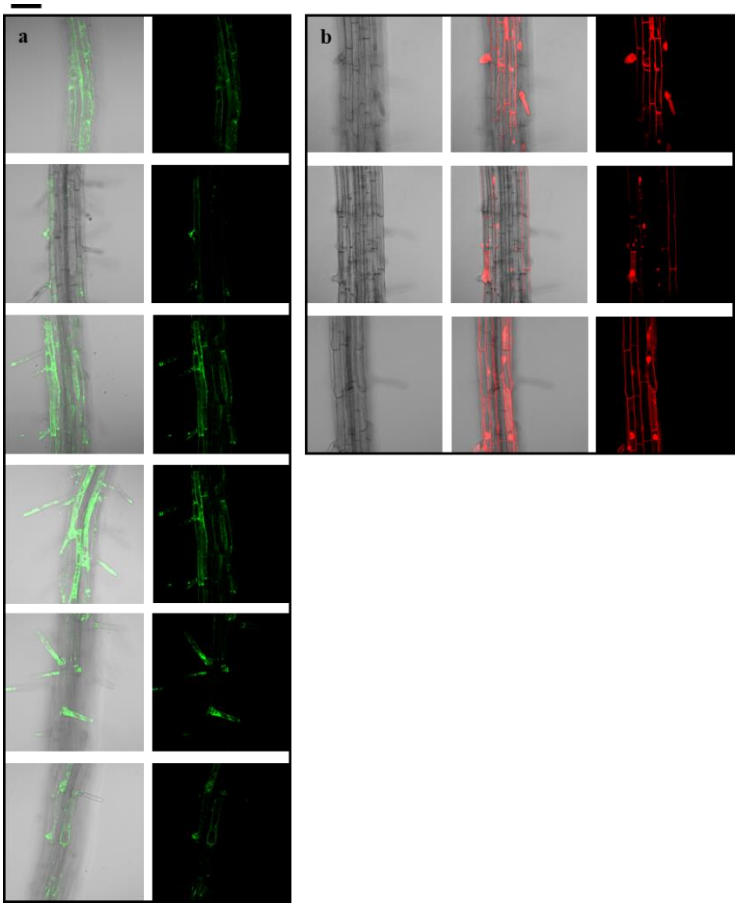

Fig. 6 *A. thaliana* seedling roots treated with Dynasore at 80 µM for 120 minutes before the addition of 15 mg L^{-1} Cu6-PLGA NPs for 10 minutes (a) or before supplementation of propidium iodide for cytotoxicity test (b). a) Intense fluorescence in the cells of the root epidermis is recognizable. Merge (bright field / fluorescence) and fluorescence images; b) in red are the nonviable cells, almost all cells are found to be viable. The scale bar represents 20 µm.

Unfortunately, limited information about PLGA NPs internalization mechanisms in plant cells are reported in the literature. Previous studies highlighted that PLGA NPs enter in *V. vinifera* suspended cells as well as in leaf tissues through stomata openings, and also absorbed by the roots (Valletta et al., 2014). Palocci et al., (2017) suggested a role of cell wall in the size selection of PLGA NPs showing that PLGA NPs with a diameter over 50 nm were able to penetrate in *Vitis vinifera* cells. In the *Arabidopsis* cells, PLGA NPs of 30 nm can enter the cells. In suspension cultures of *Chenopodium album* L., *Dioscorea deltoidea* Wall. and *Medicago sativa* L., the mean size limit was found to vary between 2.4 and 3.8 nm (Woehlecke et al., 1997). Bandmann and Homann (2012) proved that the cell wall blocks the uptake of nanobeads larger than 100 nm in BY-2 tobacco cells. The reason for the difference from species to species could depend on the structure, organization and interactions of cellulose, hemicelluloses, pectins, structural proteins and lignin (Carpita et al., 1979). Particularly, in the primary wall, pectins are known to regulate porosity through galactan and arabinan side chains of rhamnogalacturonan (Rondeau-Mouro et al., 2008). TEM analyses conducted on *Medicago sativa* suspension cultures showed that PLGA NPs passed through the cell wall and were accumulated into the cytoplasm and nucleus (Ulusoy et al., 2020). Passed through the cell wall, NPs cross the membrane by endocytosis (Wang et al., 2021), a process involving the internalization of extracellular materials or plasma membrane proteins into the cell

through a series of vesicular compartments (Murphy et al., 2005). Similar to animal cells, the major route in plants is clathrin-mediated endocytosis (CME) and starts with the invagination of clathrin-coated membrane (Chen et al., 2011). Subsequently, dynamin assembles as a collar on the neck of a budding pit, and the conformational change accompanying GTP hydrolysis causes a constriction and scission of the neck (Danino et al., 2004). However, several researches have revealed some clathrin-independent pathways, including membrane microdomain-associated endocytosis, fluid-phase endocytosis, and phagocytosis-like uptake of rhizobia in plants (Malinsky et al., 2013; Fan et al., 2015). For example, in *Arabidopsis* the membrane microdomain-associated flotillin1 (Flot1) is involved in clathrin-independent endocytosis, as demonstrated through transgenic green fluorescent protein–flotillin1 *A. thaliana* plants in combination with confocal microscopy analysis and transmission electron microscopy immunogold labeling (Li et al., 2012). According to our results, it was discovered that some clathrin-independent endocytosis pathways are dynamin-independent (Guha et al., 2003) and that some members of the ADP-ribosylation factor (Arf) and Rho subfamilies of small GTPases have key roles in regulating different pathways of clathrin-independent endocytosis (Ridley, 2006).

Macia et al. (2006) showed that Dynasore acted as a potent inhibitor of dynamin-related endocytic pathways in animal cells. The supplementation of 80 µM of Dynasore inhibited the uptake of

transferrin within 1–2 min of treatment in HeLa and astrocytes cells, and they were presumably limited by diffusion of the molecule to the coated pits on which it acted. In fact, electron micrograph images obtained from cells treated for 10 minutes with 80 µM of Dynasore showed a large number of coated pits at partial stages of late assembly that remained linked to the plasma membrane by either narrow or wide necks. They also demonstrated that extended incubation of cells with 80 µM for two days of Dynasore was not toxic and reversible. Up to now, there are no studies demonstrating the effect of Dynasore as an inhibitor of NPs endocytosis in plants.

For the first time in this study, the treatment of *A. thaliana* cell suspension cultures with Dynasore at 80 µM and 160 µM for 10 minutes did not prevent the uptake of Cu6-PLGA NPs. The treatment of *A. thaliana* roots with Dynasore at 80 µM or 160 µM for 30, 60 and 120 minutes or with Dynasore at 320 µM for 30 and 60 minutes did not prevent the uptake of Cu6-PLGA NPs and the root cells were found to be viable. Differently, the treated with Dynasore at 320 µM for 120 minutes were not viable.

The results of this study suggest that Cu6-PLGA NPs are uptaken in *A. thaliana* cell suspension cultures and roots of plantlets through a dynamine-independent pathway.

PLGA NPs traslocation in the hypocotyl

Apotome fluorescence microscopy images showed the presence of Cu6-PLGA NPs in the hypocotyl of *A. thaliana* after treatment of plantlet roots with Cu6-PLGA NPs at 15 mg L^{-1} for 1 hour (**Fig. 7**). NPs fluorescence was visible in cells of the epidermis and cortical parenchyma. Hypocotyl of untreated plants showed no autofluorescence (data not shown). Therefore, the Cu6-PLGA NPs were translocated from the root to the hypocotyl to the *A. thaliana* plantlets. This result is in agreement with other studies showing that NPs are able to take up by the root, to reach the vascular cylinder through a radial path, and then be transported to the shoot. The same results have been demonstrated in *Vitis vinifera* plant roots treated with Cu6-PLGA NPs. After 48 h of treatment the NPs were accumulated in the shoot tissues (Valletta et al., 2014). Confocal microscopy images of the sugarcane roots showed fluorescent signals of zein nanoparticles along the epidermal layer and their translocation to the cortex, to the endodermis and then to the leaves (Prasad et al., 2017).

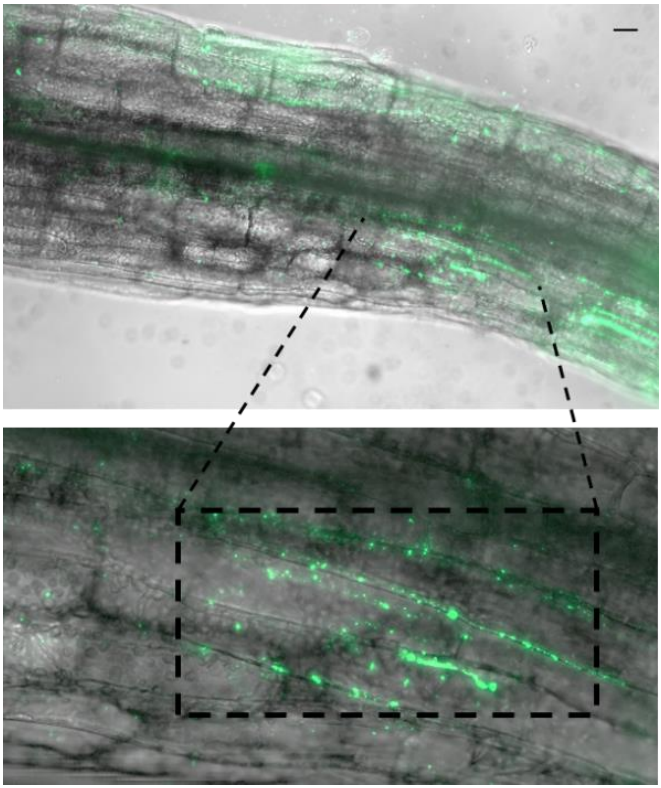

Fig. 7 Hypocotyl of *A. thaliana* after one hour with Cu6-PLGA NPs treatment of plantlet roots at the concentration of 15 mg L^{-1}. Merge (bright field / fluorescence) images obtained by ApoTome fluorescence microscope show the Cu6-PLGA NPs translocation from the root to the hypocotyl in the *A. thaliana* plantlets. The scale bar represents 50 μm.

Conclusions

In the present study, Cu6-PLGA NPs rapidly penetrated cultured cells and plantlet roots of *A. thaliana*. It has been observed that Dynasore did not inhibit the uptake of Cu6-PLGA NPs into cells and roots suggesting that the internalization of NPs could occur by a dynamin-independent pathway and, consequently, by a clathrin-independent pathway, in agreement with previous works (Valletta et al., 2014; Palocci et al., 2017). In addition, it has been observed that, in the *A. thaliana* plantlets, Cu6-PLGA NPs, translocated from the root to the hypocotyl. Further studies are essential to understand the migration of PLGA NPs through *A. thaliana* plant tissue and determine accumulation sites, especially with the prospect of using PLGA NPs as carriers of bioactive molecules in the agronomic field. In fact, PLGA-NPs could have numerous applications. Chronopoulou et al., (2019) obtained PLGA NPs loaded with MeJA, an endogenous plant defense elicitor, and demonstrated that encapsulating MeJA in PLGA NPs significantly enhanced MeJA cell uptake and MeJA-induced responses in *V. vinifera* cell cultures. De Angelis et al., (2022) demonstrated that PLGA NPs loaded with pterostilbene inhibited the growth of *Botrytis cinerea*, and thus could be used in the control of this pathogen. In conclusion, the obtained results add new information to be considered for the use of PLGA NPs in agriculture.

References

Fortunati, E., Mazzaglia, A., & Balestra, G. M. (2019). Sustainable control strategies for plant protection and food packaging sectors by natural substances and novel nanotechnological approaches. *Journal of the Science of Food and Agriculture*, 99(3), 986-1000.

Makadia, H. K., & Siegel, S. J. (2011). Poly lactic-co-glycolic acid (PLGA) as biodegradable controlled drug delivery carrier. *Polymers*, 3(3), 1377-1397.

Pérez-de-Luque, A. (2017). Interaction of nanomaterials with plants: what do we need for real applications in agriculture?. *Frontiers in Environmental Science*, 5, 12.

Proença, P. L., Carvalho, L. B., Campos, E. V., & Fraceto, L. F. (2022). Fluorescent labeling as a strategy to evaluate uptake and transport of polymeric nanoparticles in plants. *Advances in Colloid and Interface Science*, 102695.

Valletta, A., Chronopoulou, L., Palocci, C., Baldan, B., Donati, L., & Pasqua, G. (2014). Poly (lactic-co-glycolic) acid nanoparticles uptake by Vitis vinifera and grapevine-pathogenic fungi. *Journal of Nanoparticle Research*, 16(12), 1-14.

Palocci, C., Valletta, A., Chronopoulou, L., Donati, L., Bramosanti, M., Brasili, E., ... & Pasqua, G. (2017). Endocytic pathways involved in

PLGA nanoparticle uptake by grapevine cells and role of cell wall and membrane in size selection. *Plant Cell Reports*, 36(12), 1917-1928.

Chronopoulou, L., Donati, L., Bramosanti, M., Rosciani, R., Palocci, C., Pasqua, G., & Valletta, A. (2019). Microfluidic synthesis of methyl jasmonate-loaded PLGA nanocarriers as a new strategy to improve natural defenses in *Vitis vinifera*. *Scientific Reports*, *9*(1), 1-9.

Narasimhan, M., Johnson, A., Prizak, R., Kaufmann, W. A., Tan, S., Casillas-Pérez, B., & Friml, J. (2020). Evolutionarily unique mechanistic framework of clathrin-mediated endocytosis in plants. *Elife*, 9, e52067.

Fan, L., Li, R., Pan, J., Ding, Z., & Lin, J. (2015). Endocytosis and its regulation in plants. *Trends in Plant Science*, 20(6), 388-397.

Mayor, S., & Pagano, R. E. (2007). Pathways of clathrin-independent endocytosis. *Nature Reviews Molecular Cell Biology*, 8(8), 603-612.

Onelli, E., Prescianotto-Baschong, C., Caccianiga, M., & Moscatelli, A. (2008). Clathrin-dependent and independent endocytic pathways in tobacco protoplasts revealed by labelling with charged nanogold. *Journal of Experimental Botany*, 59(11), 3051-3068.

Li, R., Liu, P., Wan, Y., Chen, T., Wang, Q., Mettbach, U., ... & Lin, J. (2012). A membrane microdomain-associated protein, *Arabidopsis*

Flot1, is involved in a clathrin-independent endocytic pathway and is required for seedling development. *The Plant Cell*, 24(5), 2105-2122.

Mishev, K., Dejonghe, W., & Russinova, E. (2013). Small molecules for dissecting endomembrane trafficking: a cross-systems view. *Chemistry & Biology*, 20(4), 475-486.

Minamidate, A., Onizawa, M., Saito, C., Hikichi, R., Mochimaru, T., Murakami, M., ... & Watanabe, M. (2021). A potent endocytosis inhibitor Ikarugamycin up-regulates TNF production. *Biochemistry and Biophysics Reports*, 27, 101065.

Elkin, S. R., Oswald, N. W., Reed, D. K., Mettlen, M., MacMillan, J. B., & Schmid, S. L. (2016). Ikarugamycin: a natural product inhibitor of clathrin-mediated endocytosis. *Traffic*, 17(10), 1139-1149.

Robinson, D. G., Jiang, L., & Schumacher, K. (2008). The endosomal system of plants: charting new and familiar territories. *Plant Physiology*, 147(4), 1482-1492.

Arighi, C. N., Hartnell, L. M., Aguilar, R. C., Haft, C. R., & Bonifacino, J. S. (2004). Role of the mammalian retromer in sorting of the cation-independent mannose 6-phosphate receptor. *The Journal of Cell Biology*, 165(1), 123-133.

Macia, E., Ehrlich, M., Massol, R., Boucrot, E., Brunner, C., & Kirchhausen, T. (2006). Dynasore, a cell-permeable inhibitor of dynamin. *Developmental Cell*, 10(6), 839-850.

Chronopoulou, L., Sparago, C., & Palocci, C. (2014). A modular microfluidic platform for the synthesis of biopolymeric nanoparticles entrapping organic actives. *Journal of Nanoparticle Research*, 16(11), 1-10.

May, M. J., & Leaver, C. J. (1993). Oxidative stimulation of glutathione synthesis in *Arabidopsis thaliana* suspension cultures. *Plant Physiology*, 103(2), 621-627.

Jones, K. H., & Senft, J. A. (1985). An improved method to determine cell viability by simultaneous staining with fluorescein diacetate-propidium iodide. *Journal of Histochemistry & Cytochemistry*, 33(1), 77-79.

Woehlecke, H., Afifi, I., & Ehwald, R. (1997). Dynamics of limiting cell wall porosity in plant suspension cultures. *Planta*, 203(3), 320-326

Bandmann, V., & Homann, U. (2012). Clathrin-independent endocytosis contributes to uptake of glucose into BY-2 protoplasts. *The Plant Journal*, 70(4), 578-584.

Carpita, N., Sabularse, D., Montezinos, D., & Delmer, D. P. (1979). Determination of the pore size of cell walls of living plant cells. *Science*, 205(4411), 1144-1147.

Rondeau-Mouro, C., Defer, D., Leboeuf, E., & Lahaye, M. (2008). Assessment of cell wall porosity in *Arabidopsis thaliana* by NMR spectroscopy. *International Journal of Biological Macromolecules*, 42(2), 83-92.

Ulusoy, E., Derman, S., & Erişen, S. (2020). The cellular uptake, distribution and toxicity of Poly (lactic-co-glycolic) acid nanoparticles in *medicago sativa* suspension culture. *Romanian Biotechnological Letters*, 25(3).

Wang, J. W., Cunningham, F. J., Goh, N. S., Boozarpour, N. N., Pham, M., & Landry, M. P. (2021). Nanoparticles for protein delivery in planta. *Current Opinion in Plant Biology*, 60, 102052.

Murphy, A. S., Bandyopadhyay, A., Holstein, S. E., & Peer, W. A. (2005). Endocytotic cycling of PM proteins. *Annual Review of Plant Biology*, 56(1), 221-251.

Chen, X., Irani, N. G., & Friml, J. (2011). Clathrin-mediated endocytosis: the gateway into plant cells. *Current Opinion in Plant Biology*, 14(6), 674-682.

Danino, D., Moon, K.H., and Hinshaw, J.E. (2004). Rapid constriction of lipid bilayers by the mechanochemical enzyme dynamin. *Journal of structural biology*, 147, 259–267.

Malinsky, J., Opekarová, M., Grossmann, G., & Tanner, W. (2013). Membrane microdomains, rafts, and detergent-resistant membranes in plants and fungi. *Annual Review of Plant Biology*, 64, 501-529.

Li, R., Liu, P., Wan, Y., Chen, T., Wang, Q., Mettbach, U., ... & Lin, J. (2012). A membrane microdomain-associated protein, *Arabidopsis* Flot1, is involved in a clathrin-independent endocytic pathway and is required for seedling development. *The Plant Cell*, 24(5), 2105-2122.

Guha, A., Sriram, V., Krishnan, K. S., & Mayor, S. (2003). Shibire mutations reveal distinct dynamin-independent and-dependent endocytic pathways in primary cultures of *Drosophila* hemocytes. *Journal of Cell Science*, 116(16), 3373-3386.

Ridley, A. J. (2006). Rho GTPases and actin dynamics in membrane protrusions and vesicle trafficking. *Trends in Cell Biology*. 16, 522-529.

Prasad, R., Bhattacharyya, A., & Nguyen, Q. D. (2017). Nanotechnology in sustainable agriculture: recent developments, challenges, and perspectives. *Frontiers in Microbiology*, *8*, 1014.

De Angelis, G., Simonetti, G., Chronopoulou, L., Orekhova, A., Badiali, C., Petruccelli, V., ... & Palocci, C. (2022). A novel approach

to control *Botrytis cinerea* fungal infections: uptake and biological activity of antifungals encapsulated in nanoparticle based vectors. *Scientific Reports*, 12(1), 1-9.

Chapter 4

A novel approach to control *Botrytis cinerea* fungal infections: uptake and biological activity of antifungals encapsulated in nanoparticle based vectors

Paper published in *Scientific Reports*

DOI: 10.1038/s41598-022-11533-w

Giulia De Angelis[†1], Giovanna Simonetti[†3], Laura Chronopoulou[†2], Anastasia Orekhova[3], Camilla Badiali[1], Valerio Petruccelli[1], Francesca Portoghesi[2], Simone D'Angeli[1], Elisa Brasili[1], Gabriella Pasqua [1]* & Cleofe Palocci[2].

[1] Department of Environmental Biology, "Sapienza" University of Rome, P. le Aldo Moro 5 00185 Rome, Italy
[2] Department of Chemistry, "Sapienza" University of Rome, 00185 Rome, Italy
[3] Department of Public Health and Infectious Diseases, "Sapienza" University of Rome, 00185 Rome, Italy

Abstract

Botrytis cinerea, responsible for grey mold diseases, is a pathogen with a broad host range, affecting many important agricultural crops, in pre and post harvesting of fruits and vegetables. Commercial fungicides used to control this pathogen are often subjected to photolysis, volatilization, degradation, leaching, and runoff during application. In this context, the use of a delivery system, based on poly (lactic-co-glycolic acid) nanoparticles (PLGA NPs) represents an innovative approach to develop new pesticide formulations to successfully fight *B. cinerea* infections. In order to study NPs uptake, *B. cinerea* conidia and mycelium were treated with PLGA NPs loaded with the high fluorescent probe coumarin-6 (Cu6-PLGA NPs) and analyzed under ApoTome fluorescence microscopy. The observations revealed that 50 nm Cu6-PLGA NPs penetrated into *B. cinerea* conidia and hyphae, as early as 10 minutes after administration. Pterostilbene, a natural compound, and fluopyram, a synthetic antifungal, were entrapped in PLGA NPs, added to *B. cinerea* conidia and mycelium, and their antifungal activity was tested. The results revealed that the compounds loaded in NPs exhibited a higher activity against *B. cinerea*. These results lay the foundations for the use of PLGA NPs as a new strategy in plant pest management.

Introduction

Fungal plant pathogens are the main cause of considerable economic losses of crop plants[1]. Ascomycete *Botrytis cinerea*, responsible for grey mold diseases, is a highly successful pathogen due to its flexible infection modes, high reproductive output, wide host range, and ability to survive for extended periods as conidia and/or small hardened mycelia masses called sclerotia[2]. It is a pathogen with a broad host range, affecting many important agricultural crops, mainly in pre and post harvesting of fruit or vegetables. It is estimated that *B. cinerea* causes a $10 to 100 billion of production loss annually worldwide[3]. Due to the highly destructive nature of *B. cinerea*, it was ranked second on a list of fungal pathogens of scientific and economic importance[4]. Approximately 8% of the global fungicide market is used to control this pathogen. It is important to highlight that less than 0.1% of fungicides reach their biological targets as 90% of them are lost through photolysis, volatilization, degradation, leaching, and runoff during application[5]. In addition, fungicide usage is harmful to both the environment and human health, and *B. cinerea* has developed resistance to many conventional fungicides such as dicarboximides and benzimidazoles[6].

To overcome the fungal multi-resistance to existent drugs, it is important to explore novel antifungal agents, which may replace current control strategies. Some authors reported the activity of plant extracts or natural compounds against *B. cinerea*[7]. In this context, the generation

of drug delivery systems based on nanomaterials represents a potential alternative to develop novel formulations to successfully combat fungal infections and overcome the fungal multi-resistance to existent drugs[8]. Different studies have determined that NPs present fewer side effects and greater specificity to the infection site[9,10]. Special attention has been given to biopolymeric nanoparticles (NPs) as non-toxic and eco-friendly nanocarriers that can be successfully used for the controlled release of bioactive compounds[11]. In recent years, a variety of natural and synthetic polymers have been explored for nanoformulations. Among them, polylactic acid (PLA), polyglycolic acid (PGA), and their copolymer (PLGA) have been extensively investigated due to their biocompatibility, high solubility, stability, and effectiveness[12,13,14,15].

It has been shown that PLGA NPs have the ability to penetrate *Vitis vinifera* cell suspensions without harmful effects on cellular vitality[16,17]. As largely investigated by the authors in *V. vinifera* cell cultures, methyl jasmonate (MeJA) encapsulation in PLGA NPs significantly promoted MeJA cell uptake and the activation of MeJA-induced responses[13]. Simonetti et al.[15] have demonstrated the anti-*Candida* biofilm activity of PLGA NPs loaded with non-fermented grape pomace.

Up to now, there is relatively little and limited evidence about PLGA NPs uptake by pathogenic fungal cells[18,19], and further studies are needed in order to improve the knowledge on the effectiveness of PLGA NPs to deliver natural or conventional antifungals to microbial cells.

The present research aimed to study PLGA NPs uptake in *B. cinerea* and investigate the antifungal activity of natural and synthetic compounds entrapped in PLGA NPs against *B. cinerea* conidia and mycelium.

In order to examine NPs uptake, *B. cinerea* conidia and mycelium were treated with PLGA NPs loaded with the high fluorescent probe coumarin-6 (Cu6-PLGA NPs) and analyzed under ApoTome fluorescence microscopy. Moreover, in an effort to investigate the antimicrobial activity of antifungals delivered by NPs, pterostilbene and fluopyram were encapsulated in PLGA NPs and administered at different stages of *B. cinerea* development.

Pterostilbene is a natural antimicrobial phenolic compound derived from resveratrol, mostly contained in *V. vinifera* leaves and grape berries. It has been demonstrated that pterostilbene has no harmful effects on plant metabolism or crop yield, and it is able to inhibit the growth of several phytopathogenic fungi, such as *Leptosphaeria maculans*, *Peronophythora litchii*, *Botrytis cinerea* and others[20,21]. Schmidlin et al.[22] showed that pterostilbene was 5 to 10 times more effective than resveratrol in inhibiting the germination of conidia of *B. cinerea* and sporangia of *P. viticola*. On the other hand, fluopyram is a synthetic fungicide and nematicide compound commonly used in agriculture against *B. cinerea*.

This study provides new evidence of the use of PLGA NPs as an interesting strategy in integrated plant disease management, with the

aim to increase the potency and efficiency of natural and conventional antifungals through a controlled and targeted drug release while decreasing environmental toxicity and agricultural costs.

Materials and methods

Chemicals and Materials

Pterostilbene was purchased from Chemodex (St. Gallen, Switzerland). Poly(D,L)-lactic-co-glycolic acid (PLGA, lactide: glycolide 50:50, MW 50 kDa), Coumarin 6 (Cu6) (98%), Potato dextrose agar (PDA), Fluopyram, RPMI medium (RPMI 1640 with L-glutamine, without bicarbonate), MOPS acid, XTT [2,3-bis- (2-methoxy-4-nitro-5-sulfophenyl) -5- (carbonyl (phenylamino)]-2H-tetrazolium hydroxide] and Menadione (MEN) were purchased from Sigma-Aldrich (Milan, Italy).

Potato dextrose broth (PDB) was purchased from Formedium LTD (Hunstanton, Norfolk, England).

The microfluidic flow focusing reactor was assembled by the research group involved in the study as reported previously by Bramosanti et al.[23].

Synthesis of PLGA NPs

PLGA NPs loaded with fluopyram, pterostilbene or coumarin 6 were prepared by using an innovative microfluidic reactor with a flow-focusing configuration described previously[24]. The reactor consists of

three inlets and one main mixing outlet channel. An organic phase containing the polymer is injected into the middle channel and water is injected into the two side inlets. NPs formation occurs through a nanoprecipitation mechanism in the mixing channel and NPs can be recovered at its end. PLGA (2 mg mL^{-1}) and the selected payload were dissolved in an organic phase. Acetone was used to dissolve pterostilbene (1 mg mL^{-1}) and coumarin 6 (40 µg mL^{-1}), while fluopyram (0.2 mg mL^{-1}) was dissolved in DMSO. To optimize the amount of encapsulated fluopyram and pterostilbene, PLGA NPs were prepared with different polymer/drug ratios, respectively from 2.5:1 to 20:1 and from 2:1 to 4:1, keeping PLGA concentration constant. A PLGA/coumarin 6 ratio of 50:1 was chosen on the basis of previous works[24]. The aqueous flow rate was 2000 µL min^{-1} while the organic phase flow rate was 100 µL min^{-1} when using acetone and 400 µL min^{-1} when using DMSO. The formed PLGA-based NPs were recovered and the organic phase was eliminated under reduced pressure. The NPs aqueous suspensions were stored at 4°C until use.

PLGA NPs characterization

Dynamic light scattering (DLS) measurements were carried out using a NanoZetasizer (Malvern Instruments, Malvern, UK) to measure the mean hydrodynamic diameter of PLGA NPs and their polydispersity index. The experimental conditions used are the following: a helium neon laser operating at 633 nm, a fixed scattering angle of 173° and

constant temperature (25°C). The measured autocorrelation functions of the scattered light intensity were analyzed using the CONTIN algorithm in order to obtain the decay time distributions[25]. Decay times were used to determine the distributions of the diffusion coefficients of the particles (D), converted in turn in the distributions of the apparent hydrodynamic radii, R_H, using the Stokes-Einstein relationship: $R_H = k_BT/6\pi\eta D$ (kBT = thermal energy; η = solvent viscosity).

Particle morphology was observed by scanning electron microscopy (SEM) in both the secondary and the backscattered electron modes with an electron acceleration voltage of 20 keV, using a LEO 1450VP SEM microscope (ZEISS, Oberkochen, Germany).

The quantitative analysis of fluopyram and pterostilbene loaded in PLGA NPs was carried out by spectroscopic measurements. NPs aqueous suspensions were ultra-centrifuged at low temperature (4°C) to recover NPs. The supernatant was discarded and the pellet was dissolved in DMSO and analyzed by measuring the UV absorbance at 270 nm (for fluopyram) or at 313 nm (for pterostilbene), comparing the results with the corresponding calibration curve. The method used for fluopyram was linear within the concentration range between 0.2 and 0.8 mg mL^{-1} with R^2=0.997. The method used for pterostilbene was linear within the concentration range between 0.002 and 0.01 mg mL^{-1} with R^2=0.9822.

The encapsulation efficiency and loading capacity were calculated by using the following equations:

$$(EE\ \%) = \frac{(Total\ drug\ added - free\ non - entrapped\ drug)}{(Total\ drug\ added)} \times 100$$

$$(LC\ \%) = \frac{(Amount\ of\ total\ entrapped\ drug)}{(Total\ nanoparticle\ weight)} \times 100$$

In vitro release studies of fluopyram and pterostilbene from PLGA NPs

A fixed amount (2 mg) of fluopyram or pterostilbene-loaded PLGA NPs was suspended in 2 mL of acetate buffer at pH=4 or in 2 ml of PBS solution at pH=7.4 in a centrifuge tube. The suspensions were incubated at 25°C and maintained under magnetic stirring at 300 rpm. At fixed time intervals, 500 µL of the supernatant was collected and replaced with an equal volume of buffer in order to keep the reaction volume constant. The concentration of fluopyram or pterostilbene in the collected supernatant was spectrophotometrically determined as reported above. At each time point, the amount of released drug was calculated by normalizing the data with the total amount of drug inside the particles.

Fungal strain and culture condition

Botrytis cinerea DSM 877, obtained from the German Collection of Microorganisms (DSMZ, Braunschweig, Germany), was used in this study. This strain has been reported to show an intermediate pathogenicity[26] and it was used for the evaluation of antifungal

compounds[27]. The strain was cultured on potato dextrose agar (PDA) at 24°C. Conidia were collected from 10-day-old and the concentration was determined using a Thoma counting chamber. RPMI medium (RPMI 1640 with L-glutamine, without bicarbonate) buffered to pH 7.0 with 0.165 M MOPS was used for antifungal tests. XTT [2,3-bis- (2-methoxy-4-nitro-5-sulfophenyl) -5- (carbonyl (phenylamino)]-2H-tetrazolium hydroxide] and Menadione (MEN) were used to test the metabolic activities of *B. cinerea* cells.

Fungal uptake of Cu6-PLGA NPs

The aqueous suspension of Cu6-PLGA NPs was added to *B. cinerea* conidia and mycelium. In particular, *B. cinerea* conidia (1×10^5 conidia mL^{-1}) were inoculated into potato dextrose broth (PDB) and incubated at 24°C. After 12 h Cu6-PLGA NPs, at a final concentration of 0.1 mg mL^{-1}, were added. After 0, 10, and 60 min, the fungal suspension was placed on a microscope slide, and observed under ApoTome fluorescence microscope. For Cu6-PLGA NPs uptake in *B. cinerea* mycelium, *B. cinerea* (1×10^5conidia mL^{-1}) was cultured on glass microscope slides placed into Petri dishes containing PDB. After 24h of incubation the medium was removed and the Cu6-PLGA NPs, at a final concentration of 0.1 mg mL^{-1}, were added. After 0, 10, and 60 min, each glass microscope slide was removed from the Petri dish and observed under ApoTome fluorescence microscope. A control of

untreated conidia and mycelium was observed to reveal any auto-fluorescence.

Fluorescent analysis

Cu6-PLGA NPs treated conidia and mycelium were observed and images were acquired using an Axio Imager M2 fluorescence microscope (Zeiss, Germany), motorized on the 3 axes, using a FITC filter (λ excitation BP 455-495 nm; λ emission BP 05-555 nm). The high thickness of the sample required a Z-stack image scanning performed with an Axiocam 512 (Zeiss) monochromatic camera and ApoTome 2 (Zeiss) as fringe projection module used to remove the out of focus signal. Single plane images were obtained as Z-stack maximum projection using Zen 2.5 (Zeiss) image analysis software.

***In vitro* antifungal activity of pterostilbene and fluopyram**

In vitro antifungal activity was carried out as previously described by Meletiadis et al[28]. *B. cinerea* conidia were grown in 96-well plates with fluopyram or pterostilbene, free or entrapped in PLGA NPs. After 0, 1, 5, 24, 48, and 72 h of incubation at 24°C, XTT-menadione were added to each well to obtain final concentrations of 200 μg mL^{-1} for XTT and 25 μM for menadione. The microtitration plates were incubated for a further 2 h at 24°C and the optical density at 450 nm (OD450) was measured. A minimum of four replicates was performed. The

percentage of MA inhibition (100%−%MA) was compared with the drug-free control.

Statistical analysis

The data were expressed as mean ± SD, and P <0.05 was considered statistically significant.

Statistical criteria, p, and other parameters are shown for each experiment. The statistical data analysis was performed using the GraphPad Prism 8 software (GraphPad Software Inc., USA).

Results and discussion

NPs characterization

PLGA NPs dimensions, characterized by DLS measurements, are reported in **Table 1**. According to the used experimental conditions, PLGA NPs entrapping fluopyram, pterostilbene, or 6-coumarin, presented an average size of 50 nm, with polydispersity indexes below 0.2. Investigations by scanning electron microscopy (SEM) showed that drug-loaded PLGA NPs had a spherical morphology (**Fig. 1**). Drug loading efficiencies and loading capacities for fluopyram-PLGA NPs or pterostilbene-PLGA NPs prepared with different polymer/drug ratios are reported in **Tables 2** and **3** respectively.

The PLGA/fluopyram and PLGA/pterostilbene weight ratios that showed the best encapsulation efficiency and loading capacity were

respectively 10:1 and 2:1. These conditions were selected for all successive observations.

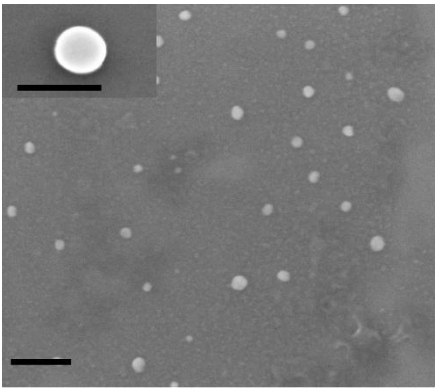

Figure 1. SEM micrograph of PLGA based NPs, dimension bar 200 nm (100 nm in the enlarged image).

Table 1. Dimensions and Polydispersity Indexes (PdI) of PLGA-based NPs, measured by DLS. Values are referred to as mean ± standard deviation.

NPs	Dimensions (nm)	PdI
Fluopyram-PLGA	47.95 ± 5.33	0.187 ± 0.06
Pterostilbene-PLGA	54.06 ± 7.64	0.119 ± 0.03
6-coumarin PLGA	48.48 ± 3.62	0.155 ± 0.02

Table 2. Drug loading efficiencies and loading capacities for fluopyram-PLGA NPs prepared with different polymer/drug ratios.

PLGA/fluopyram ratio ***(w/w)***	**Encapsulation Efficiency** ***(%)***	**Loading Capacity** ***(%)***
20:1	64 ± 1	3.2 ± 0.05
15:1	83 ± 3	5.5 ± 0.03
10:1	89 ± 1	8.9 ± 0.01
8:1	78 ± 2	9.8 ±0.05
5:1	56.3 ± 1	11.3 ± 0.1
2.5:1	37.5 ± 2	15.0 ± 0.6

Table 3. Drug loading efficiencies and loading capacities for PTB-PLGA NPs prepared with different polymer/drug ratios.

PLGA/pterostilbene ratio ***(w/w)***	**Encapsulation Efficiency (%)**	**Loading Capacity (%)**
4:1	37 ± 2	9.2 ± 0.5
2:1	75 ± 3	37.5 ± 1.5

In vitro release kinetics of fluopyram and pterostilbene from PLGA NPs

The *in vitro* release of fluopyram occurs slowly reaching a plateau after 120 h as a function of medium pH (**Fig. 2a**). In both experimental conditions at pH 4 and 7.4, the quantity of released fluopyram results to be compatible with the *in vitro* inhibition protocols of *B. cinerea* (1.25-0.07 μg ml^{-1}). Nevertheless, the release of the drug appears to be positively influenced by lower pH; in these experimental conditions, acid hydrolysis of the polymeric backbone could be favored, which would influence the release of the drug by erosion. The amount of pterostilbene released within the time interval examined was low, probably due to the poor solubility of pterostilbene in water (0.011 g L^{1}) and the hydrophobic interactions that stabilize the PLGA-pterostilbene complex. No significant change in the amount of released pterostilbene as a function of pH was observed (**Fig. 2b**). The % of pterostilbene released at pH 4, at the plateau conditions, was equal to 16 % and corresponded to 30 μg mL^{-1}, an amount compatible with the *in vitro* inhibition protocols of *B. cinerea*, in which pterostilbene was used at different concentrations between 20 and 1.25 μg mL^{-1}.

However, such results could be useful to compare *in vitro* and *in vivo* performances since in *in vivo* experiments other mechanisms that favor NPs erosion phenomena may occur.

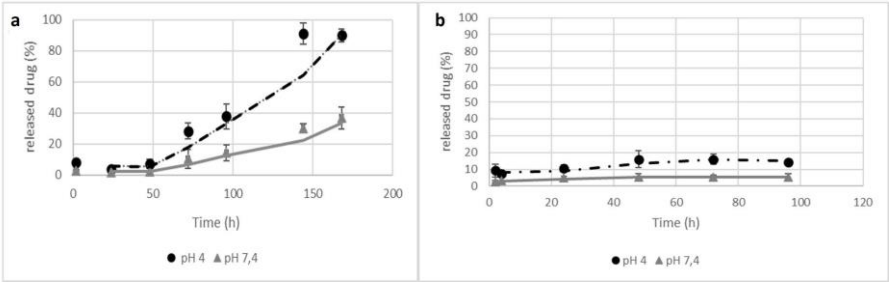

Figure 2. *In vitro* release kinetics of fluopyram (a) and pterostilbene (b) from PLGA NPs at 25 °C and different pH values.

Microscopic observations of NPs uptake in *B. cinerea* conidia and mycelium

According to the microscopic analyses, Cu6-PLGA NPs administered to *B. cinerea* enter conidia and hyphae after 10 min. It was found that NPs interacted with the conidia wall from the first stages of germination before the formation of the septum (**Fig. 3a-b**). The conidia of *Botrytis cinerea* have relatively thick cell walls (0.5 μm) consisting of two layers, a thin, dark, rough outer layer that is electron-dense under the microscope, and a thicker inner one that is transparent under electron microscopy[29]. Based on fluorescence results, optical sections and the 3D reconstruction of the ApoTome Microscope, it has been possible to observe that the fluorescent signal was present both along the conidia wall and inside conidia, throughout the whole thickness of the spore (**Fig. 3c**). The NPs fluorescent signal was well visible also in the

expanding germ tube (**Fig. 3d-e**). As the tube elongates, a large void forms in the center of the original spore.

The 50 nm Cu6-PLGA NPs were also administered to *B. cinerea* mycelium. 1 h after NPs administration, an intense signal appeared in the fungal hyphae (**Fig. 3f-h**). Fluorescence was visible in the mycelium after washing with sterile saltwater, showing that NPs penetrated or remained adhered to the hyphae. No autofluorescence was detected from the conidia and mycelium alone (data not shown). In a previous work, we demonstrated that PLGA NPs were able to penetrate the mycelium of some plant pathogenic fungi such as *A. carbonarius, A. niger* and *B. cinerea*[16]. During *B. cinerea* conidia germination, the outer spore wall breaks, and the emergent germ tube appears surrounded by the elastic inner one and by a mucilage sheath. At a very early stage, a transverse wall with a central pore is laid at the base of the germ tube[29]. Similarly, the uptake of Cu6-PLGA NPs has been previously demonstrated in fungal cells of *Aspergillus flavus.* In particular, Patel et al.[12] showed that the uptake of Cu6-PLGA NPs in *A. flavus* spores and mycelium was closely related to NPs size. In such work, NPs of 203 nm interacted with fungal cell surfaces and were efficiently internalized after 1 hour of incubation. Muse et al.[30] observed that covalently tagged poly(lactic-co-glycolic) acid nanoparticles (PLGA-tetramethylrhodamine [PLGA-TRITC]), entrapping coumarin-6 (double-tagged) with a diameter of 85–150 nm released coumarin-6 in *A. flavus* spores and hyphae while the majority of the particles

themselves did not seem to be trafficked into the interior of the cells. Nonetheless, some red fluorescence (PLGA-TRITC) was still observed within the interior of the cell, indicating that the smaller nanoparticles (30–50 nm) may have been directly endocytosed or diffused through the hyphae cell wall[30]. Other studies were carried out to test biopolymeric drug delivery systems against *B. cinerea*. In a recent work, Raj and collaborators[31] showed that chitosan-arabic gum-coated liposome 5I-1H-indole nanoparticles were potent inhibitors against *B. cinerea* growth. Up to now, despite *B. cinerea* causing significant damage to agriculture every year, few data are available on its uptake of PLGA NPs. The inhibition of spore germination should be considered effective for controlling plant disease. In this work, we showed that PLGA NPs interacted and penetrated also in the conidia of *B. cinerea*, promoting the uptake of the encapsulated compound into fungal cells, with the aim to prevent spore germination and thus fungal infection.

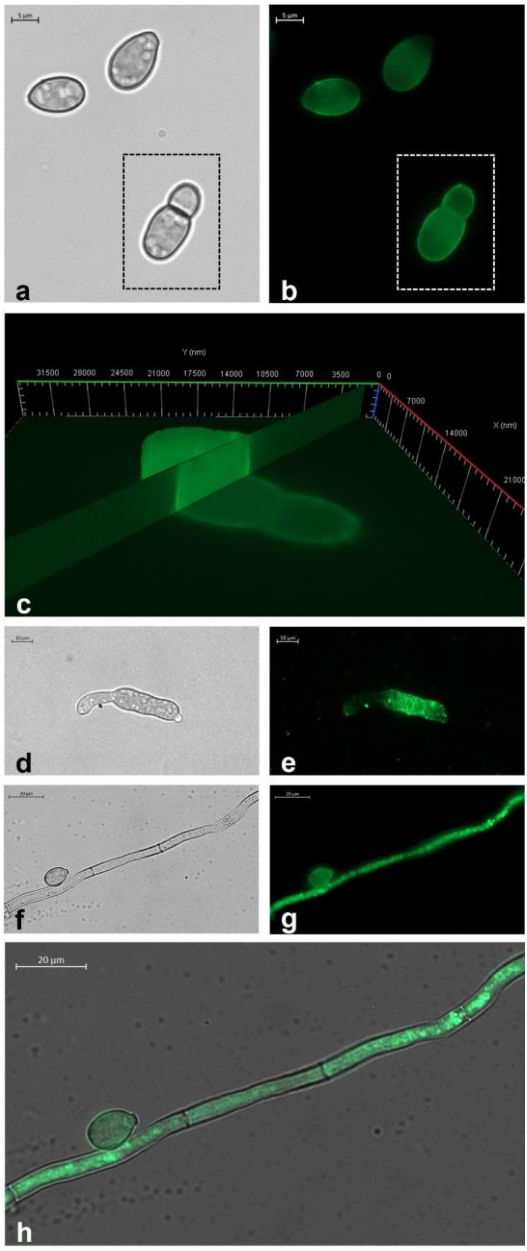
5 µm
a
5 µm
b
Y (nm)
31500 28000 24500 21000 17500 14000 10500 7000 3500 0
0
7000
14000
X (nm)
21000
c
10 µm
d
10 µm
e
20 µm
f
20 µm
g
20 µm
h

Figure 3a-h. (a) Bright field and (b) fluorescence image of *B. cinerea* conidia treated for 10 min with Cu6-PLGA NPs. NPs fluorescence signal was evident in germinated *B. cinerea* conidia (white square) and non-germinated ones. (c) 3D reconstruction of *B. cinerea* conidia treated with NPs for 10 min. The fluorescence signal was detected inside conidia, along the whole thickness of the spore. (d) Bright field and (e) fluorescence image of *B. cinerea* germ tube. The NPs fluorescence signal was well visible in the expanding germ tube after 10 min of administration. (f) Bright field and (g) fluorescence image of *B. cinerea* conidium and hypha. The fluorescence signal was well visible both in the conidium and the hypha after 1 h of administration. (h) Overlap of the bright field image and the fluorescence image which shows the localization of Cu6-PLGA NPs inside the fungal conidium and hypha.

Antifungal activity of pterostilbene or fluopyram PLGA NPs

In vitro antifungal activity of pterostilbene or fluopyram, free or loaded into PLGA NPs, against germinated and non-germinated conidia has been determined by evaluating the metabolic activity of fungal cells after 1, 5, 24, 48 and 72 hours of incubation. No statistically significant differences were observed after 1 and 5 hours of incubation between NPs loaded with pterostilbene or fluopyram and the free compounds (data not shown). Conversely, after 24 and 48 h of incubation with NPs loaded with pterostilbene or fluopyram, the metabolic activity of the conidia was lower compared to when these compounds were administered in their free form, as shown in **Fig. 4.** These data

demonstrated that after 24 and 48 h of incubation both fluopyram or pterostilbene loaded into NPs showed better antifungal activity than the free compounds (**Fig. 4**). In both experiments, empty NPs did not show antifungal activity. NPs loaded with pterostilbene, added to germinated conidia, showed significant inhibition of *B. cinerea* growth after 24 h of incubation. NPs loaded with fluopyram significantly inhibited *B. cinerea* growth, compared to free fluopyram, after 72 h of incubation, in all tested concentrations (**Fig. 5**). The antifungal activity of pterostilbene, a well-known plant phytoalexin, on *B. cinerea* has already been demonstrated by Pezet and Pont since 1990[32]. More recently, Xu and collaborators[21] reported 45% of mycelial growth reduction after treatment of *B. cinerea* with 200 μg mL^{-1} of pterostilbene. Moreover, Xu and collaborators[33] in a subsequent study showed multiple action mechanisms of pterostilbene against *B. cinerea*. After treatment with pterostilbene, *B. cinerea* changed the morphology of the hyphae and conidiophores, lost plasma membrane integrity, modulated gene expression, and increased laccase production. Some researchers reported that *B. cinerea*, through laccase secretion, can degrade and neutralize the toxicity of pterostilbene[34]. Our results show a significant and long lasting increase in activity, even at low concentrations. The significant increase in activity of pterostilbene delivered by PLGA NPs could be due to the protection of pterostilbene from fungal laccase. Moreover, the higher hydrophobicity of pterostilbene delivered by PLGA NPs could increase diffusion through

fungal membranes. On the other hand, pterostilbene with multiple mechanisms of action carries a low risk of developing resistance and its low toxicity makes pterostilbene a winning compound to fight *B. cinerea*. Synthetic fungicides are currently widely used in agriculture to fight *B. cinerea* infections. In this context, fluopyram, a synthetic pyridinyl ethylbenzaimide fungicide that inhibits succinate dehydrogenase (SDH), is commonly used to safeguard crops. Some studies reported high risks of *B. cinerea* resistance development to fluopyram and other succinate dehydrogenase inhibitors[35]. However, Dong and Hu[36] have shown that the transformation products were more toxic than fluopyram. Moreover, fluopyram shows high residue in surface soil which affects subsequent crops[37]. In this study, NPs loaded with fluopyram significantly inhibited *B. cinerea* growth, compared to free fluopyram.

Agriculture is the backbone of the economy of most countries and it was the key development in the rise of human civilization. *B. cinerea* is a well-known fungus with a wide host range that causes heavy losses in crop yields every year. The generation of drug delivery systems based on nanomaterials represents a potential alternative to developing newer formulations to successfully control fungal infections and overcome the fungal multi-resistance to existent drugs. In fact, the encapsulation protects the antifungal compound from damage such as photolysis or degradation, allowing the drug to reach the target site more efficiently with a consequent reduction in the number of applications[38,39]. In this

context, the delivery of antifungal compounds encapsulated in PLGA NPs could be considered an excellent strategy to safeguard crops against *B. cinerea.* The fluorescence microscopy observations revealed that 50 nm Cu6-PLGA NPs penetrated *B. cinerea* conidia and hyphae as early as 10 minutes after administration. Moreover, the antifungals pterostilbene and fluopyram delivered by NPs exhibited higher antifungal activity against *B. cinerea* than the corresponding antifungal compounds administered in free form. These results lay the foundation for the use of PLGA NPs in agriculture as a new strategy in plant pest management with the goal of enhancing the effectiveness of natural and synthetic antifungals through controlled and targeted drug delivery in the agronomic field.

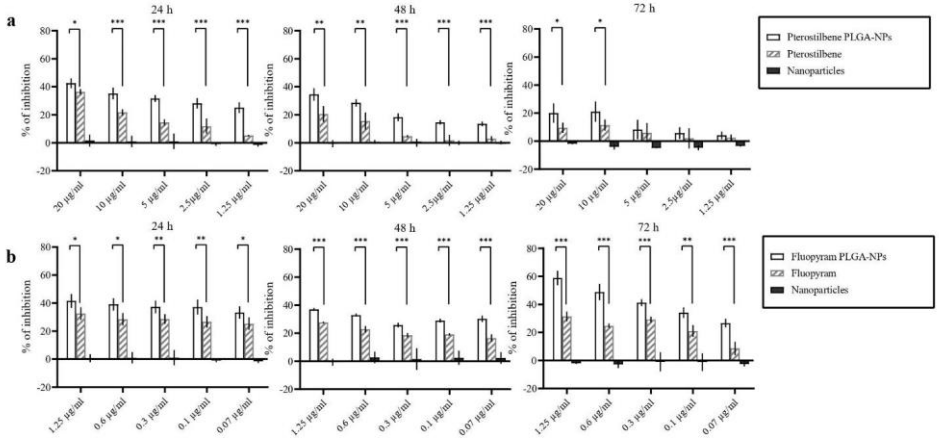

Figure 4. Activity of pterostilbene and fluopyram, free or loaded in PLGA NPs, against non-germinated conidia of *Botrytis cinerea* DSM 877 after 24, 48, and 72 h of incubation. *$P < 0.05$, **$P < 0.01$, ***$P <$ 0.001.

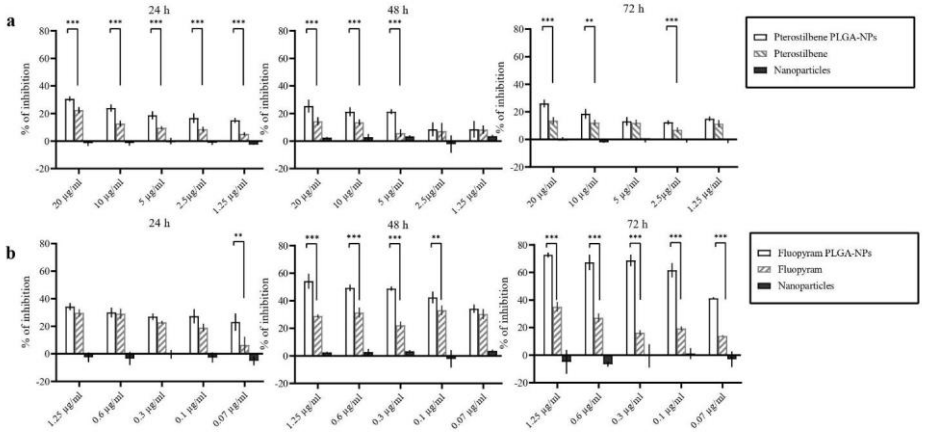

Figure 5. Activity of pterostilbene and fluopyram, free or loaded in PLGA NPs, against 12 h -germinated conidia of *Botrytis cinerea* DSM 877 after 24, 48, and 72 h of incubation. **P* < 0.05, ***P* < 0.01, ****P* < 0.001.

References

1. Cheung, N., Tian, L., Liu, X. & Li, X. The Destructive Fungal Pathogen Botrytis cinerea—Insights from Genes Studied with Mutant Analysis. *Pathogens*. **9**, 923 (2020).
2. Williamson, B., Tudzynski, B., Tudzynski, P. & Van Kan, J.A.L. Botrytis cinerea: The cause of grey mould disease. *Mol. Plant Pathol*. **8**, 561-580 (2007).

3. Weiberg, A. *et al*. Fungal small RNAs suppress plant immunity by hijacking Host RNA interference pathways. *Science*. **342**, 118-123 (2013).
4. Dean, R. *et al*. The Top 10 fungal pathogens in molecular plant pathology. *Mol. Plant Pathol*. **13**, 414-430 (2012).
5. Liang, Y. *et al*. Development of novel urease-responsive pendimethalin microcapsules using silica-IPTS-PEI as controlled release carrier materials. *ACS Sustain. Chem. Eng*. **5**, 4802-4810 (2017).
6. Droby, S., Wisniewski, M., Macarisin, D. & Wilson, C. Twenty years of postharvest biocontrol research: Is it time for a new paradigm? *Postharvest Biol. Technol*. **52**, 137-145 (2009).
7. Simonetti, G. *et al*. Prenylated flavonoids and total extracts from Morus nigra L. root bark inhibit in vitro growth of plant pathogenic fungi. *Plant Biosyst.* **151**, 783-787 (2017).
8. Usman, M. *et al*. Nanotechnology in agriculture: Current status, challenges and future opportunities. *Sci. Total Environ*. **721**, 137778 (2020).
9. Malinovskaya, Y. *et al*. Delivery of doxorubicin-loaded PLGA nanoparticles into U87 human glioblastoma cells. *Int. J. Pharm.* **524**, 77-90 (2017).

10. Sharma, A., Sood, K., Kaur, J. & Khatri, M. Agrochemical loaded biocompatible chitosan nanoparticles for insect pest management. *Biocatal. Agric. Biotechnol*. **18**, 101079 (2019).
11. Saallah, S. & Lenggoro, I. W. Nanoparticles carrying biological molecules: Recent advances and applications. *KONA Powder Part. J.* **35**, 89-111 (2018).
12. Patel, N. R., Damann, K., Leonardi, C. & Sabliov, C. M. Size dependency of PLGA-nanoparticle uptake and antifungal activity against Aspergillus flavus. *Nanomedicine*. **6**, 1381-1395 (2011).
13. Chronopoulou, L. *et al*. Microfluidic synthesis of methyl jasmonate-loaded PLGA nanocarriers as a new strategy to improve natural defenses in Vitis vinifera. *Sci. Rep.* **9**, 1-9 (2019).
14. Fukamachi, K., Konishi, Y., & Nomura, T. Disease control of Phytophthora infestans using cyazofamid encapsulated in poly lactic-co-glycolic acid (PLGA) nanoparticles. *Colloids Surf. A: Physicochem. Eng. Asp.* **577**, 315-322 (2019).
15. Simonetti, G. *et al*. Anti-Candida biofilm activity of pterostilbene or crude extract from non-fermented grape pomace entrapped in biopolymeric nanoparticles. *Molecules*, **24**, 2070 (2019).

16. Valletta, A. *et al*. Poly (lactic-co-glycolic) acid nanoparticles uptake by Vitis vinifera and grapevine-pathogenic fungi. *J. Nanoparticle Res*. **16**, 2744 (2014).
17. Palocci, C. *et al*. Endocytic pathways involved in PLGA nanoparticle uptake by grapevine cells and role of cell wall and membrane in size selection. *Plant Cell Rep*. **36**, 1917-1928 (2017).
18. Liu, J. *et al*. Fungal diversity in field mold-damaged soybean fruits and pathogenicity identification based on high-throughput rDNA sequencing. *Front. Microbiol*. **8**, 779 (2017).
19. Almeida, F., Rodrigues, M. L., & Coelho, C. The still underestimated problem of fungal diseases worldwide. *Front. Microbiol*. **10**, 214 (2019).
20. Medrano-Padial, C., Prieto, A. I., Puerto, M., & Pichardo, S. Toxicological Evaluation of Piceatannol, Pterostilbene, and ε-Viniferin for Their Potential Use in the Food Industry: A Review. *Foods*. **10**, 592 (2021).
21. Xu, D. *et al*. In vitro and in vivo effectiveness of phenolic compounds for the control of postharvest gray mold of table grapes. *Postharvest Biol. Technol.* **139**, 106-114 (2018).
22. Schmidlin, L. *et al*. A stress-inducible resveratrol O-methyltransferase involved in the biosynthesis of pterostilbene in grapevine. *Plant Physiol.* **148**, 1630-1639 (2008).

23. Bramosanti, M., Chronopoulou, L., Grillo, F., Valletta, A., & Palocci, C. Microfluidic-assisted nanoprecipitation of antiviral-loaded polymeric nanoparticles. *Colloids Surf. A: Physicochem. Eng. Asp.* **532**, 369-376 (2017).

24. Chronopoulou, L., Sparago, C. & Palocci, C. A modular microfluidic platform for the synthesis of biopolymeric nanoparticles entrapping organic actives. J. Nanopart. Res. **16**, 2703-2713 (2014).

25. Provencher, S. W. CONTIN: a general purpose constrained regularization program for inverting noisy linear algebraic and integral equations. *Comput. Phys. Commun.* **27**, 229-242 (1982).

26. Lorenzini, M., & Zapparoli, G. An isolate morphologically and phylogenetically distinct from Botrytis cinerea obtained from withered grapes possibly represents a new species of Botrytis. *Plant pathol*. **63**, 1326-1335 (2014).

27. Patzke, H., & Schieber, A. Growth-inhibitory activity of phenolic compounds applied in an emulsifiable concentrate-ferulic acid as a natural pesticide against Botrytis cinerea. *Int. Food Res. J.* **113**, 18-23 (2018).

28. Meletiadis, J. *et al*. EUROFUNG Network. Colorimetric assay for antifungal susceptibility testing of Aspergillus species. *J. Clin. Microbiol.* **39**, 3402-3408 (2001).

29. Hawker, L. E. & Hendy, R. J. An electron-microscope study of germination of conidia of Botrytis cinerea. *Microbiology*. **33**, 43-46 (1963).
30. Muse, E. S., Patel, N. R., Astete, C. E., Damann, K. E., & Sabliov, C. M. Surface association and uptake of poly (lactic-co-glycolic) acid nanoparticles by Aspergillus flavus. *Ther. Deliv*. **5**, 1179-1190 (2014).
31. Raj, V., Raorane, C. J., Lee, J. H., & Lee, J. Appraisal of Chitosan-Gum Arabic-Coated Bipolymeric Nanocarriers for Efficient Dye Removal and Eradication of the Plant Pathogen Botrytis cinerea. *ACS Appl. Mater. Interfaces*. **13**, 47354-47370 (2021).
32. Pezet, R. & Pont, V. Ultrastructural observations of pterostilbene fungitoxicity in dormant conidia of Botrytis cinerea Pers. *J. Phytopathol*. **129**, 19-30 (1990).
33. Xu, D. *et al*. Efficacy of pterostilbene suppression of postharvest gray mold in table grapes and potential mechanisms. *Postharvest Biol. Technol*. **183**, 111745 (2022).
34. Favaron, F., Lucchetta, M., Odorizzi, S., da Cunha, A.T.P., & Sella, L. The role of grape polyphenols on tran-resveratrol activity against Botrytis cinerea and fungal laccase on the solubility of putative grape PR proteins. *J. Plant Pathol*. **91**, 579–588 (2009).

35. Amiri, A., Heath, S. M., & Peres, N.A. Resistance to fluopyram, fluxapyroxad, and penthiopyrad in Botrytis cinerea from strawberry. *Plant Dis.* **98**, 532-539 (2014).
36. Dong, B. & Hu, J. Photodegradation of the novel fungicide fluopyram in aqueous solution: kinetics, transformation products, and toxicity evolvement. *Environ. Sci. Pollut. Res*. **23**, 19096-19106 (2016).
37. Zhou, J. *et al.* Study on environmental behaviour of fluopyram in different banana planting soil. *Sci. Rep.* **11**, 1-10 (2021).
38. Anandhi, S., Saminathan, V. R., Yasotha, P., Saravanan, P. T., & Rajanbabu, V. Nano-pesticides in pest management. *J. Entomol. Zool. Stud*. **8**, 685-690 (2020).
39. Du, W., Gao, Y., Liu, L., Sai, S., & Ding, C. Striking Back against Fungal Infections: The Utilization of Nanosystems for Antifungal Strategies. *Int. J. Mol. Sci.* **22**, 10104 (2021).

Author contributions

†Equally contributing authors

*Author to whom correspondence should be addressed.

G.P. C.P. and G.S. conceived the study design; G.D.A., G.S., L.C., A.O., C.B., V.P., F.P., and S.D. conducted the experiment(s); G.D.A.,

G.S. and L.C. analyzed the results; E.B., G.P., C.P. and G.S wrote the final manuscript. All authors reviewed the manuscript.

Competing interests

The authors declare no competing interests.

Chapter 5

Aspergillus section *Nigri* infections could be successfully treated with antifungal formulations applicated in nanomaterials or nanoparticles (NPs), in order to overcome the multi-resistance of fungi to existing drugs. *Aspergillus* section *Nigri* can be found in a wide variety of environments, including the hospital environment, and humans can contract invasive aspergillosis and otomycosis from these fungi (Li et al., 2015). *Aspergillus* section *Nigri* consists of several species including *A. niger*, *A. melleus*, *A. sulphureus*, *A. brasilensis*, *A. ostianus*, *A. petrakii*, *A. scletotium*, *A. carbonarius*, *A. aculeatus*, *A. japonicus*, *A. tubingensis*. In agriculture, the majority of the black *Aspergillus* species are associated with grapes, maize, onions, and peanuts, where they are cited as pathogens causing such diseases as peanut and maize seedling blight, and maize kernel rot (Palencia et al., 2010). They cause innumerable damages not only for their ability to destroy several agronomically important food crops, but also due to their capacity to produce several mycotoxins and to causing pulmonary aspergillosis, otomycosis and eye infections in humans (Sarvestani et al., 2022). In this work, the uptake of PLGA-NPs loaded with the fluorescent probe Coumarin 6 was studied in *A. brasiliensis* conidia, mycelium and biofilm by confocal microscope. In addition, it has been demonstrated that the pterostilbene, a trans-stilbene compound methylated derivative of resveratrol, can be addressed by nanoparticles to reduce the infections caused by *A. brasiliensis*, section *Nigri*, biofilm.

Poly-(lactic-co-glycolic) acid nanoparticles entrapping pterostilbene for targeting *Aspergillus* section *Nigri*

Paper published in *Molecules*

DOI: 10.3390/molecules27175424

Anastasia Orekhova [1,†], Cleofe Palocci [2,3,†], Laura Chronopoulou [2], Giulia De Angelis [4], Camilla Badiali [4], Valerio Petruccelli [4], Simone D'Angeli [4], Gabriella Pasqua [4] and Giovanna Simonetti [4,*]

Department of Public Health and Infectious Diseases, Sapienza University of Rome, P.le A. Moro 5, 00185 Rome, Italy; anastasia.orekhova@uniroma1.it (A.O.)

[2] Department of Chemistry, Sapienza University of Rome, P.le A. Moro 5, 00185 Rome, Italy; cleofe.palocci@uniroma1.it (C.P.); laura.chronopoulou@uniroma1.it (L.C.)

[3] Research Center for Applied Sciences to the safeguard of Environment and Cultural Heritage (CIABC), P. le A. Moro 5, 00185 Rome, Italy;

[4] Department of Environmental Biology, Sapienza University of Rome, P. le A. Moro 5, 00185 Rome, Italy; g.deangelis@uniroma1.it (G.D.A.); camilla.badiali@uniroma1.it (C.B.); valerio.petruccelli@uniroma1.it (V.P.); simone.dangeli@uniroma1.it (S. D'.A.); gabriella.pasqua@uniroma1.it (G.P.)

Abstract

Poly-(lactic-*co*-glycolic) acid (PLGA) is a biodegradable, biosafe, and biocompatible copolymer. The *Aspergillus* section *Nigri* causes otomycosis localized in the external auditory canal. In this research, *Aspergillus brasiliensis*, a species belonging to the *Nigri* section, was tested. Coumarin 6 and pterostilbene loaded in poly-(lactic-co-glycolic) acid nanoparticles (PLGA-coumarin6-NPs and PLGA-PTB-NPs) were tested for fungal cell uptake and antifungal ability against *A. brasiliensis* biofilm, respectively. Moreover, the activity of PLGA-PTB-NPs in inhibiting the *A. brasiliensis* infection was tested using *Galleria mellonella* larvae. The results showed a fluorescence signal, after 50 nm PLGA-coumarin6-NPs treatment, inside *A. brasiliensis* hyphae and along the entire thickness of the biofilm matrix, which was indicative of an efficient NP uptake. Regarding antifungal activity, a reduction in *A. brasiliensis* biofilm formation and mature biofilm with PLGA-PTB-NPs has been demonstrated. Moreover, *in vivo* experiments showed a significant reduction in mortality of infected larvae after injection of PLGA-PTB-NPs compared to free PTB at the same concentration. In conclusion, the PLGA-NPs system can increase the bioavailability of PTB in *Aspergillus* section *Nigri* biofilm by overcoming the biofilm matrix barrier and delivering PTB to fungal cells.

Keywords: *Aspergillus* section *Nigri*; pterostilbene; PLGA-NPs; *Galleria mellonella*; biofilm

Introduction

It is well known that despite the availability of several effective agents in the antifungal drug arena, their therapeutic outcome is less than optimal due to limitations related to drug physicochemical properties and toxicity. For instance, poor aqueous solubility and toxicity limit the formulation options and efficacy of several antifungal drugs [1]. On this basis, researchers have started exploring new opportunities for antifungal treatment, including novel antifungals and alternative approaches to treating fungal affections; for example, the use of nano vectors [2]. Moreover, recently, the development of nanotechnology and its applications in medical and health sciences has increased dramatically, allowing access to different kinds of nanoparticles (NPs), with well-defined active moieties to target human cells. A broad spectrum of drugs, such as small hydrophobic and hydrophilic drugs, as well as biological molecules, can be delivered in a controlled manner with NPs. NPs, ranging from 1 to 100 nm, can be easily employed as antifungal drug delivery vehicles. NPs have the possibility to enable closer contact with fungal cell membranes, thus facilitating their cellular uptake and controlled release of the drug within the cell environment [3–5]. Poly-(lactic-co-glycolic) acid (PLGA) is one of the

most widely used and promising biopolymers for the development of drug delivery systems [6]. It is biodegradable and its degradation products, lactic acid and glycolic acid, are metabolized in the body via the Krebs cycle [7]. Therefore, PLGA systemic toxicity is negligible, and its use has been approved by the FDA and other regulating agencies. PLGA-based NPs and microparticles are currently being studied for the development of new drug-delivery systems for various drugs (i.e., chemotherapies, antiseptics, antioxidants), and some of them have already been approved by the FDA or are in clinical phase trials [6,8]. We previously reported the activity of PLGA-NPs in entrapping pterostilbene on *Candida albicans* and *Botrytis cinerea* [9,10]. To date, there are no publications on the activity of PLGA-NPs against *Aspergillus* biofilm. *Aspergillus* is a broad fungal genus comprising more than 300 different species, distributed ubiquitously worldwide. *Aspergillus* is a genus of filamentous fungi found in many habitats such as soil, air, water, and decaying plant material, and it can develop under a wide range of environmental conditions [11]. Species belonging to *Aspergillus* section *Nigri* have been difficult to classify due to their phenotypic similarities [12]. *Aspergillus* section *Nigri* includes species causing pulmonary aspergillosis and otomycosis in humans, as well as localized and disseminated diseases in domestic and wild animals. Otomycosis, the fungal infection caused by *Aspergillus* section *Nigri*, is localized in the external auditory canal, and less commonly in the middle ear [13,14]. Currently, the treatment options

for otomycosis are still limited. The disease is hard to eradicate, and recurrence rates as high as 15% can be seen [15].

Aspergillus section *Nigr*i is rarely differentiated at the species level when originating from human specimens. Some members of *Aspergillus* section *Nigri* ('black aspergilli') are *Aspergillus niger*, *Aspergillus welwitschiae*, *A. tubingensis*, and *A. brasiliensis*. *Aspergillus welwitschiae* is often collected from the external ear canal, whereas *A. tubingensis* and *A. niger* are predominant in respiratory samples [16]. *A. brasiliensis* is a species closely related to *Aspergillus niger* [17]. Moreover, *A. brasiliensis* (DSM 1988) is a reference microorganism, used to study the fungicidal effect of disinfectants and antiseptics (UNE EN 2019) [18].

Otomycosis is a biofilm-related infection. Resistance to antifungal treatments is also mediated by the development of *Aspergillus* biofilm, which provides temporary antifungal drug resistance and protects the pathogen in a hostile environment. The biofilm matrix reduces the entry and the diffusion of antifungal agents. New strategies against biofilms are needed. Pterostilbene (PTB) is a 3,5-dimethylated derivative of resveratrol that originates from several natural plant sources and that has shown strong activity against some fungal pathogens [9,19]. Recent literature studies have reported that PTB inhibits *C. albicans* biofilm [9,20]. The effect of PTB on fungal cells was related to the downregulation of the Ras/cAMP pathway and the ergosterol biosynthesis, which both contribute to the antibiofilm effect of PTB

[21]. In the present study, the use of PTB loaded into NPs was evaluated with the aim of significantly improving drug performance [2]. In particular, PLGA-NPs entrapping PTB were employed to target *A. brasiliensis* section *Nigri* and its biofilm.

Results

NPs Preparation and Characterization

PLGA-NPs with different payloads were characterized by DLS, ζ-potential, and SEM measurements. Hydrodynamic diameter, PDI, ζ-potential, and morphology were not significantly affected by the entrapment of 6-coumarin or PTB inside PLGA-NPs. Typical samples presented an average diameter of 50 nm, with a PDI below 0.2 (Figure 1A), and had a ζ-potential of ~ −25 mV. SEM analysis revealed spherical morphology for all preparations (Figure 1B).

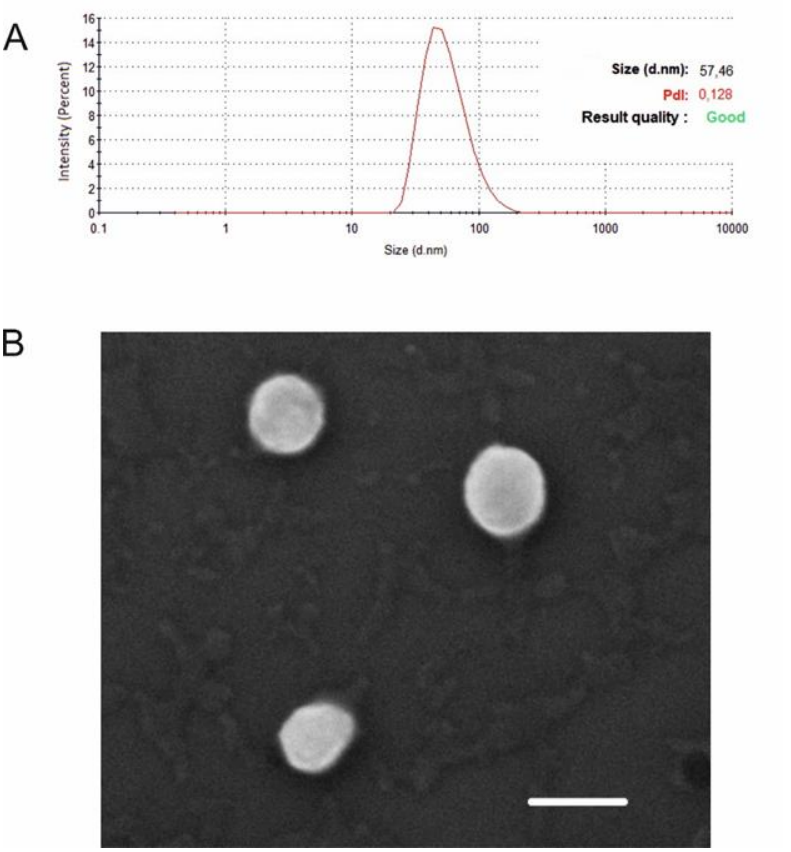

Figure 1. Size distribution by intensity and PDI of PLGA-PTB-NPs, as measured by DLS (**A**). SEM micrographs of PLGA-PTB-NPs (Scale bar: 100 nm) (**B**).

PLGA-PTB-NPs had drug content of 0.375 mg of PTB/mg of PLGA, corresponding to an encapsulation efficiency of 75%. As previously reported [10] by the authors, the amount of PTB released in buffer

solutions at different pH was low due to the poor water solubility of the drug, reaching the final value of 30 μg/mL within 5 days in plateau conditions.

Microscopic Observations of NP Uptake in *Aspergillus* Conidia, Mycelium, and Biofilm

In order to verify PLGA-NP uptake into *A. brasiliensis* conidia, mycelium, and biofilm, PLGA-NPs were loaded with the highly fluorescent probe coumarin 6, allowing them to be visualized under fluorescence microscopy. Results obtained with microscopic observations showed that 50 nm PLGA-coumarin6-NPs have the ability to penetrate conidia depending on their morphology. The conidia do not allow the internalization of NPs (Figure 2A, indicated by the yellow arrow). Only when the envelope breaks are NPs able to interact with the conidia capsule (Figure 2A, B red arrow). In the germ tube and hyphae, the fluorescence images report that 50 nm NPs were clearly visible up to 1 μm below the fungal wall (Figure 2C). The uptake of PLGA-coumarin6-NPs on biofilm was evident 60 min after administration (Figure 3A, B), the image showed that the 50 nm PLGA-NPs diffuse through the polysaccharide-derived extracellular matrix. No autofluorescence was detected from the conidia, mycelium, and biofilm alone (data not shown).

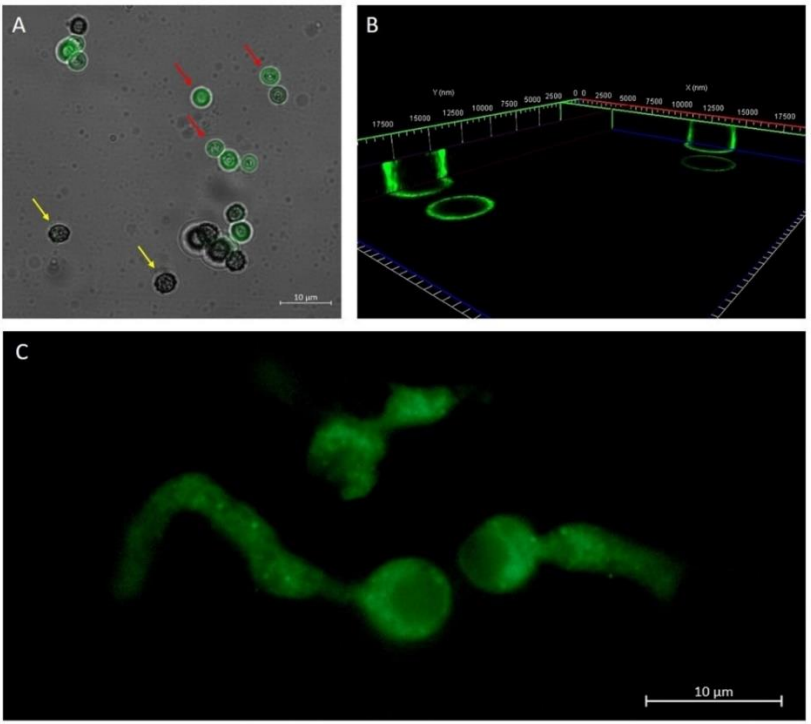

Figure 2. Overlap of the bright field image and the fluorescence image, which shows *A. brasiliensis* conidia treated for 10 min with 50 nm PLGA-coumarin6-NPs. In the first stage of conidia development (yellow square) the protective envelope did not allow interaction with NPs. In a later stage of conidia development (red square), when the envelope broke, fluorescence along the conidia capsule was observed (**A**). A 3D reconstruction of *A. brasiliensis* conidia treated with NPs for 10 min. The fluorescence signal was detected along the wall of the conidia (**B**). Fluorescence image of the hyphae of the newly germinated *A. brasiliensis* conidium treated with 50 nm PLGA-coumarin6 -NPs. The fluorescence signal inside *A. brasiliensis* hyphae is visible after 1 h of NPs administration (**C**).

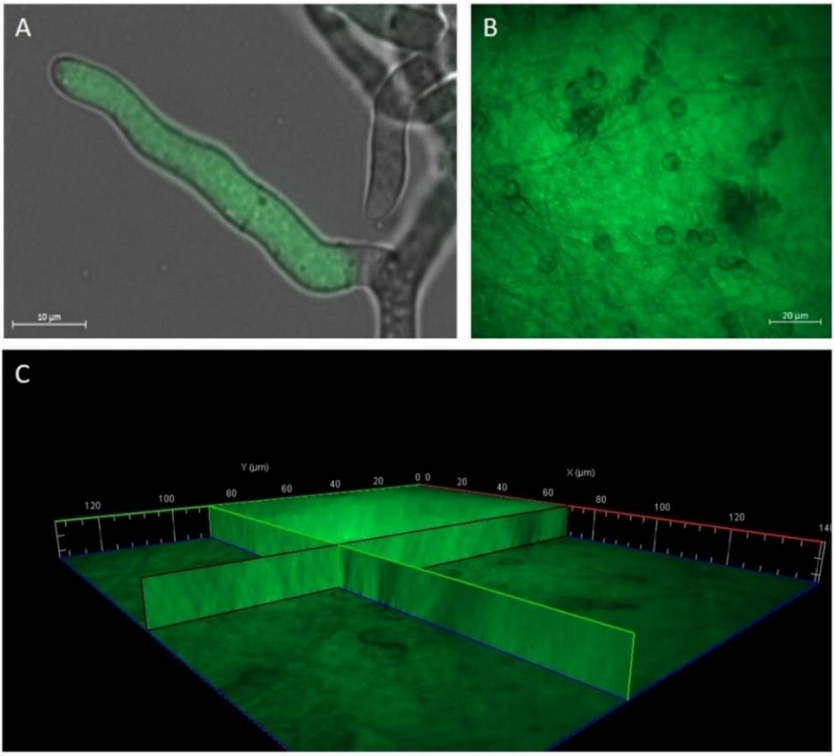

Figure 3. Observation of *A. brasiliensis* mycelium and biofilm treated with 50 nm PLGA-coumarin6-NPs. Overlap of the bright field image and the fluorescence image, which shows the localization of PLGA-coumarin6-NPs inside the fungal hypha (**A**). Presence of NPs within the biofilm (**B**). A 3D reconstruction of biofilm treated with NPs for 60 min. The fluorescence signal was detected along the entire thickness of the biofilm matrix (**C**).

Antifungal Activity of PLGA-PTB-NPs

In vitro antifungal activity of free PTB and PLGA-PTB-NPs against biofilm in formation and preformed biofilm at different stages of formation (24 h and 28 h) has been determined by evaluating the *in vitro* metabolic activity of fungal cells. The results showed that after 24 h of incubation with PLGA-PTB-NPs, the PTB loaded into PLGA-NPs showed a significantly better activity compared to free PTB in all the experiments at a concentration of 20 µg/mL (Figure 4). Empty NPs did not show antifungal activity.

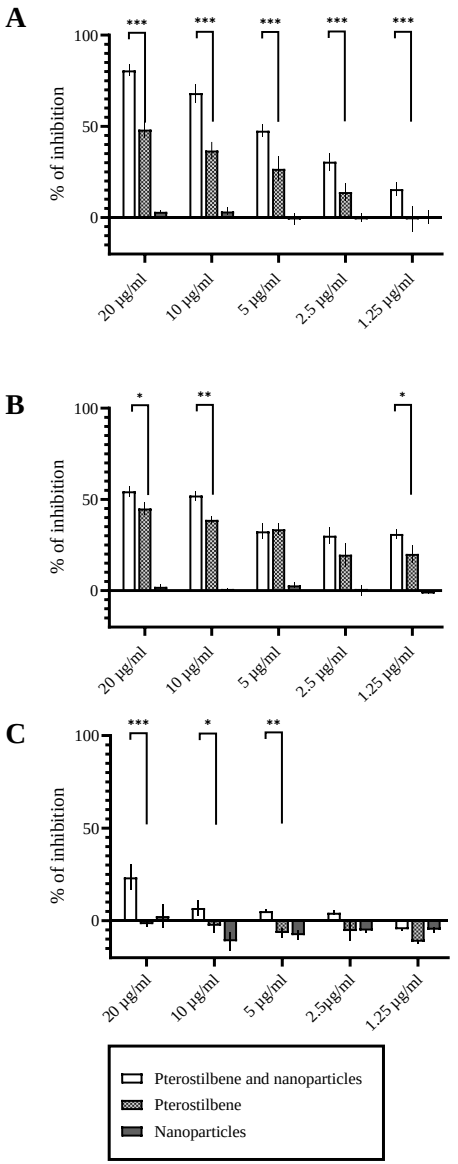
A
B
C
% of inhibition
100
50
0
***
**
*
20 µg/ml
10 µg/ml
5 µg/ml
2.5 µg/ml
2.5µg/ml
1.25 µg/ml
Pterostilbene and nanoparticles
Pterostilbene
Nanoparticles

Figure 4. Activity of free PTB and PLGA-PTB-NPs against *A. brasiliensis* (DSM 1988). Activity of free PTB and PLGA-PTB-NPs against *A. brasiliensis* biofilm in formation, after 24 h of incubation (**A**). Activity of free PTB and PLGA-PTB-NPs against *A. brasiliensis* 24 h biofilm, after 24 h of incubation (**B**). Activity of free PTB and PLGA-PTB-NPs against 48 h biofilm, after 24 h of incubation (**C**). * $p < 0.05$ compared to the control; ** $p < 0.01$ compared to the control *** $p < 0.001$ compared to the control.

Activity of PLGA-PTB-NPs on a Model of Aspergillosis in *G. mellonella*

As previously reported, *G. mellonella* is a suitable model for testing the efficacy of antifungal agents against aspergillosis [22]. *G. mellonella* larvae were infected with conidial suspensions of *A. brasiliensis*. Mortality curves were used to calculate the lethal dose (data not shown). Assessment of the efficacy of PTB or PLGA-PTB-NP treatment was based on mortality in the lethal model. A dose-dependent reduction in mortality was observed after antifungal treatment with PTB and PLGA-PTB-NPs. PLGA-PTB-NPs were more effective than free PTB. The activity of PLGA-PTB-NPs was maximal at the highest concentration (Figure 5).

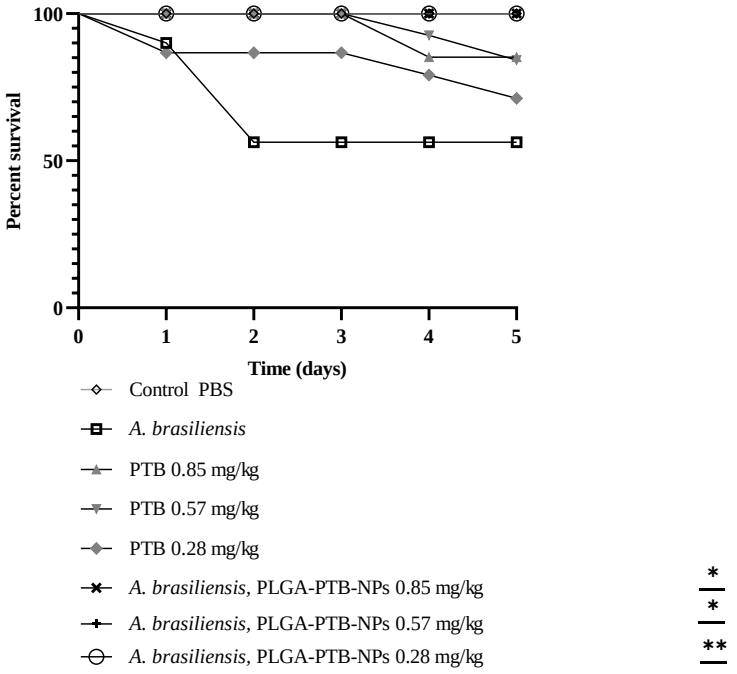

Figure 5. PLGA-PTB-NPs reduces *A. brasiliensis* virulence in *G. mellonella* model. Survival curves of *G. mellonella* larvae ($n = 10$/strain) infected via injection with 2×10^4 conidia from *A. brasiliensis* with free PTB. Larvae were monitored for 5 days post-infection. Statistical significance relative to control was judged by the Kaplan–Meier followed by Mantel–Cox log-rank tests. At least three independent biological replicates were carried out for each experiment. * $p < 0.05$ compared to the free PTB and PLGA-PTB-NPs; ** $p < 0.01$ compared to the free PTB and PLGA-PTB-NPs.

Toxicity on *Galleria mellonella* Larvae Model

PLGA-PTB-NPs were tested in an *in vivo* model by selecting the larvae of *Galleria mellonella* as a fungal *in vivo* model. *G. mellonella* was infected with *A. brasiliensis* (DSM 1988) conidia and treated with PLGA-PTB-NPs, PTB, and PLGA-NPs. To calculate the lethal dose, mortality curves were previously determined (data not shown). After inoculation with 4×10^4 to 5×10^4 conidia/larvae of *A. brasiliensis*, death was reported daily for 5 days. In the groups of untouched larvae and larvae inoculated with PBS, mortality was equal to 0%. Conversely, in the group of larvae infected with *A. brasiliensis*, the mortality rate was 45% at day 5 post-infection. Subsequently, using the same inoculum concentration, the larvae were inoculated with PLGA-PTB-NPs and PTB in a concentration range from 2.85 mg/kg to 0.089 mg/kg and from 1.35 mg/kg to 0.042 mg/kg, respectively. These results indicated a clear relationship between the concentrations of PLGA-PTB-NPs or free PTB and the mortality rate (Figure 5). The LD_{50} detected dose was more than 1.35 mg/kg for PTB and 2.855 mg/ kg for PLGA, alone and in combination (Table 1).

Table 1. Survival of *G. mellonella* larvae following administration of PLGA-NPs, PTB, and PLGA-PTB-NPs by intra-hemocoel injection. Every experiment was conducted with 10 larvae for each group in triplicate. All values are the mean of three independent experiments.

Chemical	LD_{50} (mg/kg)	Solvent
PLGA-NPs	> 2.85	H_2O
PTB	> 1.35	100 H_2O: 1 DMSO
PLGA-PTB-NPs	> 2.85–1.35	100 H_2O: 1 DMSO

Discussion

Aspergillus section *Nigri*, which include 26 species of black *Aspergillus*, are ubiquitous in the environment and in the hospital indoor environment. Clinically important species of *Aspergillus* section *Nigri*, such as *A. niger* and *A. tubingensis*, are the second most frequent agents that cause invasive aspergillosis and are the cause of otomycosis [23]. Among *Aspergillus* section *Nigri*, *A. brasiliensis* (DSM1988) has a conidial size of 3.5–4.5 μm, and growth and sporulation at 37 °C. Moreover, the growth on Czapek yeast autolysate agar with 5% NaCl is indicative of a close relationship with *A. niger* [17]. *A. brasiliensis* is used as a reference fungal species for the evaluation of the efficacy of compounds with antiseptic activity [18]. In this study, the well-

characterized strain, *Aspergillus brasiliensis* (DSM1988) (ATCC16404), was chosen for use.

Aspergillus spp. are recognized as the fungi that form biofilms [24]. The negative consequences of biofilms are widely reported [14]. *Aspergillus* diseases are often associated with biofilm formation that increases host inflammation, rapid disease progression, and mortality. Biofilm is a microbial adaptation to the environment, resulting in antimicrobial resistance. Some *Aspergillus* species are resistant to antifungal treatment. The extracellular matrix, a defining feature of biofilm, is a complex mixture of biomacromolecules which contributes to reduced antimicrobial susceptibility.

The goal of this study was to investigate the antifungal activity of pterostilbene entrapped in poly(lactic-co-glycolic) acid nanoparticles (PLGA-NPs) on *A. brasiliensis* conidia, hyphae, and biofilm. Most studies have reported the antibiofilm effect of pure natural compounds included in nanosystems against *Candida* spp. biofilms, but only a few papers have reported the activity against *Aspergillus* spp. To eradicate biofilms, it is essential that NPs penetrate the matrix because it offers protection to pathogens, reducing cells' susceptibility to antimicrobials [25]. However, knowledge of NPs–biofilm interactions is still limited. As previously reported, PLGA-NPs can penetrate fungal conidia and hyphae of species belonging to the *Aspergillus* genus. Patel and colleagues tested PLGA-NPs, loaded with coumarin 6, at 203 nm and 1206 nm and demonstrated that the uptake in *A. flavus* spores and

mycelium depends on NP size. The smaller NPs tested (203 nm) were internalized more efficiently after 1 h of incubation than the bigger ones [26]. Muse and colleagues studied the uptake of PLGA-NPs covalently tagged with tetramethyl rhodamine isothiocyanate (TRITC), a red fluorescent compound (PLGA-TRITC), and PLGA-TRITC loaded with coumarin (double tagged), showing a clear surface association between NPs and *A. flavus* cells, while smaller NPs (30–50 nm) were internalized, allowing us to observe a red fluorescence inside the cells [27]. In general, for all cell types and organisms, the results suggest that smaller NPs are internalized more effectively by cells [28]. Moreover, PLGA-based NPs have been approved for many biomedical applications, such as delivery devices, and are considered safe for in vivo testing and applications. PLGA is a well-known random copolymer with physical and mechanical properties that can be easily tuned by altering the lactide to glycolate ratio, and by using nanoprecipitation techniques, it is possible to produce biodegradable nanoparticles with a controlled size and narrow size distribution [29]. In this study, we have shown that 50 nm PLGA-coumarin6-NPs can penetrate conidia only at a later germination stage; when the envelope breaks, conidia lose the pili layer and NPs can interact with the conidia capsule. Fang et al. have described conidia structure in detail. The authors reported that the surface roughness of conidia was approximately 33 nm [30]. Moreover, 50 nm NPs have been detected within the hyphae of the newly germinated conidia, at a distance of 1

μm below the fungal wall. PLGA-coumarin6-NP uptake by fungal biofilm was largely demonstrated and 50 nm PLGA-NPs diffused through the polysaccharide-derived extracellular matrix without any difficulty and remained entrapped even after rinsing with water. Regarding the antifungal activity, the anti-*Candida* activity of NPs - PTB- PLGA against *Candida albicans* biofilm was previously reported [9]. The increase in the activity of pterostilbene during the biofilm formation and after 24 h growth confirms our results, which were obtained by means of microscopy images. Moreover, recent studies have demonstrated that fungal virulence factors have similar and overlapping roles in mammalian and *G. mellonella* hosts, implying that *G. mellonella* studies can be transferred to mammals. *G. mellonella* are beneficial organisms for elucidating virulence factors, fungal signal or regulatory pathways, and the examination of antifungal pharmaceuticals [22,31]. In this study, PLGA-PTB-NPs proved to be more effective than free PTB in reducing, in a dose-dependent manner, the mortality of *G. mellonella*. Furthermore, the concentrations used in the in vivo tests were not toxic, as demonstrated in the evaluation of toxicity on *G. mellonella* larvae (LD_{50} more than 1.35 mg/kg for PTB and 2.855 mg/kg for PLGA alone and in combination). In conclusion, the *in vitro* and *in vivo* results have demonstrated that the antifungal compounds can be addressed by nanoparticles to reduce the infections caused by *A. brasiliensis,* section *Nigri,* biofilm.

Materials and Methods

Materials

Pterostilbene (PTB) was purchased from Chemodex (St. Gallen, Switzerland). Poly(D, L)-lactic-co-glycolic acid (PLGA, lactide: glycolide 50:50, MW 50 kDa), Coumarin 6 (98%), and all other chemicals and reagent-grade solvents were purchased from Sigma-Aldrich (St. Louis, MO, USA) and used as received.

Preparation and Characterization of PLGA-PTB-NPs and PLGA-coumarin6-NPs

PLGA-NPs loaded with either PTB (PLGA-PTB-NPs) or the fluorescent probe coumarin 6 (PLGA-coumarin6-NPs) were prepared based on our previous works, using a microfluidic reactor with a flow-focusing configuration through a nanoprecipitation mechanism [9,10,32]. Dynamic light scattering (DLS) and ζ-potential measurements were carried out using a NanoZetasizer (Malvern Instruments, Malvern, UK) to measure the mean hydrodynamic diameter of PLGA-NPs and their polydispersity index (PDI). The experimental conditions used are the following: a helium–neon laser operating at 633 nm, a fixed scattering angle of 173°, and a constant temperature (25.0 ± 0.1 °C). The measured autocorrelation functions of the scattered light intensity were analyzed using the CONTIN algorithm in order to obtain the decay time distributions, used to determine the distributions of the diffusion coefficients of the particles (D), converted

into the distributions of the apparent hydrodynamic radii, R_H, using the Stokes–Einstein relationship: $R_H = k_BT/6\pi\eta D$ (k_BT = thermal energy; η = solvent viscosity). The electrophoretic mobility μ of particles, measured by combined laser Doppler velocimetry (LDV) and phase analysis light scattering (PALS), was converted into their ζ-potential using the Smoluchowski relation $\zeta = \mu\,\eta/\varepsilon$ (ε=solvent permittivity).

Particle morphology was investigated by means of scanning electron microscopy (SEM) in both the secondary and the backscattered electron modes with an electron acceleration voltage of 20 keV, using an LEO 1450VP SEM microscope (ZEISS, Oberkochen, Germany). The quantitative analysis of PTB entrapped within PLGA-NPs was carried out using spectroscopic measurements. NP aqueous suspensions were ultra-centrifuged at a low temperature (14.000 rpm, 15 min, 4 °C) to recover NPs. The supernatant was discarded, the pellet was dissolved in acetone and analyzed by measuring the UV PTB absorbance at 313 nm, and the results were compared with a calibration curve within the concentration range between 0.002 and 0.01 mg/mL ($R^2 = 0.9822$).

The encapsulation efficiency (EE) and loading capacity (LC) were calculated using the following equations:

$$EE\ \% = (\text{total drug added-free non entrapped drug})/(\text{total drug added}) \times 100 \quad (1)$$

$$LC\ \% = (\text{Amount of entrapped drug})/(\text{total nanoparticle weight}) \times 100 \quad (2)$$

For studying the in vitro PTB release from PLGA-PTB-NPs, a fixed number of NPs were suspended in an acetate buffer at pH = 4.0 or in a PBS solution at pH = 7.4 and then incubated at 25 °C under magnetic stirring. At selected time intervals, fixed amounts of supernatant were collected and their PTB content was determined using the spectrophotometric method described above.

Fungal Strain and Culture Condition

A. brasiliensis (DSM 1988), formerly *A. niger* (DSM 1988), species *Aspergillus* section *Nigri* from the German Collection of Microorganisms (DSMZ, Braunschweig, Germany) was used as a reference strain in this study. *A. brasiliensis* (DSM 1988), the quality control strain, is used in preservative testing of pharmaceuticals, and in sterility testing. The strain was grown for five days on potato dextrose agar (Sigma Aldrich, St. Louis, MI, USA). The conidia were collected with phosphate-buffered saline and the concentration was determined with a Thoma counting chamber. RPMI medium (RPMI 1640 with L-glutamine, without bicarbonate) buffered to pH 7.0 with 0.165 M MOPS was used for antifungal tests.

Fungal Uptake of PLGA-coumarin6-NPs

The suspension of PLGA-coumarin6-NPs was added to *A. brasiliensis* (DSM 1988). *A. brasiliensis* conidia (1×10^5 conidia/mL) were inoculated into 24 g/L of potato dextrose broth (PDB) and after 12 h and 24 h PLGA-coumarin6-NPs, at a final concentration of 0.1 mg/mL,

were added. Fungal suspensions were placed on a microscope slide after 10 and 60 min. Mycelium, germ tube, and conidia were observed using an ApoTome fluorescence microscope. For PLGA-coumarin6-NPs uptake in *Aspergillus* biofilm, 1×10^5 conidia/mL were cultured on glass microscope slides placed into Petri dishes containing PDB and incubated for 48 h. PLGA-coumarin6-NPs at a final concentration of 0.1 mg/mL were added to the biofilm. The biofilm was rinsed with sterile water and observed under an ApoTome fluorescence microscope after 60 min. The control of untreated conidia, mycelium and biofilm was observed to reveal any auto-fluorescence.

Microscopic Analysis

Conidia, mycelium, and biofilm treated with PLGA-coumarin6-NPs were observed, and images were acquired using an Axio Imager M2 fluorescence microscope (Zeiss, Wetzlar, Germany) motorized on the 3 axes by using a FITC filter (λ excitation BP 455-495 nm; λ emission BP 05-555 nm). The thickness of the sample provided a Z-stack image scan performed with an Axiocam 512 (Zeiss) monochromatic camera and ApoTome 2 (Zeiss) as a fringe projection module to eliminate the out-of-focus signal. Zen 2.5 (Zeiss) image analysis software was used to obtain single-plane images as Z-stack maximum projection.

In Vitro Antifungal Activity of PLGA-PTB-NPs against Biofilm Formation and Preformed Biofilm

In vitro antifungal activity against in formation and preformed biofilm was carried out as previously described [33]. *A. brasiliensis* conidia were inoculated with PLGA-PTB-NPs or free PTB and incubated in RPMI for 24 h and 48 h. Biofilm grown in 96 flat-well plates was inoculated with PLGA-PTB-NPs or free PTB.

After incubation for 24 h, the cells were washed and the metabolic activity, with 2,3-bis-(2-methoxy-4-nitro-5-sulfophenyl)-2H-tetrazolium-5-carboxamide (XTT) reduction assay, was evaluated. XTT-menadione was added, and after incubation, the optical density at 450 nm was measured. Each experiment was performed at least three times, in triplicate, on separate dates [33].

Toxicity of PLGA-PTB-NPs, Free PTB, and PLGA-NPs on *Galleria mellonella* Larvae Model

In vivo toxicity studies using the *G. mellonella* larvae were carried out as previously reported [34].

Larvae, of the sixth developmental stage of *G. mellonella* (Lepidoptera: Pyralidae, the Greater Wax Moth), (obtained from Blu Fish Rome) were stored in wood shavings in the dark at 18 °C before use. Larvae with color alterations (i.e., dark spots or apparent melanization) were excluded and those weighing 0.3–0.4 g were selected for experimental use. Larvae were injected with different PTB concentrations, free or

entrapped within PLGA-NPs, or with empty PLGA-NPs. Controls included larvae injected with or without a sterile physiological saline solution. Survival was monitored over 120 h. Larvae death was monitored by visual inspection of the color (brown–dark brown) and lack of movement after touching them with forceps. Each experiment was performed in triplicate.

In Vivo Activity of PLGA-PTB-NPs

G. mellonella larvae were infected with *A. brasiliensis* (4×10^4 to 5×10^4 conidia/larvae), with or without different concentrations of PLGA-PTB-NPs or PTB. Survival was monitored over 120 h. Larvae death was monitored by visual inspection of the color (brown–dark brown) and lack of movement after touching them with forceps. Each experiment was performed in triplicate.

Statistical Analysis

The data were expressed as mean ± s.e.m. $p < 0.05$ was considered statistically significant. Statistical criteria, *p*, and other parameters are shown for each experiment. *G. mellonella* survival was displayed via Kaplan–Meier curves. The statistical data analysis was performed using the GraphPad Prism 8 software (GraphPad Software Inc., La Jolla, CA, USA).

Author Contributions: Conceptualization, G.S., A.O., G.P., and C.P.; methodology, A.O., L.C., C.B., G.D.A., V.P., and S.D'.A.; validation,

G.S., A.O., C.P., and G.P.; formal analysis, A.O., C.P., L.C., C.B., G.D.A., and V.P.; writing—original draft preparation, G.S., A.O., G.P., C.P., L.C., C.B., G.D.A., V.P., and S.D'.A.; writing—review and editing, G.S., A.O., C.P., L.C., and G.P.; supervision, G.S., A.O., C.P., and G.P.; project administration, G.S.; funding acquisition, G.S. All authors have read and agreed to the published version of the manuscript.

Funding: This research was funded by a research project of Sapienza University (grant number: RM120172A34CFCC9).

Institutional Review Board Statement: Not applicable.

Informed Consent Statement: Not applicable.

Data Availability Statement: The data presented in this study are available in this article.

Conflicts of Interest: The authors declare no conflicts of interest.

Sample Availability: Not available.

References

1. Nucci, M.; Perfect, J.R. When Primary Antifungal Therapy Fails. *Clin. Infect. Dis.* **2008**, *46*, 1426–1433. https://doi.org/10.1086/587101.
2. Soliman, G.M. Nanoparticles as Safe and Effective Delivery Systems of Antifungal Agents: Achievements and Challenges. *Int. J. Pharm.* **2017**, *523*, 15–32. https://doi.org/10.1016/j.ijpharm.2017.03.019.

3. Nami, S.; Aghebati-Maleki, A.; Aghebati-Maleki, L. Current Applications and Prospects of Nanoparticles for Antifungal Drug Delivery. *EXCLI J.* **2021**, *20*, 562. https://doi.org/10.17179/EXCLI2020-3068.
4. Nagaraj, S.; Manivannan, S.; Narayan, S. Potent Antifungal Agents and Use of Nanocarriers to Improve Delivery to the Infected Site: A Systematic Review. *J. Basic Microbiol.* **2021**, *61*, 849–873. https://doi.org/10.1002/jobm.202100204.
5. Osanloo, M.; Assadpour, S.; Mehravaran, A.; Abastabar, M.; Akhtari, J. Niosome-Loaded Antifungal Drugs as an Effective Nanocarrier System: A Mini Review. *Curr. Med Mycol.* **2019**, *4*, 31–36. https://doi.org/10.18502/cmm.4.4.384.
6. Pardeshi, S.R.; Nikam, A.; Chandak, P.; Mandale, V.; Naik, J.B.; Giram, P.S. Recent Advances in PLGA Based Nanocarriers for Drug Delivery System: A State of the Art Review. *Int. J. Polym. Mater. Polym. Biomater.* **2021**, *1*, 1–30. https://doi.org/10.1080/00914037.2021.1985495.
7. Dinarvand, R.; Sepehri, N.; Manouchehri, S.; Rouhani, H.; Atyabi, F. Polylactide-Co-Glycolide Nanoparticles for Controlled Delivery of Anticancer Agents. *Int. J. Nanomed.* **2011**, *6*, 877. https://doi.org/10.2147/IJN.S18905.
8. Park, K.; Skidmore, S.; Hadar, J.; Garner, J.; Park, H.; Otte, A.; Soh, B.K.; Yoon, G.; Yu, D.; Yun, Y.; et al. Injectable, Long-Acting PLGA Formulations: Analyzing PLGA and Understanding Microparticle

Formation. *J. Control. Release* **2019**, *304*, 125–134. https://doi.org/10.1016/j.jconrel.2019.05.003.

9. Simonetti, G.; Palocci, C.; Valletta, A.; Kolesova, O.; Chronopoulou, L.; Donati, L.; Di Nitto, A.; Brasili, E.; Tomai, P.; Gentili, A.; et al. Anti-Candida Biofilm Activity of Pterostilbene or Crude Extract from Non-Fermented Grape Pomace Entrapped in Biopolymeric Nanoparticles. *Molecules* **2019**, *24*, 2070. https://doi.org/10.3390/molecules24112070.
10. De Angelis, G.; Simonetti, G.; Chronopoulou, L.; Orekhova, A.; Badiali, C.; Petruccelli, V.; Portoghesi, F.; D'Angeli, S.; Brasili, E.; Pasqua, G.; et al. A Novel Approach to Control Botrytis Cinerea Fungal Infections: Uptake and Biological Activity of Antifungals Encapsulated in Nanoparticle Based Vectors. *Sci. Rep.* **2022**, *12*, 7989. https://doi.org/10.1038/s41598-022-11533-w.
11. Paterson, R.R.M.; Lima, N. (Eds.) *Molecular Biology of Food and Water Borne Mycotoxigenic and Mycotic Fungi*; CRC Press: Boca Raton, FL, USA, 2015; ISBN 978-0-429-08764-6.
12. Iatta, R.; Nuccio, F.; Immediato, D.; Mosca, A.; De Carlo, C.; Miragliotta, G.; Parisi, A.; Crescenzo, G.; Otranto, D.; Cafarchia, C. Species Distribution and In Vitro Azole Susceptibility of *Aspergillus* Section *Nigri* Isolates from Clinical and Environmental Settings. *J. Clin. Microbiol.* **2016**, *54*, 2365–2372. https://doi.org/10.1128/JCM.01075-16.

13. Kamali Sarvestani, H.; Seifi, A.; Falahatinejad, M.; Mahmoudi, S. Black Aspergilli as Causes of Otomycosis in the Era of Molecular Diagnostics, a Mini-Review. *J. Med. Mycol.* **2022**, *32*, 101240. https://doi.org/10.1016/j.mycmed.2021.101240.
14. Bojanović, M.; Ignjatović, A.; Stalević, M.; Arsić-Arsenijević, V.; Ranđelović, M.; Gerginić, V.; Stojanović-Radić, Z.; Stojković, O.; Živković-Marinkov, E.; Otašević, S. Clinical Presentations, Cluster Analysis and Laboratory-Based Investigation of *Aspergillus* Otomycosis—A Single Center Experience. *J. Fungi* **2022**, *8*, 315. https://doi.org/10.3390/jof8030315.
15. Ho, T.; Vrabec, J.T.; Yoo, D.; Coker, N.J. Otomycosis: Clinical Features and Treatment Implications. *Otolaryngol. Neck Surg.* **2006**, *135*, 787–791. https://doi.org/10.1016/j.otohns.2006.07.008.
16. Gits-Muselli, M.; Hamane, S.; Verillaud, B.; Cherpin, E.; Denis, B.; Bondeelle, L.; Touratier, S.; Alanio, A.; Garcia-Hermoso, D.; Bretagne, S. Different Repartition of the Cryptic Species of Black Aspergilli According to the Anatomical Sites in Human Infections, in a French University Hospital. *Med. Mycol.* **2021**, *59*, 985–992. https://doi.org/10.1093/mmy/myab027.
17. Varga, J.; Kocsubé, S.; Tóth, B.; Frisvad, J.C.; Perrone, G.; Susca, A.; Meijer, M.; Samson, R.A. *Aspergillus brasiliensis* sp. Nov., a Biseriate Black *Aspergillus* Species with World-Wide Distribution. *Int. J. Syst. Evol. Microbiol.* **2007**, *57*, 1925–1932. https://doi.org/10.1099/ijs.0.65021-0.

18. EN14885, B. Chemical Disinfectants and Antiseptics–Application of European Standards for Chemical Disinfectants and Antiseptics. *Lond. Br. Stand. Inst.* **2015**.
19. De Filippis, B.; Ammazzalorso, A.; Amoroso, R.; Giampietro, L. Stilbene Derivatives as New Perspective in Antifungal Medicinal Chemistry. *Drug Dev. Res.* **2019**, *80*, 285–293. https://doi.org/10.1002/ddr.21525.
20. Karpiński, T.M.; Ożarowski, M.; Seremak-Mrozikiewicz, A.; Wolski, H.; Adamczak, A. Plant Preparations and Compounds with Activities against Biofilms Formed by *Candida* spp. *J. Fungi* **2021**, *7*, 360. https://doi.org/10.3390/jof7050360.
21. Li, D.-D.; Zhao, L.-X.; Mylonakis, E.; Hu, G.-H.; Zou, Y.; Huang, T.-K.; Yan, L.; Wang, Y.; Jiang, Y.-Y. In Vitro and In Vivo Activities of Pterostilbene against Candida Albicans Biofilms. *Antimicrob. Agents Chemother.* **2014**, *58*, 2344–2355. https://doi.org/10.1128/AAC.01583-13.
22. Smith, D.F.Q.; Casadevall, A. Fungal Immunity and Pathogenesis in Mammals versus the Invertebrate Model Organism *Galleria mellonella*. *Pathog. Dis.* **2021**, *79*, ftab013. https://doi.org/10.1093/femspd/ftab013.
23. Li, Y.; Wan, Z.; Liu, W.; Li, R. Identification and Susceptibility of *Aspergillus* Section *Nigri* in China: Prevalence of Species and Paradoxical Growth in Response to Echinocandins. *J. Clin. Microbiol.* **2015**, *53*, 702–705. https://doi.org/10.1128/JCM.03233-14.

24. Toyotome, T.; Hagiwara, D.; Takahashi, H.; Watanabe, A.; Kamei, K. Emerging Antifungal Drug Resistance in *Aspergillus Fumigatus* and Among Other Species of *Aspergillus*. *Curr. Fungal Infect. Rep.* **2018**, *12*, 105–111. https://doi.org/10.1007/s12281-018-0318-9.
25. Fulaz, S.; Vitale, S.; Quinn, L.; Casey, E. Nanoparticle–Biofilm Interactions: The Role of the EPS Matrix. *Trends Microbiol.* **2019**, *27*, 915–926. https://doi.org/10.1016/j.tim.2019.07.004.
26. Patel, N.R.; Damann, K.; Leonardi, C.; Sabliov, C.M. Size Dependency of PLGA-Nanoparticle Uptake and Antifungal Activity against *Aspergillus flavus*. *Nanomedicine* **2011**, *6*, 1381–1395. https://doi.org/10.2217/nnm.11.35.
27. Muse, E.S.; Patel, N.R.; Astete, C.E.; Damann, K.E.; Sabliov, C.M. Surface Association and Uptake of Poly(Lactic-Co-Glycolic) Acid Nanoparticles by *Aspergillus flavus*. *Ther. Deliv.* **2014**, *5*, 1179–1190. https://doi.org/10.4155/tde.14.85.
28. Slomberg, D.L.; Lu, Y.; Broadnax, A.D.; Hunter, R.A.; Carpenter, A.W.; Schoenfisch, M.H. Role of Size and Shape on Biofilm Eradication for Nitric Oxide-Releasing Silica Nanoparticles. *ACS Appl. Mater. Interfaces* **2013**, *5*, 9322–9329. https://doi.org/10.1021/am402618w.
29. Chronopoulou, L.; Domenici, F.; Giantulli, S.; Brasili, F.; D'Errico, C.; Tsaouli, G.; Tortorella, E.; Bordi, F.; Morrone, S.; Palocci, C.; et al. PLGA Based Particles as "Drug Reservoir" for Antitumor Drug Delivery: Characterization and Cytotoxicity Studies. *Colloids Surf. B*

Biointerfaces **2019**, *180*, 495–502. https://doi.org/10.1016/j.colsurfb.2019.05.006.

30. Fang, T.-H.; Kang, S.-H.; Hong, Z.-H.; Wu, C.-D. Elasticity and Nanomechanical Response of *Aspergillus Niger* Spores Using Atomic Force Microscopy. *Micron* **2012**, *43*, 407–411. https://doi.org/10.1016/j.micron.2011.10.011.
31. Durieux, M.-F.; Melloul, É.; Jemel, S.; Roisin, L.; Dardé, M.-L.; Guillot, J.; Dannaoui, É.; Botterel, F. *Galleria mellonella* as a Screening Tool to Study Virulence Factors of *Aspergillus fumigatus*. *Virulence* **2021**, *12*, 818–834. https://doi.org/10.1080/21505594.2021.1893945.
32. Chronopoulou, L.; Sparago, C.; Palocci, C. A Modular Microfluidic Platform for the Synthesis of Biopolymeric Nanoparticles Entrapping Organic Actives. *J. Part Res.* **2014**, *16*, 2703. https://doi.org/10.1007/s11051-014-2703-9.
33. Pierce, C.G.; Uppuluri, P.; Tristan, A.R.; Wormley, F.L.; Mowat, E.; Ramage, G.; Lopez-Ribot, J.L. A Simple and Reproducible 96-Well Plate-Based Method for the Formation of Fungal Biofilms and Its Application to Antifungal Susceptibility Testing. *Nat. Protoc.* **2008**, *3*, 1494–1500. https://doi.org/10.1038/nprot.2008.141.
34. Pandolfi, F.; D'Acierno, F.; Bortolami, M.; De Vita, D.; Gallo, F.; De Meo, A.; Di Santo, R.; Costi, R.; Simonetti, G.; Scipione, L. Searching for New Agents Active against Candida Albicans Biofilm: A Series of Indole Derivatives, Design, Synthesis and Biological Evaluation. *Eur.*

J. Med. Chem. **2019**, *165*, 93–106. https://doi.org/10.1016/j.ejmech.2019.01.012.

Palencia, E. R., Hinton, D. M., & Bacon, C. W. (2010). The black Aspergillus species of maize and peanuts and their potential for mycotoxin production. *Toxins*, *2*(4), 399-416.

Sarvestani, H. K., Seifi, A., Falahatinejad, M., & Mahmoudi, S. (2022). Black aspergilli as causes of otomycosis in the era of molecular diagnostics, a mini-review. *Journal of Medical Mycology*, *32*(2), 101240.

Chapter 6: Final conclusions

Application of the biodegradable poly lactic-co-glycolic acid nanoparticles (PLGA NPs) for developing controlled release systems of encapsulated bioactive molecules has shown immense potential in agricolture (Tong et al., 2017; Athanassiou et al., 2018). PLGA is a harmless biocompatible polymer that totally degrades into nontoxic byproducts. In fact, when hydrolysis takes place, the lactide and glycolide monomers are transformed into lactic and glycolic acids, respectively, which are metabolized by the Krebs cycle producing carbon dioxide and water. Therefore, PLGA is not toxic to humans, plants or animals (Schnoor et al., 2018). In agriculture, the main advantage of these nanoformulations is the cargo protection from volatilization, infiltration, outflow, leaching and photo-, chemio- or bio-degradation (Pandita et al., 2015). As a result, plants and soils should incorporate fewer active chemicals, reducing the environment's negative impact (Perez, 2017). For their use in the plants it is important to understand the mechanisms of the uptake, translocation, and accumulation including their potential adverse effects on plant growth and development, as well as their preventive accurate evaluation of nanoparticle-plant interactions (Sanzari et al., 2019).

The PhD project went precisely in this direction. The study has been conducted on *A. thaliana* cultured cells and plantlet roots treated with

PLGA NPs loaded with the fluorescent probe coumarin6 (chapter 3). PLGA NPs Confocal and fluorescence microscopy results demonstrated that penetrated the suspended cells and tissues of roots of *A. thaliana* rapidly, as early as 10 minutes after administration. Moreover, *A. thaliana* cells were able to internalize PLGA NPs with a maximum size of 30 nm in diameter. This represents an important information for the future applications of PLGA NPs in this species. Moreover, we observed that the inhibitor Dynasore did not inhibit the uptake of PLGA NPs into *A. thaliana* cells and seedling roots. It is known that Dynasore acts as a potent inhibitor of endocytic pathways and depend on dynamin by blocking the GTPase activity of dynamin (Macia et al., 2006). Our results suggested that the internalization of NPs could occur by Dynamin-independent pathway and consequently, mainly involve the pathway of clathrin-independent endocytosis. This result is in line with previous studies, which showed clathrin-independent endocytosis was the primary internalization pathway in grapevine cell internalization (Palocci et al., 2017). A molecular approach would be of assistance in confirming this hypothesis.

In addition, the PLGA NPs were able to be translocated from the root to the hypocotyl in the *A. thaliana* seedling. These data, as well as being useful for understanding the mechanism of PLGA NPs internalization in *Arabidopsis*, are promising for future PLGA NPs applications in the field.

As widely documented, every year pathogenic fungi cause a great deal of economic damage in agriculture by attacking plants and crops (Peng et al., 2021) and producing mycotoxins that are proven harmful to human health (Reddy et al., 2010). This problem leads to widespread use of highly effective pesticides, however, every agrochemical has some potential issues including contamination of water or residues on food products that threat the human being and environmental health (Prasad et al., 2017). For this reason, it would be desirable the development of alternative systems for the administration of bioactive compounds to plant and fungi, in order to reduce the quantity and frequency of the treatments. It has been demonstrated, for example, by Chronopoulou et al. (2019) that MeJA encapsulation in NPs increases MeJA cell uptake and activates MeJA-induced responses in *V. vinifera*. It has also been shown that by encapsulating volatile compounds their long-term efficacy is ensured by controlled release and easy handling, with positive effects on their antifungal activity on *A. niger* (Janatova et al., 2015). In this context, analyses were carried out to evaluate the effectiveness of a nanotechnological system based on biopolimeric nanoparticles (PLGA NPs). In chapter 4, the effectiveness of the nanotechnological system was evaluated by encapsulating the fluorescent probe coumarin6, the naturally-derived stilbenoid pterostilbens, or the synthetic antifungal Fluopyram. Observations with fluorescence microscopy revealed that 50 nm Cu6-PLGA NPs penetrated *B. cinerea* conidia and hyphae within 10 minutes of

administration. Moreover, pterostilbene and fluopyram delivered by NPs were more active against *B. cinerea* than the corresponding free-form antifungals. This represents an important information in order to achieving higher efficacy and reduced environmental toxicity of natural and conventional antifungals through targeted and controlled drug delivery. The study of size thresholds for NPs uptake in plants and fungi could be useful in making more specific the effect of pesticides directed exclusively to fungi. In the present studies has been also demonstrated that PLGA NPs no bigger than 30 nm entered in *A. thaliana* cultured cells. Differently, Palocci and collaborators showed that in *V. vinifera* cultured cells PLGA NPs of 50 nm entered, while the bigger ones remained attached to the cell wall (Palocci et al., 2017). In *Aspergillus flavus* hyphae, 203 nm PLGA NPs were efficiently internalized, whereas 1206 nm remained associated with cell surface (Patel et al., 2011). NPs smaller than the size exclusion limit from the cell wall and from the plasma membrane would be suitable for delivery of molecules, such as resistance inducers, targeted to plant cells. In contrast, NPs with sizes above the size exclusion limit would be preferable for substances, such as antifungals, that should be released beyond plant cells.

In chapter 5, the observations of microscopy on *Aspergillus* section *Nigri* showed an efficient 50 nm PLGA-coumarin6-NPs uptake with the fluorescence signal visible inside *A. brasiliensis* hyphae and along the entire thickness of the biofilm matrix after treatment. The PLGA-PTB-NPs have reduced *A. brasililiensis* biofilm formation and mature

biofilm demonstrating that the PLGA NP system can enhance the bioavailability of natural compounds in *A. brasiliensis* biofilm by passing the biofilm matrix barrier and delivering the molecule into fungal cells. In the same publication, *in vivo* experiments showed major reduction in mortality of infected with *A. brasiliensis* (DSM 1988) conidia *Galleria mellonella* larvae, after injection of PLGA-PTB-NPs compared to those treated with PTB administered in free form at the same concentration. Fungal biofilm infections are particularly serious because biofilm cells are relatively resistant to many common antifungal agents (Blankenship and Mitchell, 2006). Simonetti et al., (2019) observed that PLGA-PTB-NPs inhibited *C. albicans* biofilm formation and reduced *C. albicans* mature biofilm.

In conclusion, 30 nm PLGA NPs were rapidly internalized by *A. thaliana* cells and plants. The PLGA NPs were not immediately degraded and were able to be translocated from the root to the hypocotyl in *A. thaliana* seedling. In addition, 50 nm PLGA NPs were efficiently absorbed by *B. cinerea* and *A. brasiliensis* and antifungals carried by NPs were more active, against the fungi under study, than the equivalent free-form antifungals. In view of these results, by targeting and controlling drug delivery, PLGA nanoparticles may be a promising treatment to deliver resistance inducers into the plant or for enhancing the effectiveness of natural antifungals and synthetic antifungals in agriculture.

References

Athanassiou, C. G., Kavallieratos, N. G., Benelli, G., Losic, D., Usha Rani, P., & Desneux, N. (2018). Nanoparticles for pest control: current status and future perspectives. *Journal of Pest Science*, *91*(1), 1-15.

Blankenship, J. R., & Mitchell, A. P. (2006). How to build a biofilm: a fungal perspective. *Current Opinion in Microbiology*, *9*(6), 588-594.

Chronopoulou, L., Donati, L., Bramosanti, M., Rosciani, R., Palocci, C., Pasqua, G., & Valletta, A. (2019). Microfluidic synthesis of methyl jasmonate-loaded PLGA nanocarriers as a new strategy to improve natural defenses in *Vitis vinifera*. *Scientific Reports*, *9*(1), 1-9.

Janatova, A., Bernardos, A., Smid, J., Frankova, A., Lhotka, M., Kourimská, L., ... & Kloucek, P. (2015). Long-term antifungal activity of volatile essential oil components released from mesoporous silica materials. *Industrial Crops and Products*, *67*, 216-220.

Macia, E., Ehrlich, M., Massol, R., Boucrot, E., Brunner, C., & Kirchhausen, T. (2006). Dynasore, a cell-permeable inhibitor of dynamin. *Developmental Cell*, *10*(6), 839-850.

Palocci, C., Valletta, A., Chronopoulou, L., Donati, L., Bramosanti, M., Brasili, E., ... & Pasqua, G. (2017). Endocytic pathways involved in

PLGA nanoparticle uptake by grapevine cells and role of cell wall and membrane in size selection. *Plant Cell Reports*, *36*(12), 1917-1928.

Pandita, D., Kumar, S., & Lather, V. (2015). Hybrid poly (lactic-co-glycolic acid) nanoparticles: design and delivery prospectives. *Drug Discovery Today*, *20*(1), 95-104.

Patel, N. R., Damann, K., Leonardi, C., & Sabliov, C. M. (2011). Size dependency of PLGA-nanoparticle uptake and antifungal activity against *Aspergillus flavus*. *Nanomedicine*, *6*(8), 1381-1395.

Peng, Y., Li, S. J., Yan, J., Tang, Y., Cheng, J. P., Gao, A. J., ... & Xu, B. L. (2021). Research progress on phytopathogenic fungi and their role as biocontrol agents. *Frontiers in Microbiology*, 1209.

Pérez-de-Luque, A. (2017). Interaction of nanomaterials with plants: what do we need for real applications in agriculture?. *Frontiers in Environmental Science*, *5*, 12.

Prasad, R., Bhattacharyya, A., & Nguyen, Q. D. (2017). Nanotechnology in sustainable agriculture: recent developments, challenges, and perspectives. *Frontiers in Microbiology*, *8*, 1014.

Reddy, K. R. N., Salleh, B., Saad, B., Abbas, H. K., Abel, C. A., & Shier, W. T. (2010). An overview of mycotoxin contamination in foods and its implications for human health. *Toxin Reviews*, *29*(1), 3-26.

Sanzari, I., Leone, A., & Ambrosone, A. (2019). Nanotechnology in plant science: to make a long story short. *Frontiers in Bioengineering and Biotechnology*, *7*, 120.

Schnoor, B., Elhendawy, A., Joseph, S., Putman, M., Chacón-Cerdas, R., Flores-Mora, D., ... & Salvador-Morales, C. (2018). Engineering atrazine loaded poly (lactic-co-glycolic acid) nanoparticles to ameliorate environmental challenges. *Journal of Agricultural and Food Chemistry*, *66*(30), 7889-7898.

Simonetti, G., Palocci, C., Valletta, A., Kolesova, O., Chronopoulou, L., Donati, L., ... & Pasqua, G. (2019). Anti-*Candida* biofilm activity of pterostilbene or crude extract from non-fermented grape pomace entrapped in biopolymeric nanoparticles. *Molecules*, *24*(11), 2070.

Tong, Y., Wu, Y., Zhao, C., Xu, Y., Lu, J., Xiang, S., ... & Wu, X. (2017). Polymeric nanoparticles as a metolachlor carrier: water-based formulation for hydrophobic pesticides and absorption by plants. *Journal of Agricultural and Food Chemistry*, *65*(34), 7371-7378.

Chapter 7: Other publications and activities during the PhD

Giordani, C., Simonetti, G., Natsagdorj, D., Choijamts, G., Ghirga, F., Calcaterra, A., Quaglio, D., De Angelis, G., Toniolo, C. & Pasqua, G. (2020). Antifungal activity of Mongolian medicinal plant extracts. Natural product research, 34(4), 449-455.

Mulinacci, N., Valletta, A., Pasqualetti, V., Innocenti, M., Giuliani, C., Bellumori, M., De Angelis., G, Carnevale, A., Locato, V., Di Venanzio, C. & Pasqua, G. (2019). Effects of ionizing radiation on bio-active plant extracts useful for preventing oxidative damages. Natural product research, 33(8), 1106-1114.

Winner of the call for Avvio alla Ricerca 2019

- Lab2go tutoring activity
- Tutoring activity (as part of the Morphofunctional Botany courses for Environmental Sciences Degree).
- Summer School in Plant Phenotyping, Metaponto 3-5 July 2019. Organized by the Working Groups in "Cell and Molecular Biology" and "Biotechnology and Differentiation" of the Italian Botanical Society.
- IV° Electron and confocal microscopy course in botany at Science Area of Via Campi, Modena 10- 13-14 December 2021